

PREPARATION AND CHARACTERIZATION OF  
CHITOSAN-GELATIN/HYDROXYAPATITE SCAFFOLDS FOR  
HARD TISSUE ENGINEERING APPROACHES

A THESIS SUBMITTED TO  
THE GRADUATE SCHOOL OF NATURAL AND APPLIED SCIENCES  
OF  
MIDDLE EAST TECHNICAL UNIVERSITY

BY

CANSEL IŞIKLI

IN PARTIAL FULFILLMENT OF THE REQUIREMENTS  
FOR  
THE DEGREE OF MASTER OF SCIENCE  
IN  
BIOMEDICAL ENGINEERING

JANUARY 2010

Approval of the thesis:

**PREPARATION AND CHARACTERIZATION OF  
CHITOSAN-GELATIN/HYDROXYAPATITE SCAFFOLDS  
FOR HARD TISSUE ENGINEERING APPROACHES**

submitted by **CANSEL IŞIKLI** in partial fulfillment of the requirements for the degree of **Master of Science in Biomedical Engineering Department, Middle East Technical University** by,

Prof. Dr. Canan Özgen \_\_\_\_\_  
Dean, Graduate School of **Natural and Applied Sciences**

Prof. Dr. Zülfü Aşık \_\_\_\_\_  
Head of Department, **Biomedical Engineering**

Prof. Dr. Nesrin Hasırcı \_\_\_\_\_  
Supervisor, **Chemistry Dept., METU**

Prof. Dr. Vasıf Hasırcı \_\_\_\_\_  
Co-supervisor, **Biology Dept., METU**

**Examining Committee Members:**

Prof. Dr. Duygu Kısakürek \_\_\_\_\_  
Chemistry Dept., METU

Prof. Dr. Nesrin Hasırcı \_\_\_\_\_  
Chemistry Dept., METU

Prof. Dr. Zülfü Aşık \_\_\_\_\_  
Engineering Sciences Dept., METU

Prof. Dr. Kezban Ulubayram \_\_\_\_\_  
Faculty of Pharmacy, Hacettepe University

Assoc. Prof. Dr. Caner Durucan \_\_\_\_\_  
Metallurgical and Materials Engineering Dept., METU

**Date:** 20.01.2010

**I hereby declare that all information in this document has been obtained and presented in accordance with academic rules and ethical conduct. I also declare that, as required by these rules and conduct, I have fully cited and referenced all material and results that are not original to this work.**

Name, Last name: Cansel Işıklı

Signature:

# ABSTRACT

## PREPARATION AND CHARACTERIZATION OF CHITOSAN-GELATIN/HYDROXYAPATITE SCAFFOLDS FOR HARD TISSUE ENGINEERING APPROACHES

Işıklı, Cansel

M.Sc., Department of Biomedical Engineering

Supervisor: Prof. Dr. Nesrin Hasırcı

Co-supervisor: Prof. Dr. Vasıf Hasırcı

January 2010, 127 pages

Hard tissue engineering holds the promise of restoring the function of failed hard tissues and involves growing specific cells on extracellular matrix (ECM) to develop “tissue-like” structures or organoids. Chitosan is a linear amino polysaccharide that can provide a convenient physical and biological environment in tissue regeneration attempt. To improve chitosan’s mechanical and biological properties, it was blended with another polymer gelatin. 1-ethyl-3-(3-dimethylaminopropyl)-carbodiimide (EDC) and N-hydroxysuccinimide (NHS) were used to crosslink the chitosan-gelatin matrix to produce stable structures. These natural polymers are mechanically weak especially to serve as a bone substitute and therefore, an inorganic calcium phosphate ceramic, hydroxyapatite, was incorporated to improve this aspect.

The objective of this study was to develop chitosan-gelatin/hydroxyapatite scaffolds for a successful hard tissue engineering approach. For this reason, two types of hydroxyapatite, as-precipitated non-sintered (nsHA) and highly crystalline sintered (sHA) were synthesized and blended into mixtures of chitosan (C) and gelatin (G)

to produce 2-D (film) and 3-D (sponge) structures. The physicochemical properties of the structures were evaluated by scanning electron microscopy, X-Ray Diffraction (XRD), Fourier Transform Infrared-Attenuated Total Reflectance spectrometer (FTIR-ATR), differential scanning calorimetry, contact angle and surface free energy measurements and swelling tests. Mechanical properties were determined through tensile and compression tests. In vitro cell affinity studies were carried out with SaOs-2 cells. MTS assays were carried out to study cell attachment and proliferation on the 2-D and 3-D scaffolds. Several methods such as confocal, fluorescence and scanning electron microscopy were used to examine the cell response towards the scaffolds.

Cell affinities of the samples were observed to change with changing chitosan-gelatin ratio and hydroxyapatite addition into the matrices. XRD and FTIR results confirmed the purity of the hydroxyapatite synthesized. Mechanical test results showed that 2-D and 3-D chitosan-gelatin/hydroxyapatite constructs have similar properties as bones, and in vitro studies demonstrated that the prepared matrices have the potential to serve as scaffold materials in hard tissue engineering applications.

**Keywords:** Chitosan, Gelatin, Hydroxyapatite, Scaffold, SaOs-2, Hard Tissue Engineering

# ÖZ

## KİTOSAN-JELATİN/HİDROKSİAPATİT DESTEK YAPILARIN SERT DOKU MÜHENDİSLİĞİ YAKLAŞIMLARI İÇİN HAZIRLANMASI VE KARAKTERİZASYONU

Işıklı, Cansel

Yüksek Lisans, Biyomedikal Mühendisliği Bölümü

Tez Yöneticisi: Prof. Dr. Nesrin Hasırcı

Ortak Tez Yöneticisi: Prof. Dr. Vasıf Hasırcı

Ocak 2010, 127 sayfa

Doku mühendisliği, zarar görmüş doku ve organların fonksiyonlarını yeniden kazanmasını hedefleyerek, hücre dışı matris üzerinde belli hücrelerin büyütülmesi ile doku-benzeri organı yapılar geliştirmek temeline dayanır. Lineer bir amino polisakarid olan kitosan doku yenilenmesi sürecinde uygun fizyolojik ve biyolojik çevreyi sağlar. Kitosan mekanik ve biyolojik özelliklerini geliştirmek amacı ile, bir başka polimer olan jelatin ile karıştırılmıştır. 1-etil-3-(3-dimetilaminopropil)-karbodiimid (EDC) ve hidroksisaksinimid (NHS) kararlı kitosan-jelatin yapılar oluşturmak için çapraz bağlayıcı olarak kullanılmıştır. Bu doğal polimerler özellikle kemik tedavisi uygulamalarında mekanik açıdan zayıf oldukları için bu özellikleri geliştirmek amacı ile içlerine inorganik kalsiyum fosfat seramiği hidroksiapatit eklenmiştir.

Bu çalışma başarılı bir sert doku mühendisliği yaklaşımı için kitosan-jelatin/hidroksiapatit destek yapılar geliştirmeyi hedeflemiştir. Bu amaçla, çöktürülmüş katılaştırılmamış (nsHA) ve yüksek kristaliniteye sahip katılaştırılmış (sHA) olmak üzere iki çeşit hidroksiapatit sentezlenmiş, iki-boyutlu (film) ve üç-boyutlu (köpük) yapılar üretmek için kitosan (C) ve jelatin (G) karışımlarının içine

eklenmiştir. Yapıların fiziko kimyasal özellikleri taramalı elektron mikroskobu (SEM), X-Ray Difraktometre, FTIR-ATR, DSC, kontakt açısı ve yüzey enerji ölçümleri ve şişme testleri ile incelenmiştir. Mekanik özellikler gerilme ve basınç testleri ile gözlenmiştir. Örneklerin in vitro çalışmaları, SaOs-2 hücreleri ile etkileşimi sonucu belirlenmiştir. Destek yapılar üzerindeki hücre yapışmasını ve çoğalmasını gözlemlemek için MTS ölçümleri yapılmıştır. Hücrelerin destek yapılarına karşı davranışları konfokal, floresan ve taramalı electron mikroskopları gibi çeşitli metodlarla incelenmiştir. XRD ve FTIR sonuçları saf hidroksiapatit sentezlendiğini kanıtlamıştır. Mekanik test verileri iki- ve üç-boyutlu kitosan-jelatin/hidroksiapatit yapıların sert doku mühendisliğinde kullanıma uygun değerlere sahip olduğunu göstermiştir. Örneklerin hücre etkileşimleri kitosan-jelatin oranlarının değişimi ve hidroksiapatit eklenişiyle de geliştirilmiştir.

**Anahtar Kelimeler:** Kitosan, Jelatin, Hidroksiapatit, Destek Yapı, SaOs-2, Sert Doku Mühendisliği

*To my precious family...*



## ACKNOWLEDGEMENTS

I would like to express my gratitude to my supervisor Prof.Dr. Nesrin Hasırcı for, her valuable advices, continuous guidance, encouragement and giving me a chance to be a part of her highly qualified laboratory throughout my study. I am deeply thankful for her motivation and support to complete this thesis.

I would like to express my deep appreciation to Prof. Dr. Vasıf Hasırcı for enlightening my professional and academic vision with his support, leadership and guidance. I am also thankful for making me a member of BIOMAT group that gave me the possibility of joining many international academical organizations supported by this team.

I am grateful to Assoc.Prof. Caner Durucan and his lab team for their support in preparation and characterization of hydroxyapatite component of the matrices.

My sincere acknowledgements go to Tuğba Endođan and Aysel Kızıltay for their great patience, support, help and friendship as great lab partners. I am also thankful to Tuğba Endođan for her patience and help in microscopic examinations and to Aysel Kızıltay for her guidance in cell culture tests.

I would like to appreciate BIOTECH laboratories for *in vitro* studies, microscopic examinations, freeze-drying, contact angle measurements. I would like to thank to Chemistry Department for DSC analysis and to Sedat Canlı, METU Central Laboratory and Cengiz Mehmet Tan and his staff, for their support provided during SEM examinations. I wish to thank to all BIOMAT group members and especially to Dr. Eda Ayşe Aksoy for their support.

TUBITAK is gratefully acknowledged for the financial support via grant no 109M325.

I am really grateful to founder of Turkish Republic; Mustafa Kemal Atatürk for his revolutions in education and woman rights that provide me to study under these conditions.

I would like to thank to my dear friends İrem Alp, Yasemen Hintliođlu, Emre Öđütçü, Bahadır Dođan, Can Nebigil, Berk Müjde, Füsun Akman, Dođa Atay and all members of Association of Flamenko Ankara for their precious friendship and support. I am also thankful to Elif Vardar for her valuable friendship and support in every part of my life.

Finally, I would like to give special thanks to my mother Hülya Işıklı, my father Zafer Işıklı, my dear brother Canberk Işıklı, my aunt Oya Fırat and my dearest grandmother Memnune Fırat for their patience, encouragement and endless love.

# TABLE OF CONTENTS

ABSTRACT.....	iv
ÖZ.....	vi
ACKNOWLEDGEMENTS.....	ix
TABLE OF CONTENTS.....	xi
LIST OF TABLES.....	xv
LIST OF FIGURES.....	xvi
ABBREVIATIONS.....	xix
CHAPTERS	
1.INTRODUCTION .....	1
1.1 Tissue Engineering .....	1
1.2 Components of Tissue Engineering .....	2
1.2.1 Scaffolds.....	2
1.2.1.1 Scaffold Materials.....	4
1.2.1.1.1 Biodegradable Polymers.....	5
1.2.1.1.2 Bioceramics.....	7
1.2.1.1.3 Biocomposites.....	9
1.2.1.2 Scaffold Preparation Techniques.....	10
1.2.1.2.1 Solvent Casting Method.....	13
1.2.1.2.2 Freeze-Drying Technique.....	13
1.2.1.2.3 Crosslinking Process.....	14
1.2.2 Active Molecules .....	16
1.2.3 Cells .....	18
1.3 Hard Tissue Engineering .....	19

1.4	Components of Hard Tissue Engineering .....	21
1.4.1	Scaffolds in Hard Tissue Engineering .....	22
1.4.1.1	Scaffold Materials in Hard Tissue Engineering.....	23
1.4.1.1.1	Chitosan.....	24
1.4.1.1.2	Gelatin.....	27
1.4.1.1.3	Hydroxyapatite.....	29
1.4.1.1.4	Biocomposites of Chitosan-Gelatin/Hydroxyapatite.....	32
1.4.2	Active Molecules in Hard Tissue Engineering .....	35
1.4.3	Cells in Hard Tissue Engineering .....	36
1.5	Characterization of Scaffolds .....	37
1.5.1	Chemical Structure.....	37
1.5.2	Surface Examination .....	38
1.5.3	Swelling Degree .....	42
1.5.4	Mechanical Properties.....	43
1.5.5	Thermal Analysis .....	45
1.5.6	Pore Size Distribution .....	45
1.5.7	Biocompatibility.....	46
1.6	The Aim of This Study.....	46
2.	EXPERIMENTAL .....	48
2.1	Materials.....	48
2.2	Methods .....	49
2.2.1	Hydroxyapatite Synthesis .....	49
2.2.2	Chitosan-Gelatin/Hydroxyapatite Scaffolds Preparation.....	49
2.2.2.1	Chitosan, Gelatin and Chitosan-Gelatin Films.....	49
2.2.2.2	Chitosan-Gelatin/Hydroxyapatite Films.....	50
2.2.2.3	Chitosan-Gelatin/Hydroxyapatite Porous Sponge Scaffolds.....	52
2.3	Characterization.....	53
2.3.1	X-Ray Diffraction (XRD) .....	53

2.3.2	Scanning Electron Microscopy .....	53
2.3.3	Fourier Transform Infrared-Attenuated Total Reflectance (FTIR-ATR) Analysis .....	53
2.3.4	Differential Scanning Calorimetry (DSC) Analysis .....	53
2.3.5	Contact Angle and Surface Free Energy Measurements .....	54
2.3.6	Swelling Tests .....	54
2.3.7	Mechanical Tests.....	54
2.3.8	Cell Viability Tests .....	55
2.3.8.1	Preparation of Scaffolds for Cell Seeding.....	55
2.3.8.2	Cell Culture and Cell Seeding.....	55
2.3.8.3	Cell Proliferation Test.....	55
2.3.8.4	Cell Morphology.....	56
3.	RESULTS AND DISCUSSION .....	57
3.1	Hydroxyapatite Synthesis.....	57
3.2	Hydroxyapatite Characterization Results .....	58
3.2.1	X-Ray Diffraction Examination.....	58
3.2.2	FTIR-Attenuated Total Reflectance Spectroscopy Analysis .....	59
3.2.3	Morphologies of Hydroxyapatite Particles .....	60
3.3	Film Preparation .....	61
3.4	Film Characterization .....	63
3.4.1	FTIR-Attenuated Total Reflectance Spectroscopy Analysis .....	63
3.4.2	Differential Scanning Calorimetry Results .....	66
3.4.3	Mechanical Properties of Film Structures.....	70
3.4.4	Surface Hydrophilicity .....	72
3.4.5	Surface Morphology Analysis .....	75
3.4.6	Swelling Behavior of Film Structures.....	77
3.4.7	Cell Affinity and Proliferation of Film Structures .....	79
3.5	Porous Scaffold Preparation .....	87
3.6	Porous Scaffold Characterization .....	88

3.6.1	FTIR-Attenuated Total Reflectance Examination .....	88
3.6.2	Scaffold Morphology .....	89
3.6.3	Mechanical Properties .....	91
3.6.4	Cell Viability on Porous Structures .....	94
4.	CONCLUSIONS.....	98
	REFERENCES.....	101
	APPENDIX.....	127
	A. DSC CURVES OF C-G FILMS .....	127

## LIST OF TABLES

### TABLES

Table 1 Biomaterials used in human body with some examples, forms and application areas .....	4
Table 2 Natural polymer types with different sources and examples .....	6
Table 3 Bioceramics with different types, medical devices and functions .....	8
Table 4 Polymeric scaffold processing methods with advantages and disadvantages .....	12
Table 5 Chemical structures of crosslinkers. ....	15
Table 6 Mechanical properties of cortical and spongy bones .....	44
Table 7 Compositions of the prepared films. ....	51
Table 8 Compositions of the prepared sponge structures .....	52
Table 9 Adsorbed water evaporation and decomposition temperatures of chitosan-gelatin and chitosan-gelatin/non-sintered hydroxyapatite composite films. .	69
Table 10 Mechanical properties of crosslinked (C-G) blend and (C-G/nsHA) composite films .....	71
Table 11 Contact angle values of the uncrosslinked, crosslinked (x) chitosan-gelatin blend and crosslinked chitosan-gelatin/nsHA composite (x/nsHA) films.....	73
Table 12 Surface free energy parameters (acidic and basic components) of test liquids according to acid-base approach.....	74
Table 13 SFE values of chitosan-gelatin films .....	75
Table 14 Swelling ratios (% w/w) of crosslinked blend and composite films.....	78
Table 15 Comparison of Young's modulus (E) and Ultimate Compression Strength of crosslinked Chitosan-Gelatin and Chitosan-Gelatin/Hydroxyapatite porous scaffolds with those of cancellous bone. ....	93

## LIST OF FIGURES

### FIGURES

Figure 1 Scanning electron microscope micrographs of (a) poly( $\xi$ -caprolactone) based rapid prototyped 3-D scaffold (b) gelatin-based scaffolds prepared by freeze-drying method (c) micropatterned polymeric films obtained from the PDMS replica of the Si template (d) electrospun fiber morphologies of gelatin/PCL.....	10
Figure 2 Reaction mechanisms of carboxylic group activation by EDC and amide bond formation with amine addition. ....	16
Figure 3 Bone regeneration by using scaffolds and seeded cells.....	21
Figure 4 Graph of mass and weight loss of the scaffold versus time for bone/cartilage tissue engineering approaches.....	23
Figure 5 Derivation of chitosan from chitin.....	25
Figure 6 (A) Chemical structures of amino acid sequences, and (B) proposed chemical structure of gelatin.....	27
Figure 7 Crystallographic structure of hydroxyapatite viewed along the c-axis. ....	30
Figure 8 Contact angle of a liquid drop with surface free energy vectors; A, B and C showing interfacial tension between air and liquid, solid and liquid, solid and vapor respectively. ....	39
Figure 9 A tensile stress-strain curve of a viscoelastic material .....	43
Figure 10 Hydroxyapatite synthesis.....	57
Figure 11 XRD patterns of hydroxyapatite powders (a) non-sintered, and (b) sintered .....	58
Figure 12 FTIR-ATR spectra of hydroxyapatite powder (a) non-sintered and (b) sintered .....	59
Figure 13 SEM micrographs of non-sintered (a and b) and sintered (c and d).....	60



Figure 14 Pictures of (a)xC, (b)xC-G:3-1, (c)xC-G:1-1, (d)xG, (e)xC/nsHA, (f) xC-G:3-1/nsHA, (g) xC-G:1-1/nsHA, and (h) xG/nsHA films. ....	61
Figure 15 Schematic illustration of (A) gelatin carboxyl group activation by EDC and reaction of activated gelatin complex with (B) chitosan, (C) gelatin, and (D) NHS activated gelatin reactions. ....	62
Figure 16 FTIR spectra of uncrosslinked chitosan-gelatin films. ....	64
Figure 17 FTIR spectra of crosslinked chitosan-gelatin films. ....	65
Figure 18 FTIR spectra of crosslinked chitosan-gelatin/non-sintered hydroxyapatite composite films. ....	65
Figure 19 DSC of crosslinked chitosan-gelatin blend films .....	67
Figure 20 DSC of crosslinked chitosan-gelatin/nsHA composite films .....	68
Figure 21 SEM micrographs of crosslinked chitosan-gelatin (left column) and chitosan-gelatin/nsHA composite (right column) films X5000 .....	76
Figure 22 Swelling behavior of crosslinked chitosan-gelatin blends. ....	78
Figure 23 Swelling behavior of crosslinked chitosan-gelatin/nsHA composite samples. ....	79
Figure 24 SaOs-2 proliferation on films .....	81
Figure 25 Fluorescence microscopy images of crosslinked chitosan-gelatin blend films with SaOs-2 cells cultured on them for 1 and 7 days (x20). ....	82
Figure 26 Fluorescence microscopy images of crosslinked chitosan-gelatin/nsHA composite films seeded with SaOs-2 cells. After 1 and 7 days (x20). ....	83
Figure 27 SEM images of cell morphology of SaOs-2 cells seeded on crosslinked chitosan-gelatin blend films cultured for 1 day and 7 days .....	85
Figure 28 SEM images of SaOs-2 cells seeded on crosslinked chitosan-gelatin/nsHA composite films and cultured for 7 days .....	87
Figure 29 SEM micrographs of spxC-G:1-1/sHA porous scaffolds frozen (a) at -80°C (b) in N <sub>2</sub> (liq), and (c) on N <sub>2</sub> (liq). ....	88
Figure 30 FTIR-ATR analysis of crosslinked various chitosan-gelatin sponges.....	89

Figure 31 Scanning electron microscopy images of chitosan-gelatin-based three-dimensional porous scaffolds. Second column presents the magnified version of the first column.....	90
Figure 32 Scanning electron microscopy images of chitosan-gelatin/non-sintered hydroxyapatite (x5000) magnitude and chitosan-gelatin/sintered hydroxyapatite scaffolds pore walls (x250) magnitude.....	91
Figure 33 Comparison of Young's modulus (E) of crosslinked chitosan-gelatin, chitosan-gelatin/non-sintered hydroxyapatite, chitosan-gelatin/sintered hydroxyapatite porous scaffolds, obtained in compression tests.....	92
Figure 34 Ultimate compression strengths (UCS) of crosslinked chitosan-gelatin, chitosan-gelatin/non-sintered hydroxyapatite, chitosan-gelatin/sintered hydroxyapatite porous scaffolds.....	93
Figure 35 SaOs-2 osteosarcoma proliferation on sponges assessed by MTS assay	94
Figure 36 Confocal images of the cross-section of SaOs-2 cells seeded crosslinked chitosan-gelatin blend, chitosan-gelatin/nsHA and chitosan-gelatin/sHA composite porous scaffolds cultured for 1 and 7 days.....	95
Figure 37 SEM images of SaOs-2 cells seeded on crosslinked chitosan-gelatin blend, chitosan-gelatin/nsHA and chitosan-gelatin/sHA composite porous scaffolds cultured for 1 and 7 days.....	96
Figure 38 DSC analysis of uncrosslinked chitosan-gelatin films. ....	127

## ABBREVIATIONS

$\gamma$	Surface Tension
BSA	Bovine serum albumin
C	Chitosan
CaCO <sub>3</sub>	Calcium carbonate
Ca(NO <sub>3</sub> ).4H <sub>2</sub> O	Calcium Nitrate
DAPI	4', 6-diamidino-2-phenylindole
DIM	Diiodomethane
DMSO	Dimethyl Sulfoxide
DSC	Differential Scanning Calorimetry
DW	Deionized Water
E	Elasticity (Young's Modulus)
ECM	Extracellular Matrix
EDC	1-ethyl-3-(3-dimethylaminopropyl)-carbodiimide
FA	Formamide
FBS	Fetal bovine serum
FTIR-ATR	Fourier Transform Infrared-Attenuated Total Reflectance
G	Gelatin
HA	Hydroxyapatite
MTS	(3-(4,5-dimethylthiazol-2-yl)-5-(3-carboxymethoxyphenyl)-2-(4-sulfophenyl)-2H-tetrazolium)
N <sub>2</sub> (liq)	Liquid nitrogen
NaOH	Sodium hydroxide
(NH <sub>4</sub> ) <sub>2</sub> HPO <sub>4</sub>	Diammonium phosphate
NHS	N-hydroxysuccinimide
nsHA	Non-sintered hydroxyapatite

PBS	Phosphate buffered saline
PFA	Paraformaldehyde
PI	Propidium iodide
RGD	Arginine-glycine-aspartic acid
SAB	Strain at break
SaOs-2	Human osteosarcoma cell line
SEM	Scanning Electron Microscope
SFE	Surface Free Energy
sHA	Sintered hydroxyapatite
sp	Sponge
TCP	Tissue culture plate
T <sub>g</sub>	Glass Transition Temperature
UCS	Ultimate Compression Strength
UTS	Ultimate Tensile Strength
x	Crosslinked
XRD	X-Ray Diffraction

# CHAPTER 1

## INTRODUCTION

### *1.1 Tissue Engineering*

The need for the organ transplantation is one of the main health problems around the world because of organ shortage resulting with about 8000 deaths on the waiting lists in last years [Pomfret, 2008]. Posttransplantation period also has some complications that limits the tissue transplantation such as; transmission of the diseases or immune reactions [Lalan et al., 2001]. Therefore, around the world, about 600 million dollar per year is spent by more than 70 different companies for the invention of new applicable engineered biomaterials to increase the health standards and to overcome the drawbacks of organ or tissue transplantation [Lysaght et al., 2001]. Thus, researches that aim to find new solutions to these arising health problems and limitations, have revealed an interdisciplinary area named as; tissue engineering.

Tissue engineering which is still developing branch of science, aims to mimic the nature, using the supporting engineered structures with or without cell addition, for restoring the function of damaged tissues [Garner, 2004]. Therefore, materials which are compatible with the biological media, are the fundamental elements of tissue engineering and used in various biomedical applications [Barnes et al., 2008]. In tissue engineering approach; two main strategies can be applied to the required area; a polymeric matrix or a matrix loaded with cells, depending on the healing ability of damaged part of the body [Atala et al., 2007]. In each case, the material used to produce two dimensional or three dimensional constructs should have good

matching with the applied body site. These biomaterials acting as scaffolds, cells and signalling factors (e.g. growth factors) enhancing the regeneration [Basmanav et al., 2008] are the major components of tissue engineering. The keys of successful tissue engineering approaches are; choosing the correct biomaterial with required properties and having an appropriate engineering performance for subsequent healing process. Researchers try to investigate new applicable tissue engineering approaches dealing with some challenges and claim that despite all the limitations, in future, many patients will be treated by advanced tissue engineered biomaterials [Giannoudis et al., 2005]. Therefore, great knowledge in chemistry, biology, materials science and medicine is needed for research in tissue engineering that is an interdisciplinary area.

Following sections will focus on the properties of tissue engineering components for successful applications.

## ***1.2 Components of Tissue Engineering***

This section examines the definitions and properties of fundamental components of tissue engineering approach which are; scaffolds, cells and bioactive molecules since the properties of these components are very crucial for a successful tissue regeneration process.

### ***1.2.1 Scaffolds***

Scaffolds behave as templates for growing cells or for delivery materials (genes or drugs), and are implanted into diseased body part [Widmer et al., 1998]. Choosing the material and designing procedure of the scaffold structure, are the first steps to obtain a useful and applicable end product to the damaged tissue site. Implantable scaffolds can be prepared as two-dimensional (2-D) film forms or three-dimensional (3-D) porous structures, depending on the shape and position of the implantation site. The essential roles of scaffolds are; to create a convenient

environment for the cell ingrowth, so that cells can adhere to the matrix, proliferate and differentiate in the desired direction, to improve the mechanical property of the unhealthy tissue and to maintain these features until the completion of new healthy tissue formation [Kim et al., 2001]. Scaffold characteristics are very important parameters to observe the new tissue formation on the applied part of the body. They must have an appropriate chemistry that provides an interface varying with the local physiological and biological changes and that encourages the extracellular matrix remodeling [Venugopal et al., 2007].

Porosity of the 3-D structure is one of the main factors that affect the tissue growth into the matrix, cell viability is provided by the channels through the scaffold with easy oxygen and nutrient transportation.

Scaffold surface is another important factor, because initial cell attachment begins on the surface of the material and subsequent tissue formation depends on the initial cell-material interaction. Therefore, functional groups existing on the scaffold surface can enhance or diminish cell adhesion.

Furthermore, tissue engineered scaffolds must have compatible properties with the damaged part of the tissue without causing any toxic or allergenic reactions [Liu et al., 2007]. While scaffolds degrade in time after implantation, they release some chemicals and they may change the pH or biological properties of the environment. That's why, not only the tissue engineered scaffold material but also degradation products are important. They must be non-toxic to prevent immune response or encapsulation of construct (meaning fibrous tissue formation around the implant) which are termed as host response of body to implanted material.

Surface area to volume ratio is another key factor for successful scaffold material affecting scaffold-cell interaction. Greater surface area to volume ratio means greater water uptake and greater interactions with cells. Therefore, the number of cells adhered to the material increases. On the other hand, high porosity supplies easier transport of metabolites enhancing cell growth. For degradable materials; degradability of the scaffold occurs in shorter time compared to bulk structures [Lu et al., 1999].

In the following sections, properties of scaffold materials are described in details.

### ***1.2.1.1 Scaffold Materials***

Polymers, ceramics, composites and metals, are the main classes of biomaterials used in the tissue damages in different forms as it is illustrated in Table 1 [Park et al., 2007].

Table 1 Biomaterials used in human body with some examples, forms and application areas.

Materials	Examples	Biomaterial Forms	Applications
Polymers	PLLA, PLGA, PCL, PMMA, polyamides, polystyrene, polyethylene, polyurethanes, polyethyletherketone, silicone, chitosan, silk, gelatin, Ulvan, fibroin, collagen	Fibers, hydrogels, 2-D or 3-D porous or non-porous constructs	Sutures, soft (e.g. heart valves) or hard (e.g. dental) tissue implants, hip socket
Ceramics	Calcium phophates (e.g. $\beta$ -Tricalcium phosphate, hydroxyapatite), bioglass, calcium aluminate, alumina, zirconia	Particulate constructs, 2-D or 3-D porous or non-porous constructs	Othopedic implants, dental implants
Composites	Carbon nanotubes and fibers, PLGA-calcium phosphate, chitosan-gelatin/hydroxyapatite composites	Fibers, 2-D or 3-D porous or non-porous constructs,	Bone cement, dental resin, tissue engineered scaffolds
Metals	Titanium-based alloys, gold, silver, Cobalt-based alloys, steel, platinum	2-D or 3-D porous or non-porous constructs	Bone implants, hip prostheses, screws, pins, plates



Biomaterial has lots of different definitions changing with time related to the improvements in technologies used, application areas or approaches. In 1992, European Society for Biomaterials Consensus Conference II defined biomaterial as; “a material intended to interface with biological systems to evaluate, treat, augment or replace any tissue, organ or function of the body”.

According to the recent approaches, biomaterials may also be defined as; “the materials, both synthetic and natural, that are implanted in the human body for the purposes of promoting improved human health” [Guelcher and Hollinger, 2006].

In tissue engineering, some types of these biomaterials are used to design modified constructs with cells and with or without active molecules in order to improve regeneration and healing process in defected tissue site of body. These types of structures are called as scaffolds as described previously and have some important characteristics to prevent undesired results in postimplantation periods. For example, degradation product of the construct may result with some effects such as; allergenic, cancerogenic reactions, encapsulation or immune responses. Therefore, in recent years, much more attention has been paid to biodegradable polymers and bioactive ceramics as scaffold materials because of their high biological and chemical resemblance to natural tissue. These materials that are used especially in tissue engineering approaches, are summarized in the following sections.

#### ***1.2.1.1.1 Biodegradable Polymers***

Biodegradability of a material depends on its origin, chemistry, degradability and environment [Mohanty et al., 2000]. In recent studies, biodegradable polymers are emphasized as candidate scaffold materials because some types have great resemblance to natural extracellular matrix with a soft, tough, and elastomeric proteinaceous network structure that perform mechanical stability and structural integrity for damaged hard tissues [Chu, 2008]. Mohanty et al. classified biodegradable polymers as; biosynthetic, semi-biosynthetic and chemo-biosynthetic types with respect to their material classes. Furthermore, biodegradable polymers

are also divided into two major categories according to their chemistries and origins: natural biopolymers and synthetic polymers.

Polymers synthesized by living organisms are called as natural biopolymers and classified into four main categories; polysaccharides, proteins, lipid/surfactants and speciality polymers [Krajewska et al., 2005 and Kaplan et al., 1998], the categorization of natural polymers is illustrated as Table 2.

Table 2 Natural polymer types with different sources and examples.

Polymer Type	Source	Examples
Polysaccharides	Red sea weeds, plant cell walls, exoskeleton of insects and crustacea, animal cells, bacteria	Plant/algal: starch, cellulose, pectin, konjac, ulvan, alginic acid Animal: hyaluronic acid, chondroitin sulphate Fungal: pullulan, elsinan, scleroglucan Exoskeletal: chitin, chitosan Bacterial: levan, xanthan
Proteins	Blood, hard and soft tissues of animals, silk	Soy, serum, albumin, collagen, gelatin, fibroin, polyamino acids, elastin, fibrin
Lipids/surfactants	Vegetable oils and extractions	Acetoglycerides, waxes, surfactants
Speciality polymers	Vegetable extractions	Lignin, shellac, natural rubber

Limitations of their applications are; nonreproducible productions and variations of isolation from biological sources (batch variation), and their different solubilities [Chen et al., 2005]. Natural biodegradable polymers have been examined in the literature as delivery agents in cancer therapies [Vorhies et al., 2009], scaffolds for cartilage and bone tissue engineering approaches [Lu et al., 2001], or autologous

aortic vascular designs [Shum-Tim et al., 1999] etc. There are several natural polymers used in hard tissue engineering such as; collagen [Zheng et al., 2007], silk fibroin [Altman et al., 2003], alginate [Li et al., 2005], chitosan [Peter et al., 2010] and gelatin [Liu et al., 2009]. In next sections, chitosan and gelatin properties will be examined to explain the reasons of their usages in this project.

The other type of biodegradable polymers is synthetic polymers. The most commonly used synthetic biodegradable polymers are polyesters such as; poly (glycolic acid) (PGA), poly(lactic acid) (PLA), poly(lactic acid-co-glycolic acid) (PLGA) copolymers, poly(L-lactide), poly(trimethylene carbonate) (PTMC) copolymers, poly(hydroxybutyrate) and poly(3-hydroxybutyrate-co-3-hydroxyvalerate) (PHBV) in tissue engineering approaches. The reasons of increasing number of tissue engineering researches on polyesters are their easy degradation by hydrolysis of ester linkages and resorbable degradation products. However, this easy and fast degradation may result with sudden mechanical strength loss of polyester based scaffolds, which is an undesirable reaction in tissue engineering applications [Gunatillake et al., 2003]. A number of other polymers such as; poly(dioxanone), poly( $\xi$ -caprolactone) (PCL) homopolymers and copolymers are also examined as scaffold materials. For example, in a recent study, it was validated that PHBV implants in the rat tibia defects resulted with induced mild tissue with bone deposition without any fibrous tissue formation at 4 weeks post surgery [Wu et al., 2009]. Moreover, PCL/PLGA blend scaffolds showed no cytotoxic effect and great cell proliferation as promising tissue engineering materials for further studies [Lucchesi et al., 2010].

#### ***1.2.1.1.2 Bioceramics***

Ceramics are defined as highly crystalline, inorganic materials bonded with combination of ionic, covalent and metallic bonds [Carter 2007]. Ceramics that are designed and fabricated for the repair and reconstruction of diseased and damaged part of the body, are called as bioceramics.

In orthopedic applications, bioceramics have great advantages. For instance, they release negligible amount of ions and cause less aging effect reducing wear rate [Chevalier 2009]. Hydroxyapatite (HA) ( $\text{Ca}_{10}(\text{PO}_4)_6(\text{OH})_2$ ), Bioglass<sup>®</sup> ( $\text{Na}_2\text{O}-\text{CaO}-\text{SiO}_2-\text{P}_2\text{O}_5$ ),  $\beta$ -tricalcium phosphate ( $\beta$ -TCP) ( $\text{Ca}_3(\text{PO}_4)_2$ ) and bioactive glasses are attractive bioactive ceramics used in bone tissue engineering studies because of the lack of encapsulation problem seen in most of the other bone implants [Kokubo et al., 2003].

Some examples of bioceramics used in biomedical applications are summarized in Table 3 [Thamaraiselvi and Rajeswari et al., 2004].

Table 3 Bioceramics with different types, medical devices and functions.

Types	Devices	Function
Dense hydroxyapatite, $\text{Al}_2\text{O}_3$ , Bioglass, vitreous carbon	Osseous tooth replacement implants	Replace diseased, damaged or loosened teeth
High-density alumina, metal bioglass coatings	Artificial total hip, knee, shoulder, elbow, wrist	Reconstruct arthritic or fractured joints
Dense-apatite, Polytetra fluoro ethylene (PTFE)-carbon composite, porous $\text{Al}_2\text{O}_3$ , bioglass,	Alveolar bone replacements, mandibular reconstruction	Restore the alveolar ridge to improve denture fit

In 1971, the first observation of chemical bond formation between hydroxyapatite crystals and bone has been reported [Hench et al., 1971]. After this proof, it was suggested that bioactive ceramics like hydroxyapatite induce bond formation between implanted material and surrounding osseous tissue and enhance bone tissue formation. *In vivo* and *in vitro* studies focusing on the examination of bone-bioceramic bond formation summarized the progress as; dissolution, precipitation

and ion exchange [El-Ghannam et al., 1997] accompanied by adsorption and incorporation of biological molecules [El-Ghannam et al., 1999]. It was also stated that bioactive ceramics such as: HA or TCP are excellent materials for stimulation of cells for bone repair in tissue engineering approaches [Duchenyne et al., 1999]. One of the most attractive characteristics of bioactive ceramics in tissue engineering applications is their controlled bioresorption rates that can be controlled by their chemical structures [Hench et al., 1997].

### ***1.2.1.1.3 Biocomposites***

For tissue engineering applications, polymers are ductile and not rigid enough, and ceramics are too stiff and brittle. Therefore, combinations of polymers with bioceramics can provide improved mechanical and biological properties with desired stiffness elasticity and porosity required for tissue engineering approaches. So, in many recent studies, ceramics like hydroxyapatite or tricalcium phosphate have been added into the polymeric scaffolds to produce biocomposite constructs [Supova, 2009].

There are tremendous number of studies that aim to fabricate biocomposites for successful bone tissue engineering approaches. For instance, in a recent study, 3-D scaffolds prepared by lyophilization of the mixtures of chitosan and bioactive glass particles, indicated great biocompatibility towards MG-63 cells with high amount cell spreading and it was reported that these types of biocomposites have great potential to be used in tissue engineering applications without any cytotoxic effect [Peter et al., 2010]. In another recent research, it was investigated that porous PHBV-hydroxyapatite composite scaffolds prepared by modified thermally induced phase-separation technique, showed improved stiffness, strength, and *in vitro* bioactivity with addition of HA by controlling the surface characteristics and porosities of the samples. As a result, it was reported that these novel PHBV-HA composite scaffolds may be served as promising three-dimensional structures in bone tissue engineering applications [Jack et al., 2009]. Furthermore, calcium phosphate/collagen structures as chondrocyte carriers [Kose et al., 2004], nano-

hydroxyapatite incorporated poly(L-lactic acid) scaffolds as bone tissue engineering scaffolds [Wei et al., 2003], two-dimensional biodegradable polyester constructs with  $\beta$ -tricalcium phosphate as guided bone regeneration materials [Kikuchi et al., 2004] are some of the successful examples studied biocomposites for bone tissue engineering approaches.

### ***1.2.1.2 Scaffold Preparation Techniques***

Properties of final scaffold products strongly depend on their preparation techniques. Pore size and surface characteristics are the most important properties that are affected from scaffold preparation method as they are shown in Figure 1 [Yilgor et al., 2008, Ulubayram et al., 2002, Yucel et al., 2010, Zhang et al., 2004].

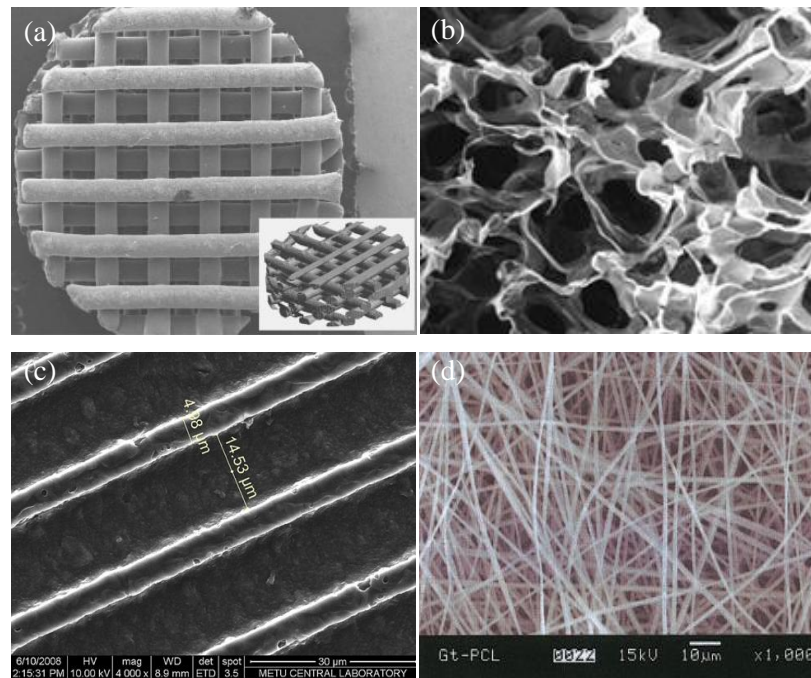


Figure 1 Scanning electron microscope micrographs of (a) poly( $\xi$ -caprolactone) based rapid prototyped 3-D scaffold (b) gelatin-based scaffolds prepared by freeze-drying method (c) micropatterned polymeric films obtained from the PDMS replica of the Si template (d) electrospun fiber morphologies of gelatin/PCL.

There are various types of scaffold preparation techniques and some of them can be classified as; solvent casting with or without particle leaching, membrane lamination, peptide self assembly, phase separation, freeze-drying, electrospinning, 3-D micro plotting, rapid prototyping, micro patterning, melt molding, extrusion, and fiber bonding.

Different preparation methods give the chance to create scaffolds with different desirable shapes and dimensions. Surface modifications, porosity control, pore wall thicknesses are some of the parameters that can be varied with preparation processes depending on the need in the application area.

All of the scaffold production methods has some advantages and disadvantages as summarized in Table 4 [Yang et al., 2001, Ma et al., 2006 and Murphy et al., 2007] and different forms of materials such as; fibers, porous structures, hydrogels and membranes may be obtained by these fabrication methods.

Stabilities of the produced scaffolds must be provided for desired time periods because these engineered materials must support cell growth on themselves in aqueous media and be stable as the cells grow and then decompose in extended periods. Crosslinking processes can be applied to enhance the stabilities of easily soluble tissue engineered scaffolds by some physical and/or chemical modifications. In this study, solvent casting and freeze-drying techniques and crosslinking process are used to fabricate 2-D and 3-D chitosan-gelatin/hydroxyapatite composite structures and therefore these techniques will be discussed in the following sections.

Table 4 Polymeric scaffold processing methods with advantages and disadvantages.

Processes	Advantages	Disadvantages
Solvent casting and particulate leaching	Controlled porosity up to 93%	Lack of mechanical strength for load-bearing tissue
Membrane lamination	3-D porous matrix	Lack of mechanical strength for load-bearing tissue
Peptide self assembly	Control of porosity, fiber diameter, bioactive degradation products	Expensive, complex design parameters, limited micro-size and mechanical properties
Phase separation	Keeping of molecular activity	Lack of scaffold morphology control
Freeze-drying	High porosity and interconnectivity	Surface skin formation depending on the process conditions, time consuming
Electrospinning	Control of porosity and pore size and fiber thickness	Pore size decrease because of fiber thickness, limited mechanical properties
3-D micro plotting	Design-based, good mechanical properties	Very smooth surface that may be undesired for cells attachment
Rapid prototyping	Complex geometries and very fine structures, controlled porosity, medical scan	Expensive, limited polymer types
Micropatterning	Guided spatial organization of cells	Only for 2-D constructs
Melt molding	Lack of harsh organic solvent	Risk of degradation and inactivation of molecules because of high temperature
Extrusion	Control of porosity	Limited mechanical properties, risk of degradation and inactivation of molecules because of temperature
Fiber bonding	Simplicity	Lack of porosity control



### ***1.2.1.2.1 Solvent Casting Method***

Solvent-casting is a well-known polymeric film production technique and it has been widely used in tissue engineering studies to prepare two-dimensional scaffolds. In solvent-casting method; polymers are dissolved in a solvent and the prepared polymer solution is casted into a mold as thin layer and then dried at room temperature on shelf or in an oven for evaporation of the solvent. Solvent evaporation rate marginally affects the structure of the casted film [Bu et al, 2002]. There are several advantages of this technology such as; low cost, uniform thickness distribution and extremely low haze which are very important properties for scaffold surfaces [Siemann et al, 2005].

### ***1.2.1.2.2 Freeze-drying Technique***

Freeze-drying is based on freezing of the prepared polymer solution to form solid solvent crystals in the construct and then, removing these solid crystals by sublimation, which leave empty interconnected pores through the scaffold, with maximum 90% porosities. Freezing time and annealing stage are critical points that control the porosity level of freeze-dried material [Murphy et al., 2007]. To prevent collapse of freeze-drying sample or any back melting, there must be a balance between heat transfer and solvent sublimation [Rey et al., 2004]. If, freezing time is too short and uncontrollable, scaffolds with heterogeneous porosity are obtained because of non-uniform nucleation and growth of solvent crystals.

Different pore sizes may be observed in the regions that are called as hot spots where the contact between the sample dish and freeze-dryer shelf is poor. These points formed as a result of less heat conduction and augmented temperature of sample [O'brien et al., 2004].

### ***1.2.1.2.3 Crosslinking Process***

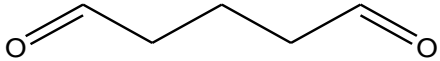
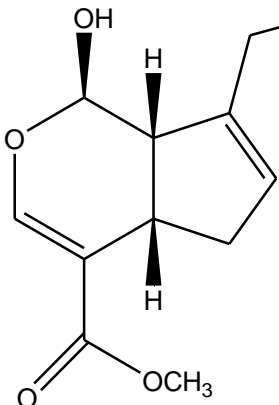
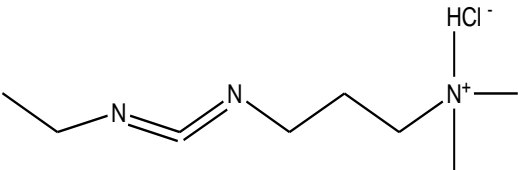
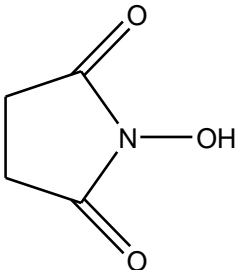
Crosslinking is mostly needed for chemical or physical modifications of biodegradable polymeric scaffolds because degradability of the biomaterials must be extended to the desired time period before the implantation process. If the polymeric construct does not have a suitable degradation period for the applied region of injured tissue, healing process within the scaffold application may be unsuccessful. If the degradation rate is too fast, the scaffold will disappear before complete healing. If it is too slow, matrix will stay in the applied area more than needed. This rate can be adjusted by the type and the amount of crosslinkers used. There are many different crosslinking agents used as stabilizing agents of natural biodegradable polymeric constructs such as; glutaraldehyde, genipin, 1-ethyl-3-(3-dimethylaminopropyl)-carbodiimide (EDC) and *N*-hydroxysuccinimide (NHS) (Table 5).

The major advantages of water-soluble amide-type crosslinkers such as; 1-ethyl-3-(3-dimethylaminopropyl)-carbodiimide (EDC) and *N*-hydroxysuccinimide (NHS) are their lower toxicity and better compatibility with respect to other crosslinkers [van Wachem et al., 2001].

Another attractive property of EDC/NHS is the absence of additional chemical entities that are incorporated into the matrix at the end of the process.

In EDC/NHS crosslinking reaction carboxyl groups of the matrices are usually activated with EDC in the presence of NHS and the activated carboxyl groups then react with nucleophiles, such as primary amine groups, to form stable zero-length amide bonds with increased stability [Rafat et al., 2008]. EDC activated reaction mechanisms are given in Figure 2.

Table 5 Chemical structures of crosslinkers.

Crosslinking Agent	Chemical Structure
Glutaraldehyde	
Genipin	
1-ethyl-3-(3-dimethylaminopropyl)-carbodiimide	
<i>N</i> -hydroxysuccinimide	

Recently, it was proposed that in addition to amide bond formation, ester links are also formed between activated carboxyl groups and hydroxyl groups [Everaerts et al., 2008].

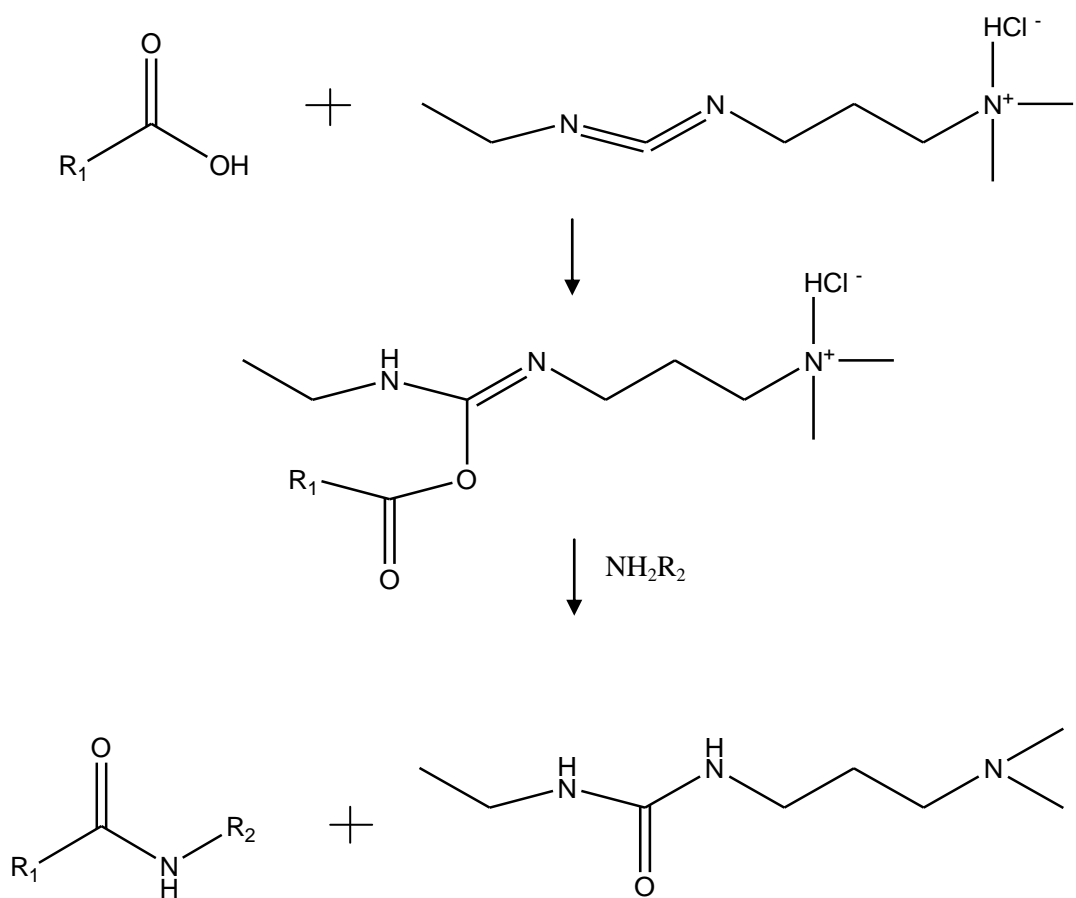


Figure 2 Reaction mechanisms of carboxylic group activation by EDC and amide bond formation with amine addition.

It was reported that EDC/NHS crosslinking has resulted with higher modulus of elasticity and stability in gelatin based scaffolds compared to glutaraldehyde crosslinked constructs [Ulubayram et al., 2002].

### 1.2.2 Active Molecules

The extracellular matrix (ECM) contains various complex structures and macromolecules to maintain the cells viabilities. Many different signaling

molecules are found in ECM providing cell-cell, cell-ECM interactions for cell migration, proliferation and differentiation. Some signaling compounds are growth factors and they stimulate and guide the cell behavior with different signal transduction pathways. These active molecules can be incorporated to the implanted sample to enhance the cell attachment on the scaffold materials by physical adsorption or chemical bonding. Glycosaminoglycans (GAGs), proteoglycans and adhesive proteins are the main types of ECM elements that may be used to enhance cell attachment [Rosso et al., 2004]. Some of these proteins that contain Arginine-Glycine-Aspartic acid (RGD) like sequences are highly preferred in tissue engineering applications to increase the cell attachment on the scaffold surface by these cell recognition sites. Cell membrane components integrins, that provide cell-environment communication bind to these RGD groups on the material surface and provide improved cell adhesion. There are various studies that aimed to immobilize RGD sequences on the scaffold surfaces. For example, it was reported that chitosan-alginate-hyaluronan based scaffolds were modified with covalent attachment of RGD-containing proteins. After cell seeding process, these modified complexes showed neocartilage formation and when they were implanted into the damaged rabbit knee cartilage, they demonstrated repair of tissue in one month [Hsu et al., 2004].

The other commonly used bioactive molecules used in tissue engineering applications are transforming growth factor  $\beta$ 1 (TGF- $\beta$ 1) in new cartilage tissue formation [Guo et al., 2007], vascular endothelial growth factors (VEGF) in cardiac tissue engineering [Sheridan et al., 2000], basic fibroblast growth factor (bFGF) in adipose tissue regeneration [Kimura et al., 2003], epidermal growth factor (EGF) in the design of new biomimetic constructs [Imen et al., 2009] and platelet-derived growth factor (PDGF) in periodontal applications [Zhang et al., 2007].

### **1.2.3 Cells**

In tissue engineering, the reason of cell addition into the polymeric carrier is to expand the cells under *in vitro* conditions on this scaffold material and to enhance *in vivo* tissue regeneration because the defect site is not left empty to heal but rather filled with a substitute tissue which is already actively healing. Cell number and cell type are chosen by taking into consideration the application area, regeneration ability of cells and repair mechanism of the damaged tissue site [Carole et al., 2000].

Cells, added on the construct can be from patient's own body (autograft), from another human (allograft) or from an animal donor (xenograft). These cells can be mature cells or stem cells of various levels of development.

In recent studies, stem cells, such as human amniotic fluid-derived, adipose-derived, umbilical cord and bone marrow stem cells, gained much attention in biomimetic strategies because of their potential to differentiation into the desired cell type with some stimulants [Liao et al., 2008]. For example, it was reported that mesenchymal stem cells seeded onto porous hydroxyapatite scaffolds along with bioactive agents demonstrated enhanced bone and cartilage tissue formation [Yoshikawa et al., 2005].

In general, in simple tissue engineered approaches more concentrated on scaffold development, cells used are generally cell lines. For this purpose, certain types of cells that are harvested from the tissue of a living system, are proliferated and maintained to form first subculture, a monolayer. The system rising from the outgrowth of this primary monolayer is called as cell line [Freshney et al., 2006]. Cell lines have great advantages such as they are easy to produce and handle, well characterized, have less tendency to phenotypic problems than their primary cells. Human osteosarcoma cell lines SaOs-2 and MG-63, fibroblast 3T3 and mouse calvaria MC3T3-E1 cell lines are some of the most popular cell lines used in bone and skin tissue engineering studies.

Moreover, vascular endothelial cells, myoblasts, chondrocytes and kidney cells are other cell types widely used in tissue engineering approaches [Malafaya et al.,

2007]. For instance, it was proved that endothelial cells enhanced vascular smooth muscle cell adhesion and spreading after coculturing in porous polyethylene terephthalate membranes. This result showed that endothelial cell seeded scaffolds have great potential to use in vascular grafts [Wang et al., 2007].

Cell attachment and adhesion are critical steps in tissue engineering approaches. Former is known as a short-term event involving physicochemical interactions like van der Waals and ionic interactions between the cell and the material surface. However, cell adhesion is a longer-term process dependent on several environmental factors such as signal transduction promoting the action of transcription factors and gene expression regulated by biological agents [Anselme et al., 2000]. Therefore, choice of the cell type and material is very critical to obtain a successful tissue engineering approach.

In brief, tissue engineered scaffolds loaded with cells can be implanted into the defect site for the new tissue formation, and gradual degradation of the scaffold material is required and the formed metabolites should not cause any immune response or other cytotoxic effect.

Based on the organ systems, tissue engineering may be subdivided either by organ systems (such as hepatic tissue engineering, cardiac tissue engineering) or by tissue properties (such as hard tissue engineering and soft tissue engineering) or by strategies (aim to replace a metabolic or a structural function) [Saltzman et al., 2004]. In the following sections, hard tissue engineering will be explained as this study aims at producing the two-dimensional (2-D) and three-dimensional (3-D) matrices prepared for hard tissue engineering applications.

### ***1.3 Hard Tissue Engineering***

According to 2006 research results over 1.5 million people suffer from bone related diseases in the world [White et al., 2006]. Since the regeneration of bone tissue is limited, there have recently been extensive research efforts on developing new technologies and strategies specifically employing hard tissue engineering.

Hard tissue engineering has emerged to regain the properties of the defected bone as an alternative approach to tissue transplantation methods that have problems such as; immune response or tissue rejection in allografting and donor site limitation in autografting [Naughton et al.,1995, Mizutani et al, 1990 and Moore et al.,1984].

Two different forms of hard tissue are found in the bone; cancellous bone (trabecular) containing pores, and compact bone (cortical) made up of protective outer shells. Bone tissue also contains two main phases; organic phase formed by type I collagen and glycosaminoglycans giving tensile strength to bone tissue, and inorganic phase including hydroxyapatite-like minerals providing higher compressive strength for bone structure. Combination of these different phases provides highly improved mechanical property to the natural bone.

Osteogenic precursor cells (bone lining cells), osteoblasts, osteoclasts, osteocytes, and the hematopoietic (blood cell production) elements of bone marrow are the cellular components of bone [Anderson et al., 2000]. Precursor cells are inactive cells but remodeling of bone tissue with osteoblast production and new bone matrix mineralization creates a living environment in bone tissue. Osteocytes maintain the bone matrix and osteoclasts resorb this matrix [Marks et al., 2002]. Living bone tissue acts as a dynamic tissue and healing of bone proceeds with dynamic mechanisms of bone deposition, resorption and remodeling. Different hormonal and pathological effects also have influences on new bone formation [Kalfas et al., 2001]. Because of the diversity of bone structure and the variations of effects on healing process, the design of tissue engineered material becomes very complicated. Although, there exist some difficulties in clinical applications, healing of bone fractures in 6 months by the help of tissue engineered implants has been reported [Quarto et al., 2001].

Hard tissue engineering components have different characteristics depending on the properties of bone tissue. Thus, the following sections will focus on the characteristics of these components used in hard tissue engineering.



### 1.4 Components of Hard Tissue Engineering

In hard tissue engineering approaches; similar to the other tissue engineering applications; there exist three main components; scaffolds, active molecules and cells that are chosen according to their availabilities for the required bone healing application.

*In vitro* bone tissue engineering aims to expand the cells in the scaffolds (which either contains ceramic particles or not) and to use these scaffolds as filling material in the defected bone region as described in Figure 3.

Furthermore, there are other interesting hard tissue engineering approaches in which *in vivo* bone tissue engineering is aimed and the cells are expanded in the body on the osteoinductive scaffolds, using the body as a bioreactor. Then this cellularized construct is implanted into the defected tissue site in the same body, resulting with tissue regeneration [Bao et al., 2008].

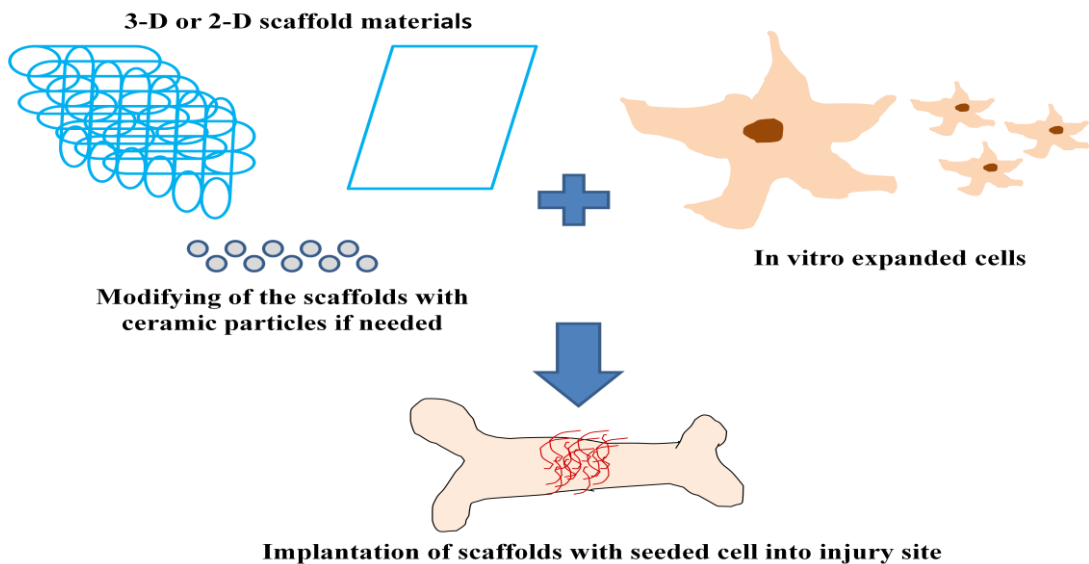


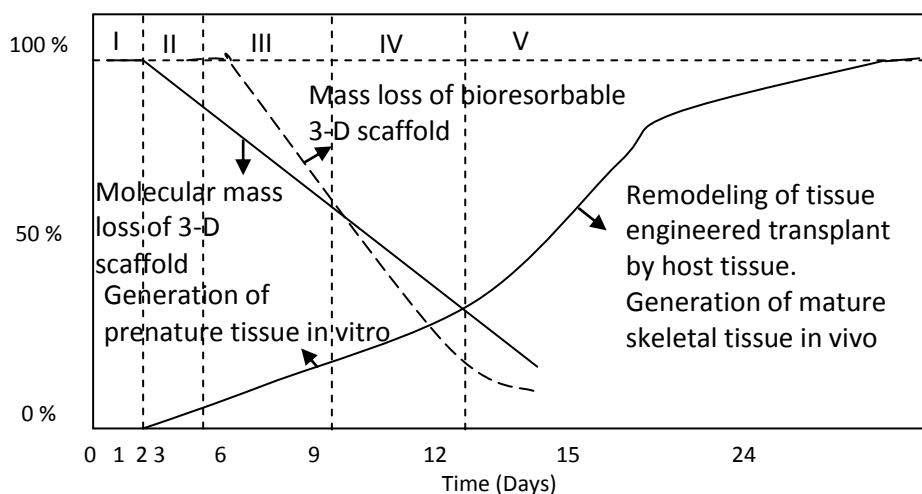
Figure 3 Bone regeneration by using scaffolds and seeded cells.

There are different successful approaches that aim to induce bone tissue formation by scaffold application such as; using of micropatterned two-dimensional biodegradable polymeric structures [Kenar et al., 2006]. In a recent study, collagen-polysaccharide based porous scaffolds were fabricated with two different layers. One side of this layer stimulates cartilage growth and the other side contains calcium phosphate to stimulate bone growth in defected tissue site. So, this approach has a great potential to use in knee implants [Gibson et al., 2009 ].

#### ***1.4.1 Scaffolds in Hard Tissue Engineering***

Two-dimensional and three dimensional constructs known as scaffolds; provide the needed environmental conditions for initial cell adhesion and subsequent proliferation in hard tissue engineering applications and the design of these constructs affects the shape of the regenerated tissue.

Scaffold properties such as; surface chemistry, mechanical similarities to bone tissue, biodegradability depending on the material chemistry, and biocompatibilities of degradation products, are very important factors for successful hard tissue engineering approach. For biodegradable constructs; controlled degradation also is needed because scaffolds must retain their physical properties for at least 6 months in defected bone tissue site. Otherwise, scaffold may degrade before the complete healing process causing some unfilled regions in the bone tissue as it is seen in Figure 4 [Hutmacher et al., 2000]. Figure 4 shows the mass and weight loss of the scaffold and remodeling of the healing tissue as a function of time.



- I Hydration  
 II Hydration and Degradation  
 III Degradation and Mass Loss  
 IV Resorption and Metabolization  
 V Metabolization

Figure 4 Graph of mass and weight loss of the scaffold versus time for bone/cartilage tissue engineering approaches.

Chemical structure and molecular weights of polymers, and crystallinities of ceramics are the main parameters that affect the resorption kinetics and degradation rate of scaffolds. Pore sizes of the hard tissue engineered scaffolds may have influences on mechanical properties of the sample. Thus, pore sizes with the range of 100-500  $\mu\text{m}$  are supposed to be ideal for new vessel formation through the matrix maintaining the mechanical strength of the material in a required range in hard tissue engineering applications.

#### ***1.4.1.1 Scaffold Materials in Hard Tissue Engineering***

There are various raw materials used in scaffold preparation for bone tissue engineering because of the importance of scaffold chemistry. These materials can be classified as; natural or synthetic biodegradable polymers, ceramics and

composites of these materials and their harvested forms with natural extracellular matrices [Badylak et al., 2002] in different forms like; microparticles, hydrogels, fibers, 3-D porous or 2-D membranes. Although there is an intense research in this area; there is still need for the investigations and improvement of novel materials with required properties such as; biocompatibility, biodegradability, and mechanical strength for clinical applications [Malafaya et al., 2007]. In recent studies, some natural polymers such as; chitosan and gelatin with high resemblance to bone tissue and great mechanical behaviors have been the subject of great interest. Ceramics, like hydroxyapatite, that mimic the inorganic part of the bone tissue, are also candidate materials for scaffold materials in hard tissue engineering. Properly designed composites of these two types of materials; natural polymers and ceramics, can provide highly improved mechanical and biocompatible properties in bone tissue engineering applications.

So, in the following sections natural biodegradable polymers; chitosan and gelatin, bioceramics; hydroxyapatite will be discussed in details to explain the reasons of their usages in this project.

#### ***1.4.1.1.1 Chitosan***

Chitin, (the second most abundant polysaccharide after cellulose), is produced by the removal of proteins and the dissolution of  $\text{CaCO}_3$  that exist in crab shells and cell walls of fungi. Chitosan is obtained by NaOH treatment of chitin at  $120^\circ\text{C}$  for 1-3h to produce deacetylated chitosan and formed by  $\beta$ -(1-4) linked D-glucosamine residues with *N*-acetyl-glucosamine groups (Figure 5). Deacetylation value of chitosan can change between 30% and 90% and molecular weight may vary from 300 to 1000 kD [Madihally et al., 1999].

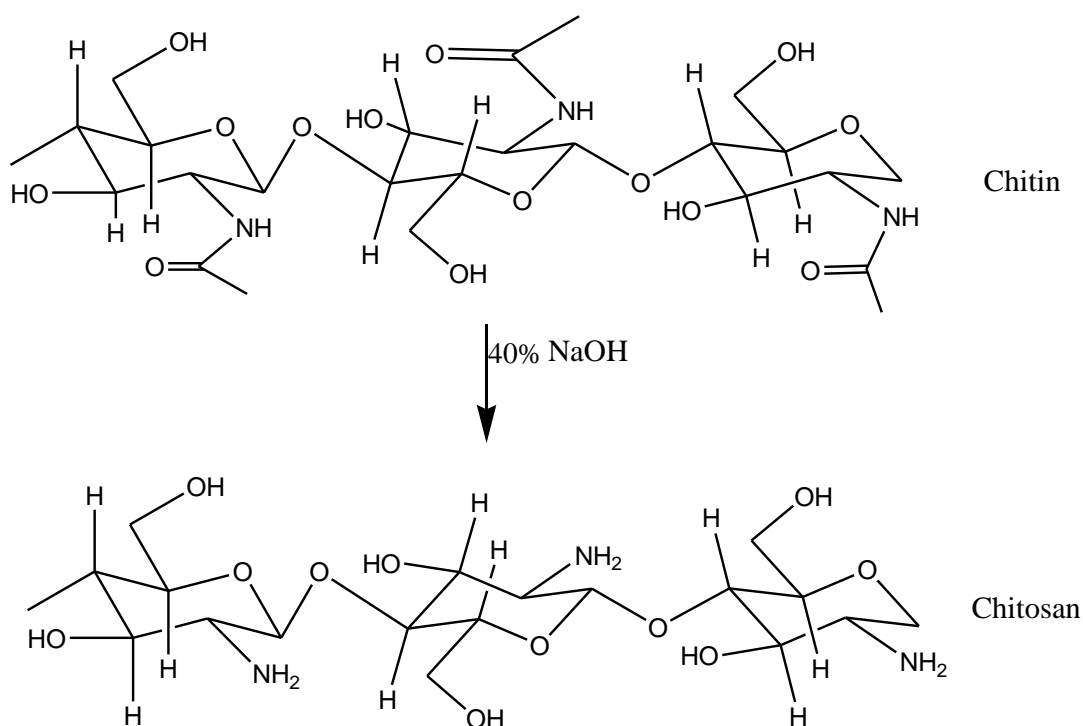


Figure 5 Derivation of chitosan from chitin.

Deacetylation of chitosan implies the change of acetyl groups of chitin to primary aliphatic amino groups in chitosan structure. Chitosan can react with other polymers through N-acetylation and Schiff reactions [Kumar et al., 2000]. *In vivo* degradation of chitosan takes place by lysosyme enzyme, and with an inverse proportality highly depends on the deacetylation degree and crystallinity of chitosan [Di Martino et al., 2005], as well as pH of the preparation solution [Davies et al., 1969].

Chitosan is insoluble in water or in solutions with pH above 7, but it is soluble in acidic environment with the help of the protonated free amino groups on glucosamine. Acetic acid is most commonly used solvent of chitosan [Dornish, 2001]. Studies on chitosan has displayed that it enhances osteogenesis [Klokkevold et al., 1996], osteoconductivity [Tang et al., 2008], and has scar reducing ability in soft tissue [Ishihara et al., 2002]. It is also indicated in the literature that chitosan has hemostatic [Ong et al., 2008], fat binding [Gades et al., 2005], wound healing

[Muzarelli et al., 1977, Hiroshi et al., 2001], bioadhesive [George et al., 2006], antimicrobial properties [Rabea et al., 2003, Zivanovic et al., 2007, Sarasam et al., 2008] and it is biologically renewable [Khor et al., 2003].

Since its reactive functional groups bind to drugs and it has non-toxic metabolites [Suheyla et al., 1997], chitosan has been applied to a wide range of tissue engineering approaches such as; gene [Dang et al., 2006] or drug delivery for controlled release of bioactive agents as micro- or nano- particles [Agnihotri et al., 2004], antimicrobial agent against several viruses and bacteria types [Rabea et al., 2003], additive for enrichment of bone cements [Rochet et al., 2009], scaffolds for soft tissue engineering applications [Wang et al., 2005]. In addition, Seol et al. reported that freeze-dried chitosan scaffolds showed sufficient histological results cooperated *in vitro* bone formation with seeded rat osteoblasts [Seol et al., 2004].

Limitations of chitosan are its low degradation rate and brittleness. To overcome these difficulties, blending with ceramics and/or polymers has been investigated in recent studies [Hong et al., 2009]. For example, in bone tissue engineering approaches; calcium phosphate cements displayed enhanced mechanical properties and biocompatibility with addition of chitosan [Xu et al., 2005]. Moreover, since chitosan has a positively charged nature, its polyelectrolyte formation ability with anionic polymers is an attractive point in chitosan-based blend structure formation. For instance, chitosan-alginate hybrid porous structures showed great stability, extended mechanical property and great cell affinity toward the osteoblast cells due to ionic interactions [Li et al., 2005], polyacrylic acid-chitosan polyelectrolyte complexes with HA particles also have been examined and the results revealed that human osteosarcoma cells showed good attachment and spreading [Sailaja et al., 2006]. Since this type of structures can be modified in physicochemical manner by changing the mixing ratios and processing techniques of the blend polymers, they are promising candidate materials as hard tissue engineered scaffolds [de Oliveira et al., 2008].

### 1.4.1.1.2 Gelatin

Gelatin is a polypeptide, produced by hydrolytic cleavage of collagen protein [Kuijpers et al., 1999] that is the major constituent of human bone and skin and also animal extracellular matrix [Buckwalter et al., 2005]. It contains 19 amino acids joined by peptide linkages. It contains alanine, arginine, glutamic acid while the major amino acids in gelatin are glycine (30%) and proline/hydroxyproline (25%). Chemical structures of amino acid sequences, and proposed chemical structure of gelatin are given in Figure 6.

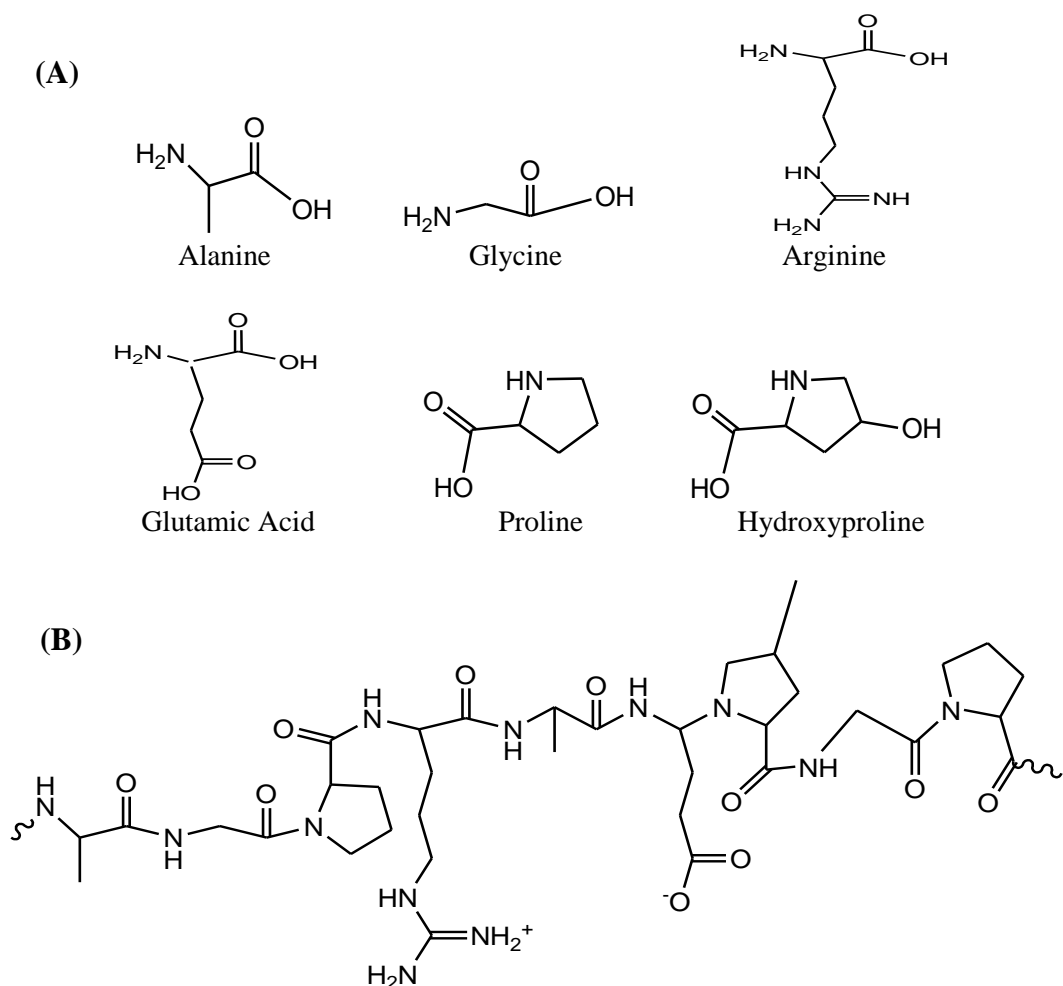


Figure 6 (A) Chemical structures of amino acid sequences, and (B) proposed chemical structure of gelatin.

Collagen has been used in many tissue engineering applications as a scaffold material but it has some limitations such as; potential pathogen transmission, immune rejection, limited handling, insufficient mechanical properties, and poor controlled biodegradability [Ma et al., 2004]. Since gelatin is the denatured form of collagen, it has lower antigenicity property and controllable degradation rate [Yao et al., 2004]. There are different sources of gelatin such as; fish [Norland et al., 1990], bovine [Chomarat et al., 1994] or porcine skins [Huang et al., 2005]. There exist two types of gelatin named with respect to collagen pretreatment method before the extraction process [Djagny et al., 2001]. Type A gelatin extracted and processed by acidic pretreatment from collagen, and Type B obtained by alkaline pretreatment converting glutamine and asparagine residues into glutamic and aspartic acid, resulting with higher carboxylic acid content than Type A [Johns et al., 1977]. Alkaline treatment causes hydrolysis of amide group of collagen and negatively charged gelatin is obtained with higher amounts of carboxyl groups. So, these chemical features facilitate the interaction of gelatin with positively charged molecules to form polyion complexes [Tabata et al., 1998].

The most attractive property of gelatin for tissue engineering is; its Arg–Gly–Asp (RGD)-like sequence that enhances the promotion of initial cell adhesion on the gelatin based scaffolds [Ito et al., 2003]. Gelatin is water-soluble and degrades *in vivo* very fast [Rohanizadeh et al., 2008]. Therefore, crosslinking agents like gluteraldehyde [Martuccia et al., 2006], genipin [Bigi et al., 2003] or carbodiimides [Everaerts et al., 2008] are used to stabilize gelatin structures prolonging its existence in application area.

Gelatin can be hydrolyzed by a variety of the proteolytic enzymes to yield its constituents of amino acid or peptide components. This nonspecificity is a desirable factor in intentional biodegradation [Kumar et al., 1981]. Reasons of arising studies on gelatin as scaffold material are its biodegradability and biocompatibility of itself and side products. Other major advantages of gelatin are; its plasticity, low immunogenicity, adhesiveness and low cost [Young et al., 2005].



Gelatin-based blend biomaterials have been widely investigated in preparation of microspheres of controlled release of bioactive agents [Defail et al., 2006]. It was reported that successful gelatin-based scaffolds with adipose-derived and muscle-derived stem cells for cartilage and bone tissue engineering were achieved [Guilak et al., 2004, Suna et al., 2005]. In another study, it was suggested that gelatin-based structures modified with nano-hydroxyapatite particles showed osteoblast stimulations [Kim et al., 2005]. There exist many other tissue engineered constructs based on gelatin such as; artificial skin substitutes [Kawai et al., 2000], scaffolds for cardiac tissue engineering [Rosellini et al., 2009] and wound dressing material [Ulubayram et al., 2001]. Gelfilm<sup>®</sup> and Gelfoam<sup>®</sup> are commercial gelatin-based two-dimensional and three-dimensional tissue engineered constructs produced by Pfizer company for hemeostatic devices or absorbable implants in neurosurgery and thoracic or ocular surgery [Pfizer Co., 2007].

#### ***1.4.1.1.3 Hydroxyapatite***

Hydroxyapatite ( $\text{Ca}_{10}(\text{PO}_4)_6(\text{OH})_2$ ) has a chemical structure and crystallography very similar to the inorganic component of the bone tissue, so it has attracted much attention in bone tissue engineering studies.

As it is seen from the Figure 7 [Manafi et al., 2008], in crystalline structure of HA,  $\text{PO}_4^{3-}$  molecules are in tetrahedral form and  $\text{Ca}^{2+}$  ions and  $\text{OH}^-$  ions exist in space and along the c-axis, respectively.

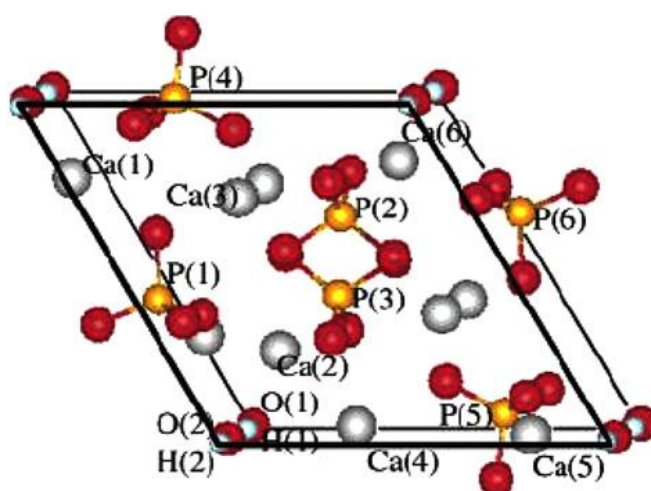


Figure 7 Crystallographic structure of hydroxyapatite viewed along the c-axis.

Calcium and phosphate precursors such as calcium acetate-triethyl phosphate, calcium nitrate-diammonium nitrate, calcium carbonate-di-ammonium hydrogen phosphate can be used to develop hydroxyapatite phases. There are different methods for synthesis of HA such as dry and wet methods (precipitation), hydrothermal method and mixed material preparation conducted with mechanochemical milling treatment [Mamoru et al., 2003]. Wet method which is the most popular HA synthesis, is based on the slow precipitation reaction between calcium and phosphate precursors under controlled pH. Hydrothermal technique uses high temperatures and pressure for HA synthesis reaction. In general, HA synthesis proceeds with sintering process which means heat treatment at 800-1000°C increasing the crystallinity of the synthesized HA [Gerike et al., 2006]. It was reported that 3-D porous scaffold materials obtained by impregnating a polyurethane sponge with HA particles, followed by burning the sacrifice polymeric template and sintering the final HA porous structure. Then, these constructs has demonstrated bioactive and biocompatible behaviors towards the mouse lung fibroblasts [Oliveira et al., 2009]. However, sintering has some limitations; it decreases the biodegradability of HA with high crystallinity. It was reported that, commercially available non-sintered HA based bone substitute Nanobone<sup>®</sup> showed

better histological results and vascularized tissue growth compared to encapsulated sintered HA particles [Abshagen et al., 2009].

Hydroxyapatite has three available forms; dense blocks, porous blocks, and granules. However, each of these forms has some limitations: Dense HA problems arise from manufacturing with large-scale fracture and granules migration in the body is uncontrollable macroporous HA has a ragged surface [Shareef et al., 1993]. Composite materials, obtained by HA incorporation into natural polymeric network, may eliminate these problems and provide convenient environment with basic resorption products of HA buffering acidic by-products of polymers such as; polyesters [Shikinami et al., 1998].

The dissolution rate of synthetic HA mainly depends on the type and concentration of the buffered or unbuffered solutions, pH of the solution, degree of the saturation of the solution, solid/solution ratio, the composition and crystallinity of the HA phase [Rezwana et al., 2006]. Another important feature of hydroxyapatite is its bioactivity which is coming from partial degradation property of calcium phosphate leading higher bonding ability between bone and HA. It was stated that augmented initial flash spread of serum proteins gives higher biocompatibility to hydroxyapatite implants as compared to the hydrophobic polymers [Hutmacher et al., 1998]. Hydroxyapatite application increased mainly because of its osteoconductivity [Woodard et al., 2007] and it has started to be used as substitutes for autogenous bone grafts in bone defects [Byrd et al., 1993].

Some of the recent investigations have demonstrated that hydroxyapatite is a convenient bioactive ceramic for improving the properties of polymeric scaffolds. It was reported that chitosan/nano-hydroxyapatite composite constructs, prepared by calcium and phosphate precursors solutions addition into chitosan solution and lyophilization method, have showed improved bioactivity and osteoblast cell differentiation when compared to pure chitosan sponges [Kong et al., 2006]. In another novel study, it was observed that chitosan hydrogel-hydroxyapatite membranes, prepared by wet synthesis of HA on chitosan hydrogel soaking it into calcium and phosphate precursors, demonstrated increased biocompatibility

towards MG-63 osteosarcoma cells [Madhumathi et al., 2009]. In another recent study, gelatin-hydroxyapatite-fibrin hybrid porous scaffolds that release bone morphogenetic protein-2 bioactive agent, indicated non-cytotoxic effects towards human bone-marrow mesenchymal cells and these structures were used to repair critical-size segmental bone defects of rabbit. As a result, it was suggested that gross specimen, X-Ray, bone histomorphology and bone mineral density assay showed that these constructs had good osteogenic capability and repair ability for the segmental bone defect completely in 12 weeks [Liu et al., 2009].

#### ***1.4.1.1.4 Biocomposites of Chitosan-Gelatin/Hydroxyapatite***

Polymeric films and porous 3-D scaffolds that are used in hard tissue engineering applications, need to be raised mechanical properties and higher osteoconductivity. Moreover, bioactive ceramics need improved osteogenicity and osteoinductivity. So, the combination of the polymers and ceramics have gained attention due to the improved mechanical and biological properties [Schnettjer et al., 2003].

Gelatin which is a protein with RGD-like sequences, contains free carboxyl groups on its backbone and has the potential to blend with chitosan which is a polysaccharide, to form a network by hydrogen bonding. There are many different studies focusing on chitosan-gelatin blend scaffolds in hard and soft tissue engineering approaches because both chitosan and gelatin are natural, biocompatible and biodegradable polymers. It was reported that; in chitosan-gelatin film structures prepared by casting of solutions in different ratios and at different temperatures (22°C and 60°C) and plasticized with water or polyols; gelatin addition lowers the crystallinity of chitosan because of chitosan incorporation in gelatin network and dilution effect of gelatin. Moreover, results revealed that increase in the total plasticizer content (water, polyols) of these blends led to higher gas permeability (CO<sub>2</sub> and O<sub>2</sub>) of the structures and lower preparation temperature resulted with higher crystalline gelatin formation [Arvanitoyannis et al., 1998]. In a recent tissue engineering study, researchers tried to fabricate porous chitosan-

gelatin hybrid structures with well-organized fluidic channels and hepatic chambers by combining rapid prototyping, micropatterning and freeze-drying techniques aiming the production of artificial liver. Since hepatocytes (liver cells) lose their characteristics after harvesting from liver, it is hard to create an environment to prolong cell viabilities in tissue engineering approaches but according to the results of this study; chitosan-gelatin based well-defined porous constructs demonstrated enhanced hepatocyte affinity compared to non-defined porous constructs and it was stated that these types of materials could be candidate structures not only for hepatic tissue engineering but also for vascular designs [Jiankang et al., 2009].

In a cartilage tissue engineering study, combined with gene therapy, freeze-dried chitosan-gelatin scaffolds were filled with plasmid DNA encoding transforming growth factor beta-1. Ultimate constructs showed plasmid release for 3 weeks in PBS solution and chondrocytes-specific ECM synthesis [Guo et al., 2006]. Porous 3-D chitosan-gelatin structures were used as controlled released drug delivery constructs against many diseases such as; diabetes and cardiovascular diseases [Dogan et al., 2009, Xiaoyan et al., 2008]. Another interesting design based on chitosan-gelatin blends is the production of contact lenses. It was reported that in solvent-casted chitosan-gelatin blends, while chitosan enhanced mechanical strength and antibacterial activity, gelatin increased the hydrophilicity and gas permeability of the structures [Xin-Yuan et al., 2004]. Optimization of chitosan-gelatin blend preparation conditions is another area that most of the studies focused on. For example, in a study about thermodynamic and kinetic parameters of bilayer chitosan-gelatin porous scaffolds, prepared by freeze-drying technique, it was described that prefreezing temperature has a crucial influence on mono- or bi-layer structure formation. Furthermore, it was reported that the lower the concentration of solution in same volume samples demonstrate, less density, larger pore size and smaller tensile strength on the scaffolds at wet state [Mao et al., 2003]. In another research, for *in vitro* characterization, mechanical behaviors and cell affinities of 2-D and 3-D chitosan-gelatin blends in different ratios towards the fibroblasts and human umbilical vein endothelial cells (HUVECs) scaffolds have been compared.

Results of tensile test in dry conditions exhibited that gelatin addition increased the break stress and stiffness, whereas in wet state an opposite trend was obtained. Furthermore, compression tests in wet conditions indicated that gelatin content increase in 3-D samples increased the stiffness of structures. Cell adhesion analysis demonstrated that 3-D structures showed better fibroblast cell morphologies and higher cell survival. In addition, HUVECs had spherical shape and less cell viability on pure chitosan scaffolds with respect to the chitosan-gelatin blend scaffolds [Huang et al., 2005]. In animal tests of chitosan-gelatin wound dressing sponges with rat models, it was suggested that antibacterial property of chitosan comes from the replacing radical amido groups with positive charge in its molecule chains. So, when hydrogen bonds break between chitosan and gelatin or water, antibacterial effect of structure increases. However, at the same time, formation of new amido bonds may decrease this activity. Thus, there is a critical point that chitosan-gelatin sponges shows the best antibacterial activity affected from the preparation conditions [Deng et al., 2007].

Previous studies have demonstrated that polyelectrolyte complex formation ability of positively charged chitosan and negatively charged gelatin makes them ideal to use as raw material in preparation of scaffold constructs. However, highly improved mechanical property and biocompatibility with bone cells are needed for successful hard tissue engineering application. So, addition of an inorganic ceramics like hydroxyapatite may enhance these properties [Mohamed 2008]. Ceramic/polymer composites have attracted attention mostly in hard tissue engineering. For example, it was reported that, layered silicate montmorillonite addition to chitosan-gelatin composite scaffolds has shown good mechanical property and cell viability for potential hard tissue engineering application [Zheng et al., 2007]. In a recent study, chitosan-gelatin films with sintered micro- and nano-sized HA were prepared by suspension of HA and tris buffer solutions of calcium nitrate-sodium phosphate, respectively. Chemical characterization results of these films revealed that polar interactions between  $\text{Ca}^{2+}$  and OH and  $\text{NH}_2$  groups of gelatin, and hydrogen bonds between OH groups of HA and OH,  $\text{NH}_2$  and COOH groups of chitosan-gelatin

blend are the driving forces in nano-HA and micro-HA formation, respectively. Furthermore, mesenchymal stem cell behavior on these films showed very good biocompatibility and high osteogenic differentiation [Li et al., 2009]. Histological investigations of the 3-D sintered hydroxyapatite/chitosan-gelatin structures that are prepared by phase separation method also have indicated high osteoconductivity and good biocompatibility towards the osteoblast cells [Zhao et al., 2002].

The limitation of highly crystalline sintered HA bone substitutes was observed as the encapsulation problem after 8 months of implantation on pigs. However as-precipitated non-sintered HA based constructs indicated almost complete degradation after 8 months and new bone tissue formation in the defected area [Gerike et al., 2006]. Moreover, clinical applications of non-sintered HA hard tissue substitute in human oral and maxiofacial surgeries resulted without any postoperative inflammatory reaction [Bienengräber et al., 2006]. Therefore, novel approaches like non-sintered HA addition into chitosan-gelatin blends in both 2-D and 3-D forms and optimization of chitosan-gelatin ratio in composite constructs or comparison of chitosan-gelatin structures with non-sintered and sintered hydroxyapatite particles are needed in the literature. Therefore, in order to be sure about the applicability of the products; the effects of chemical composition and type of hydroxyapatite on the physicochemical properties of scaffolds and cell-material interactions must be examined and optimized for successful hard tissue engineering approaches.

#### ***1.4.2 Active Molecules in Hard Tissue Engineering***

In bone tissue engineering applications, differentiation of the cells is very important to achieve new bone tissue formation. Thus, the active molecules that stimulate the differentiation of the cells, may be used and released from the scaffold. To enhance the angiogenesis, growth factors such as; vascular endothelial growth factor or fibroblast growth factor can be added into the scaffolds in hard tissue engineering approaches [Griffith et al., 2002]. Bone morphogenic proteins (BMP) are other

bioactive molecule used in hard tissue engineering because of their crucial role in bone morphogenesis. It was demonstrated that BMP loaded scaffolds have strong efficacy in inducing bone formation [Geiger et al., 2003]. Moreover, viral or non-viral gene delivery is also used in hard tissue engineering with different gene types such as; pBMP-2 genes or TGF- $\beta$  encoding plasmids. For example, Bonadio et al. reported that collagen scaffolds incorporated to the gene (pMat-1) for peptide fragment of human parathyroid hormone (hPTH 1–34) that regulates bone growth, provided new bone formation related to dose of gene [Bonadio et al., 1999].

Initial cell adhesion on the scaffolds has mechanisms including cell membrane and extracellular matrix (ECM) components. In bone matrix, there are several glycoproteins containing integrin-binding arginine-glycine-aspartic acid (RGD) sequences. Thus, scaffold materials with RGD-like sequences may have advantages like enhancement of cell affinities. It was reported that hydroxyapatite surfaces with Arginine-Glycine-Aspartic Acid (RGD) sequence modification showed improved osteoblast-like cell adhesion compared to unmodified substrates [Kilpadi et al., 2003].

### ***1.4.3 Cells in Hard Tissue Engineering***

Bone tissue engineering is based on the osteogenic cell-based therapy for the orthopedic diseases [Xia et al., 2004]. For successful bone tissue engineering, precursor cell differentiation and extracellular matrix formation are essential [Ignatiusa et al., 2005].

Osteoblast cells, that are present in bone matrix, are the main elements in bone remodeling process. Proliferation and differentiation ability of osteoblast-like cells on monolayer and 3-D porous collagen-based scaffolds also have been shown [Wiesmann et al., 2003]. The other reasons of osteoblast usage in tissue engineering experiments are their extracellular matrix production ability and mineralization [Brunette et al., 1999].



One of the most known cell lines used in bone tissue engineering studies, is the osteosarcoma cell line SaOs-2 cells. Malignant bone tumors are called osteosarcomas and consist of cells with abnormal cellular functions like immortality [Pautke et al., 2004]. This property is an advantage for studying material-cell interactions because these cells are easier to handle even though they do not always behave as the osteoblasts do. Studies of the cells on 3-D composite constructs showed that, chemical composition, porosity and pore size of the scaffold influence SaOs-2 cell growth and morphology. It was also shown that cell ingrowth into pores was possible in all scaffolds that have pores with diameters of 200-1000  $\mu\text{m}$ . It was also reported that chemical compositions of composites with different ion percentages led to different differentiation ability and solvent dehydrated bone was the most clinically applicable one when compared to tricalcium phosphate and bioglass [Mayr-Wohlfart et al., 2001]. Moreover, it was suggested that osteoblasts seeded on porous lactide- and glycolide-based constructs showed three-dimensional tissue formation with great similarity to natural bone in 12 weeks and claimed that these biodegradable polymeric constructs may be used clinically in bone regeneration [Shea et al., 2004].

## ***1.5 Characterization of Scaffolds***

The properties of scaffold materials are the key factors in cell-material interaction and subsequent healing processes. Therefore, chemical, physical, thermal, surface properties and cell interactions of the materials must be analyzed very carefully before the application to prevent any undesired reaction.

### ***1.5.1 Chemical Structure***

Chemical structure of the scaffolds must be examined to see the effects of treatments such as crosslinking or blending with different materials. Blending different polymers and forming composite structures with the addition of ceramics must be predefined in atomic scale to create a stable construct.

Fourier Transform Infrared-Attenuated Total Reflectance (FTIR-ATR) spectroscopies are successful, well-known methods to examine the chemical compositions of the samples with micro scale resolution. They also give information about phase composition to examine the degree of crystallinity [Blazewicz et al., 2001].

In FTIR spectroscopy; tested material must include vibrational modes in its atomic or molecular composition to obtain an infrared band. For instance, hydroxyapatite ( $\text{Ca}_{10}(\text{PO}_4)_6(\text{OH})_2$ ) has only OH and  $\text{PO}_4^{3-}$  vibrational modes, so only those bands can be seen from FTIR spectra. ATR provides surface examination of samples with FTIR combination. The principle of ATR is based on the reflection of IR beam between different phases close to the surface [Lacefield et al., 1999].

X-Ray diffraction (XRD) is another tool to identify the purity and composition of crystalline materials. It can be applied to hydroxyapatite crystals to ensure the completion of HA crystal formation and therefore biological suitability of the synthesized material. X-Ray examination of the sample informs about the presence of calcium phosphates and impurities in the crystal structure [Wise et al., 1995].

### ***1.5.2 Surface Examination***

Biological interactions (e.g. cell adhesion, proliferation and migration) between implanted material and defected tissue begin on the surface of the implanted construct. Thus, surface characteristics such as water contact angle, surface free energy (SFE), surface topography of the prepared material must be examined carefully.

Contact angle ( $\theta$ ) of a liquid, is the angle between the tangent line from the droplet of that liquid to the touch of the solid surface and liquid-solid interfaces as shown in Figure 8, changing from 0 to 180 degrees. Materials with water contact angle value lower than 90 degrees called as wettable (hydrophilic), while with contact angle value higher than 90 degrees known as unwettable (hydrophobic).

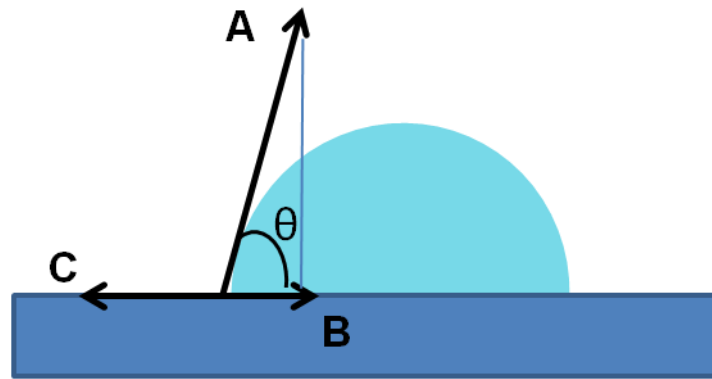


Figure 8 Contact angle of a liquid drop with surface free energy vectors; A, B and C showing interfacial tension between vapor and liquid, solid and liquid, solid and vapor respectively.

Surface free energy which is another term in surface interactions concept, can be obtained from the contact angle values of various liquid drops with known surface tension, placed on the solid surface. Surface free energy (SFE) of a material is defined as the work required to bring the molecule from the interior bulk phase to its surface to have a surface with a unit area;  $1\text{m}^2$  and its dimension is energy per unit area;  $\text{J}/\text{m}^2$  [Erbil et al., 2006].

As a general trend, the contact angle becomes lower when the SFE of the solid and liquid become closer. So, the relation between the contact angle and the intermolecular forces of the surface can be written as Young's equation:

$$\gamma_{sv} - \gamma_{sl} = \gamma_{lv} \cos \theta \dots\dots\dots(1.1)$$

where  $\gamma_{sv}$ ,  $\gamma_{lv}$  and  $\gamma_{sl}$  are the surface tensions for solid/vapor, liquid/vapor and solid/liquid interfaces, respectively. According to this equation, Belloncle et al. remarked that for a given liquid, increasing of the surface tension of the solid increases the absorption ability of this surface [Belloncle et al., 2006].  $\gamma_s$  and  $\gamma_l$  terms also can be used Instead of  $\gamma_{sv}$  and  $\gamma_{lv}$ , respectively, for low energy surfaces.

SFE includes different components such as; polar, dispersive, acidic and basic and total SFE components calculated by means of Zisman, Harmonic Mean, Geometric Mean and Acid Base approaches [Ozcan et al., 2008].

In Zisman approach, cosine of the contact angles ( $\theta$ ) of different liquids are plotted against SFE values of these liquids and Zisman equation uses slope of the regression line  $b$ , the contact angles ( $\theta$ ) and the surface tension of the liquids  $\gamma_l$ :

$$\cos \theta = 1 + b (\gamma_c - \gamma_l) \dots \dots \dots (1.2)$$

to calculate the , critical surface tension  $\gamma_c$  which is equal to SFE of the sample.

Wu et al., reported that the SFE of the materials has polar ( $\gamma^p$ ) and dispersive ( $\gamma^d$ ) components and used Harmonic Mean Equation (Eq. 1.3) or Geometric Mean Equation (Eq 1.4) to calculate the interfacial free energy between solid and liquid ( $\gamma_{sl}$ ).

$$\gamma_{sl} = \gamma_s + \gamma_l - 4 \left( \frac{\gamma_l^d \gamma_s^d}{\gamma_l^d + \gamma_s^d} + \frac{\gamma_l^p \gamma_s^p}{\gamma_l^p + \gamma_s^p} \right) \dots \dots \dots (1.3)$$

$$\gamma_{sl} = \gamma_s + \gamma_l - 2 \left( \sqrt{\gamma_l^d \gamma_s^d} + \sqrt{\gamma_l^p \gamma_s^p} \right) \dots \dots \dots (1.4)$$

According to another method which is known as Acid-Base approach, surface free energy is accepted as the summation of Lifshitz–van der Waals ( $\gamma^{LW}$ ) and Lewis acid ( $\gamma^+$ ) and base ( $\gamma^-$ ) components (Eq 1.5) [Gindl et al., 2001]:

$$(\cos \theta + 1)\gamma_l = 2 \left( \sqrt{\gamma_l^{LW} \gamma_s^{LW}} + \sqrt{\gamma_l^+ \gamma_l^-} + \sqrt{\gamma_l^- \gamma_s^+} \right) \dots \dots \dots (1.5)$$

For SFE measurements of film structures; it was suggested that the surface energies of thin films depend on the molecular forces of film material and the interactions or attractive forces of substrates [Abbasian et al., 2004]. Therefore, the same polymer may have different SFE values depending on the preparation process and the type of the mold.

In the literature, the factors of surface properties on biocompatibility of material are summarized as; the interfacial free energy, balance between the hydrophilicity and the hydrophobicity on the surface, type of functional groups, type and density of surface charges. It is suggested that desired surface properties highly depend on the biomedical application area of the material and the values of interfacial free energies of the material and the implanted surface. The difference between these SFEs must be minimum. For example, blood contacting surfaces must have interfacial free energies very close to water ( $\gamma_l^d = 21.8 \frac{\text{dyn}}{\text{cm}}$ ,  $\gamma_l^p = 50.8 \frac{\text{dyn}}{\text{cm}}$ ) because blood plasma has aqueous nature but since polar component of water is so high only dispersive component similarity may be satisfactory for blood-contacting materials [Wang et al., 2004]. Moreover, there exist various methods to modify polymeric surfaces increasing the polar surface free energy such as; ultraviolet radiation, chemical etching and plasma discharge. When degradable tissue engineered scaffolds are considered, the balance between hydrophilicity and hydrophobicity becomes more important because cell attachment and cell adhesion on material, swelling and degradation are affected from this balance. It was reported that polymeric surfaces with high hydrophilic behavior coming from hydrophilic groups (e.g. OH) on the surface of material enhanced cell adhesion. So, it is suggested that minimum interfacial energy must be obtain for higher cell adhesion [Ponsonnet et al., 2003]. However, this high hydrophilic character may increase degradation rate of scaffold in implanted area and may prevent the completion of new tissue formation through the construct. As a result, all these parameters (cell affinity of the surface, biodegradation rate etc.) must be taken into account in surface hydrophilicity examinations.

Surface topography also is another important fact influencing the cell behavior on the material surface and can be examined by different microscopic techniques. Atomic force microscopy (AFM) is one of the most common methods used in surface investigation and based on imaging of surface with a tip and laser sending electron beams to the cantilever. AFM gives excellent topographic contrast and direct measurements of surface properties with quantitative height information [Braga et al., 2004].

Scanning electron microscopy (SEM) also provides information about surface morphologies of the samples. SEM uses finely focused electron beams to irradiate the surface area of the sample. Then, signals are produced from the electrons interactions with surface of material resulting with secondary, backscattered electrons, characteristics X-Rays and other photons at different energy levels [Goldstein et al., 2003].

### ***1.5.3 Swelling Degree***

Swelling behavior of the biomaterial in physiological conditions must be investigated before the implantation to ensure that the scaffold would be swellable in aqueous media in the required time. Maximum water swelling value of a material is also known as water uptake ability of the material. To test the swelling of a material, it should be immersed into the prepared physiological solutions and the weight changes in different time intervals should be detected. Swelling ratio of polymeric structures is affected by the pH of the solution, molecular weight and crosslinking density of polymers and temperature of the environment. For example, materials containing amino groups show higher swelling in acidic solutions because of protonated amino groups but substances with carboxylic groups indicate best swellability at pH near 7. Materials composed of both acidic and basic groups may demonstrate increased swelling behavior at pH values higher or lower than pH 4-5 [Jagur-Grodzinski et al., 2009]. It is preferable that the scaffolds must reach to the equilibrium swelling states in short time intervals such as 1-24 hours instead of days.

### 1.5.4 Mechanical Properties

Mechanical properties of the scaffolds can be examined based on the stress-strain curves which inform about the hardness and toughness of the tested material.

Stress is the force intensity applied to the material and strain is the deformation or length change with changing force intensity on the material [Vincent 1990].

As it is seen from the Figure 9, a stress-strain curve of a solid may give data about yield and ultimate strength values, elastic and plastic behaviors of material. Initial linear part of the line shows the elastic region in which the deformation is reversible; if applied force is removed, material can take its original shape.

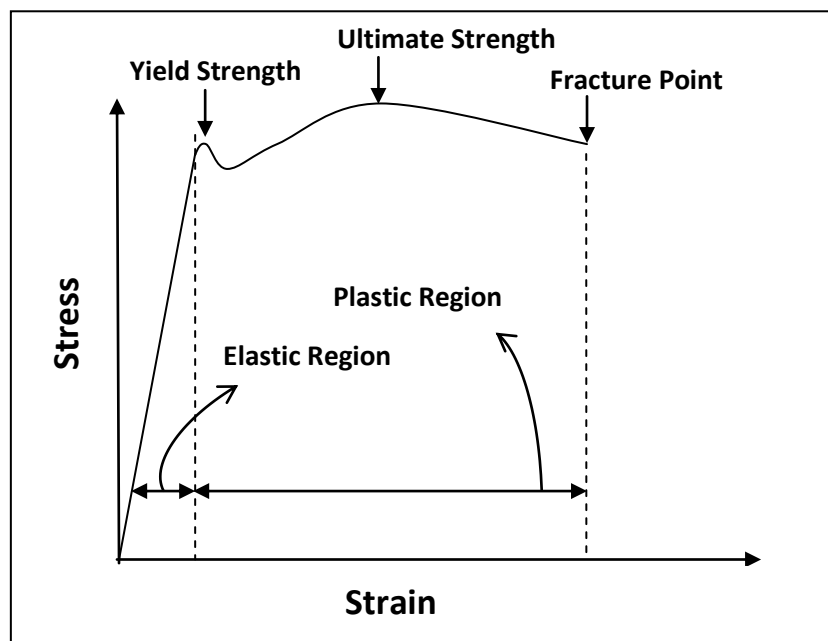


Figure 9 A tensile stress-strain curve of a viscoelastic material.

In elastic region stress is proportional to strain and slope of the curve gives Young's modulus (modulus of elasticity,  $E$ ) of the sample. However, in plastic region; deformation is irreversible and yield strength is the starting point of plastic region in some materials like metals. In general, it is difficult to define original yield point,

therefore, an offset (0.2%) yield point is used. Area under the curve gives the toughness of the material. Ultimate tensile strength is the peak strength in plastic region and fracture point at the end of plastic region is the breaking point that sample fractures [Keene 1999]. Since ceramics have high modulus of elasticity, they can easily cause undesirable results in bone implant applications. So, biocomposites of polymer-ceramics have the advantages of flexibility with respect to hard ceramics [Teoh 2000].

Mechanical behavior of the prepared constructs can be tested by using mechanical test machines. After applying controlled forces to the material, its behavior under tensile or compression stress is analyzed. Force versus extension graphs may be obtained by these test applications and elasticity, ultimate tensile or compression strength, strain at break values may be calculated.

Mechanical values of cortical and spongy bones are given in Table 6 [Hench et al., 1993]. So, hard tissue engineered 2-D or 3-D scaffolds must show almost similar results with these mechanical values depending on their implantation area (cortical or spongy bone).

Table 6 Mechanical properties of cortical and spongy bones.

Mechanical Property	Cortical Bone	Spongy Bone
Compressive Strength (MPa)	100-230	2-12
Tensile Strength (MPa)	50-150	10-20
Strain Failure (%)	1-3	5-7
Fracture Toughness (MPa.m <sup>1/2</sup> )	2-12	-
Young's Modulus (GPa)	7-30	0.05-0.5



### ***1.5.5 Thermal Analysis***

Polymeric materials can be affected from environmental temperature changes during preparation or implantation processes and some chemical transitions may occur because of these thermal variations. Glass transition, denaturation and crystallization temperatures, evaporation temperature of adsorbed water or solvents are some of the important phenomena that are dependent on the temperature alterations and heat flow rate on the material. Thermal properties of the biomaterials can be investigated by different methods such as; thermogravimetric analysis (TGA), differential thermal analysis (DTA) and differential scanning calorimetry (DSC). DSC is defined as the measurement of temperature changes of a sample and a reference in a certain heat flow rate by using a special temperature program [Höhne et al., 2003]. So, in thermal analysis results of polymeric scaffolds, it was expected to see the variations in decomposition or water/solvent evaporation temperatures with changing preparation conditions.

### ***1.5.6 Pore Size Distribution***

Porosity of the 3-D framework affects cell migration into scaffold and vascularization process. Pore size and size distribution of the matrices can be controlled by polymer type or polymer-particle ratios in blend or composite structures. New blood vessels formation into the scaffolds by host tissue ingrowth is called angiogenesis and it is essential for healing process [Carmeliet 2000]. It was reported that the development of functional vessels and tissue ingrowth into the scaffold increase with increasing pore diameter and pores with sizes of 250-300  $\mu\text{m}$  showed the best neovascularization results [Druecke 2004]. Thus, observation and calculation of the pore size distribution of scaffolds are very important in tissue engineering approaches. There are several methods to investigate the pore shape and size of the scaffolds e.g. Scanning electron microscopy (SEM), mercury porosimetry etc.

### ***1.5.7 Biocompatibility***

Biocompatibility may be simply defined as the effect of non-living material on the implanted living system after the recognition of the differences between non-living and living structures by the body [Black, 2006]. It was explained that there are two main principles in biocompatibility concept; absence of cytotoxic effect and biofunctionality of the material [Kirkpatrick et al., 2005].

The best way of observing the material biocompatibility is to analyze its affinity towards the seeded cells and subsequent cell behavior. Therefore, cell morphology and number of proliferated cells on the scaffolds must be specified with the experiments and calculations as one of the preliminary steps of biocompatibility testing. In general; MTS (3-(4,5-dimethylthiazol-2-yl)-5-(3-carboxy methoxyphenyl)-2-(4-sulfophenyl)-2H-tetrazolium) or MTT (3-(4,5-Dimethyl thiazol-2-yl)-2,5-diphenyltetrazolium bromide, a tetrazole) cell proliferation assays are applied to quantify the mitochondrial activities of the cells on the scaffold by using UV-Vis spectrophotometry. Data is obtained as a change in absorption intensity and is proportional to the living cell number.

Cell morphology is examined by microscopic methods such as; light, fluorescence and confocal microscopies to serve as an indicator of cell-material interaction.

### ***1.6 The Aim of This Study***

This study is focused on the preparation and characterization of chitosan-gelatin/hydroxyapatite scaffolds in both two-dimensional and three-dimensional forms to judge their potential to serve as tissue engineering scaffolds.

Since scaffold properties are very important to achieve proper cell-material interactions in tissue engineering applications, optimization of scaffold characteristics was aimed within the context of this research. Chitosan and gelatin were selected since they are natural biodegradable polymers and have significant resemblance to natural ECM components. These properties make them very attractive as scaffold materials. However, the mechanical and osteogenic properties

must be improved to served in hard tissue engineering applications. Hydroxyapatite which exists in the bone structure, was chosen as an additive to improve the mechanical strength of the polymeric matrix. So, two natural polymers, a polypeptide, gelatin, and a polysaccharide, chitosan, were combined with a bioactive ceramic, hydroxyapatite in 2-D and 3-D structures. In this study, calcium phosphate was synthesized and two types of hydroxyapatite, non-sintered and sintered, were produced from this synthesized calcium phosphate.

Two-dimensional polymeric blends (films) were prepared for the optimization of chitosan-gelatin blend ratio that will be used in further processes. EDC/NHS were used as crosslinkers because of their low toxicity. The crosslinked and uncrosslinked chitosan-gelatin blends were compared by examining their chemical, thermal, mechanical and surface properties.

Chitosan-gelatin blend films were mixed with hydroxyapatite in order to enhance the osteogenic activity of the biopolymeric scaffolds and to create a convenient environment for the new tissue formation by keeping the pH of the medium at a suitable value. The effects of the two types of hydroxyapatites, sintered or non-sintered hydroxyapatites, on the physicochemical properties of the scaffolds were examined by FTIR-ATR, thermal analysis, tensile tests, contact angle measurements and surface free energy calculations.

Highly porous sponges with optimized chitosan-gelatin/hydroxyapatite compositions were produced by freeze-drying technique.

Chemical, thermal and mechanical properties of all scaffolds were investigated by FTIR-ATR, DSC analysis and compression tests, respectively. SEM micrographs were taken done to obtain detailed information about the surface topography and cell morphologies after attachment experiments. Surface chemistry of the scaffolds were studied by using several surface free energy calculation approaches after contact angle measurements. Biocompatibility of scaffolds were tested by using human osseosarcoma SaOs-2 cell line. Cell numbers were determined by MTS assay, the attachment and the morphologies of the cells were evaluated by different microscopic methods such as fluorescence and confocal microscopies.

## CHAPTER 2

### EXPERIMENTAL

#### *2.1 Materials*

Hydroxyapatite precursors  $\text{Ca}(\text{NO}_3)_2 \cdot 4\text{H}_2\text{O}$  and  $(\text{NH}_4)_2\text{HPO}_4$  were purchased from Merck (Germany). 25%  $\text{NH}_4\text{OH}$  solution was also obtained from Merck (Germany). Chitosan powder (deacetylation degree = min 85%), 1-ethyl-3-(3-dimethylamino propyl)-carbodiimide (EDC), N-hydroxysuccinimide (NHS) and acetic acid were purchased from Sigma (Germany). Type A gelatin from bovine skin was obtained from Difco (USA). Sodium hydroxide was supplied from J.T. Baker (Holland). Bovine serum albumin (BSA) was obtained from Fluka (USA). Dulbecco's Modified Eagle Medium (DMEM, high glucose and low glucose), RPMI-1640 and fetal bovine serum (FBS) were obtained from HyClone (USA). Penicillin/Streptomycin (Pen/Strep) solution was also a product of HyClone (USA). Trypsin-EDTA (0.25%), glutaraldehyde and cacodylic acid (sodium salt) were obtained from Sigma (USA). Alexa Fluor 488 phalloidin and 4',6-diamidino-2-phenylindole (DAPI) were obtained from Chemicon (USA). Nucleocounter reagents were supplied by Chemometec (Denmark). MTS kit was obtained from Promega Corporation (USA).

## **2.2 Methods**

### **2.2.1 Hydroxyapatite Synthesis**

Hydroxyapatite (HA) powder was prepared by the method of Jarcho et al [Jarcho and Bolen, 1976]. Briefly, 0.5 M  $\text{Ca}(\text{NO}_3)_2 \cdot 4\text{H}_2\text{O}$  and 0.3 M  $(\text{NH}_4)_2\text{HPO}_4$  solutions were prepared separately in deionized water (DW) and pH of the solutions were adjusted to 11-12 by addition of  $\text{NH}_4\text{OH}$  solution. Calcium solution (100 mL) was added into phosphate solution (100 mL) dropwise, with  $\text{NH}_4\text{OH}$  addition to maintain pH at 11-12 continuously. Final solution was stirred at room temperature for 2 h and stirred at  $90^\circ\text{C}$  for 1 h. Then the solution was cooled down to room temperature and stirred overnight. After filtration, the filtered slurry was dried at  $80^\circ\text{C}$  overnight and the obtained non-sintered hydroxyapatite (nsHA) was ground. For the preparation of sintered hydroxyapatite (sHA),  $1000^\circ\text{C}$  heat treatment was applied for 3h to the nsHA powder.

### **2.2.2 Chitosan-Gelatin/Hydroxyapatite Scaffolds Preparation**

#### **2.2.2.1 Chitosan, Gelatin and Chitosan-Gelatin Films**

For chitosan films, chitosan solution (C, 2% w/v) was prepared in acetic acid solution (1% v/v) and filtered through sintered glass with pore size 2. To prevent bubble formation in casted films because of vacuum filtering process, all filtered chitosan solution placed into ultrasound machine for 10 min. As a result of these procedures, smooth chitosan blend films were obtained.

For gelatin films, gelatin solution (G, 2% w/v) was prepared in distilled water stirring the solution for 2 h in  $50^\circ\text{C}$  water bath.

For chitosan-gelatin blend films, chitosan solution and gelatin solution were mixed at the ratios of 3-1, 1-1 and 1-3 (w-w) under agitation for 2 h at  $50^\circ\text{C}$ .

The prepared solutions (chitosan, gelatin and chitosan-gelatin blend solutions) were poured into the plastic petri dishes and dried in oven at  $40^\circ\text{C}$  for 48 h. Prepared films

were named as C, C-G:3-1, C-G:1-1, C-G:1-3, G where the numbers define the weight ratios of chitosan to gelatin in the films.

### ***2.2.2.2 Chitosan-Gelatin/Hydroxyapatite Films***

Chitosan-Gelatin/non-sintered hydroxyapatite (C-G/nsHA) were prepared keeping the polymer:hydroxyapatite mass ratio constant as; 2:1.

C/nsHA film was prepared by adding 0.5 g of nsHA into 50 mL DW and ultrasonicated at least 20 min for a complete dispersion of nsHA in DW, and then stirring extra 1 h. Then, this nsHA suspension was poured into the 2% (w/v) 50 mL chitosan solution under agitation and mixed at overnight room temperature.

For C-G:3-1/nsHA composite preparation, 4% (w/v) 25 mL nsHA suspension in DW was added into 2% (w/v) 75 mL chitosan solution and stirred overnight. Then, 0.5 g of powder gelatin was added into this mixture under agitation and mixed in water bath at 50°C for 2 h.

In C-G:1-1/nsHA film preparation, 2% (w/v) 50 mL nsHA suspension was added into 2% (w/v) 50 mL chitosan solution and stirred overnight. 1 g of powder gelatin was added into this mixture and mixed in water bath at 50°C for 2 h.

In G/nsHA film preparation 4% (w/v) 50 mL G solution was stirred with 2% (w/v) 50 mL nsHA suspension in water bath at 50°C for 2 h.

All final mixtures were poured into plastic petri dishes and placed into 40°C oven and named as; C-G for blend films and C-G/nsHA for composite structures.

The prepared films were also subjected to crosslinking treatment. For this purpose, EDC/NHS (5/1 M/M) solution was prepared in ethanol:phosphate buffer solution (80:20 v:v) (pH 5.5; 50 mM). Film samples were immersed in this solution for 24 h at room temperature, then treated with 1 M NaOH solution for 2 h to neutralize acetic acid and then washed several times with distilled water until pH was neutralized. At the end, crosslinked films were dried at room temperature and named as xC-G for blend films and xC-G/nsHA for composite structures. The prepared film compositions are summarized in Table 7.

Table 7 Compositions of the prepared films.

<b>Samples*</b>	<b>Chitosan (g)</b>	<b>Gelatin (g)</b>	<b>HA (g)</b>	<b>EDC/NHS (5/1 M/M) treatment #</b>
<b>C</b>	1	-	-	-
<b>C-G:3-1</b>	1.25	0.75	-	-
<b>C-G:1-1</b>	1	1	-	-
<b>C-G:1-3</b>	0.75	1.25	-	-
<b>G</b>	-	2	-	-
<b>xC</b>	1	-	-	+
<b>xC-G:3-1</b>	1.25	0.75	-	+
<b>xC-G:1-1</b>	1	1	-	+
<b>xC-G:1-3</b>	1.25	0.75	-	+
<b>xG</b>	-	2	-	+
<b>C/nsHA</b>	1	-	0.5	-
<b>C-G:3-1/nsHA</b>	1.25	0.75	1	-
<b>C-G:1-1/nsHA</b>	1.25	0.75	1	-
<b>G/nsHA</b>	-	2	1	-
<b>xC/nsHA</b>	1	-	0.5	+
<b>xC-G:3-1/nsHA</b>	1.25	0.75	1	+
<b>xC-G:1-1/nsHA</b>	1	1	1	+
<b>xG/nsHA</b>	-	2	1	+
<b>xC/sHA</b>	1	-	0.5	+
<b>xC-G:3-1/sHA</b>	1.25	0.75	1	+
<b>xC-G:1-1/sHA</b>	1	1	1	+
<b>xG/sHA</b>	-	2	1	+

\* Amounts are in 100 mL

C=chitosan, G=gelatin, x=crosslinked structure, nsHA=non-sintered HA, sHA=sintered HA

# Positive sign defines application of crosslinking

For contact angle measurements, all film samples were prepared as described and casted on microscope slides to obtain smooth surfaces.

### 2.2.2.3 Chitosan-Gelatin/Hydroxyapatite Porous Sponge Scaffolds

Three-dimensional sponge structures of chitosan-gelatin (spC-G), chitosan-gelatin/nsHA (spC-G/nsHA) and chitosan-gelatin/sHA (spC-G/sHA) composite preparation procedures were same as the solution preparation steps of C-G:1-1 blend and C-G:1-1/nsHA composite films, respectively. Amounts of ingredients used in the preparation of these porous sponge structures is summarized in Table 8. Prepared solutions (1.5 mL) were put into well clusters (24-well tissue culture cluster) in 15 mm thickness (in height) and frozen in different ways. Some samples were put -80°C, some to -20°C keeping on vapor of liquid N<sub>2</sub> and some dipped in liquid N<sub>2</sub> and all kept in these conditions for 24h. All frozen spC-G, spC-G/nsHA and spC-G/sHA composite samples were lyophilized at least for 30 h. For the following experiments only scaffolds frozen at -20°C keeping on vapor of N<sub>2(liq)</sub> were used. The prepared 3-D constructs were subjected to crosslinking treatment. For this purpose, EDC/NHS (5/1 M/M) solution was prepared in ethanol:phosphate buffer solution (80:20 v:v) (pH 5.5; 50 mM). Sponge samples were immersed in this solution for 24 h at room temperature, then treated with 1 M NaOH solution for 2 h to neutralize acetic acid and then washed several times (during 24 h) with distilled water until pH was neutralized. Crosslinked sponges were freeze-dried again and named as; spxC-G, spxC-G/nsHA and spxC-G/sHA, where sp defines sponge structure and x defines crosslinked structure. The prepared sponge compositions are summarized in Table 8.

Table 8 Compositions of the prepared sponge structures.

Samples*	Chitosan (g)	Gelatin (g)	nsHA (g)	sHA (g)	EDC/NHS (5/1 M/M) treatment
spxC-G	1	1	-	-	+
spxC-G/nsHA	1	1	1	-	+
spxC-G/sHA	1	1	-	1	+

\* Amounts all in 100 mL



## **2.3 Characterization**

### **2.3.1 X-Ray Diffraction (XRD)**

The crystal structure of the synthesized and ground non-sintered and sintered hydroxyapatite samples (nsHA and sHA) were characterized by X-ray diffraction (XRD). The patterns were recorded with a Rigaku X-Ray diffractometer model Ultima D/MAX 2200/PC using CuK $\alpha$  radiation generated at 40 kV and the scan speed was 2°/min.

### **2.3.2 Scanning Electron Microscopy**

Morphology and microstructure of sHA and nsHA powders, surface morphologies of the film structures and porous structures of sponge scaffolds, cell behaviours on 2-D and 3-D constructs were investigated by scanning electron microscopy (SEM). The fracture sections of the samples were sputter-coated with Au prior to examinations.

For sintered HA (sHA) and non-sintered HA (nsHA) powder examination, JSM-6400 Electron Microscope (JEOL), equipped with NORAN System 6 Xray Microanalysis system was used. Scaffolds structures were examined with QUANTA 400F Field Emission SEM.

### **2.3.3 Fourier Transform Infrared-Attenuated Total Reflectance (FTIR-ATR) Analysis**

Chemical compositions of the prepared scaffolds were examined with FTIR-ATR (Perkin Elmer, FT-IR System, USA).

### **2.3.4 Differential Scanning Calorimetry (DSC) Analysis**

Differential scanning calorimeter (DSC, DuPont 2000, France) was used to examine the thermal properties of the prepared blend films with a constant heating rate of 10°C/min under nitrogen flow in the 25°C-350°C temperature range.

### ***2.3.5 Contact Angle and Surface Free Energy Measurements***

Contact angle and surface free energy measurements of the films were done by a goniometer (CAM 200, Finland) at room temperature. 5 $\mu$ L liquid drops of deionized water (DW), diiodomethane (DIM), formamide (FA) and dimethylsulfoxide (DMSO) were dropped on the samples and the contact angles of at least five drops were measured and averaged. Zisman, Harmonic Mean and Geometric Mean and Acid Base approaches were used to calculate surface free energy (SFE) values.

### ***2.3.6 Swelling Tests***

Crosslinked film samples (20 mm x 10 mm) were weighed and then put in 0.01 M phosphate buffered saline (PBS) at pH 7.4 at 37°C. At certain time intervals (1, 3, 6, 12, 24, and 48 h) swollen films were taken out, excess water on the surface was removed with a filter paper by gentle contact and then the samples were weighed. For each sample, three parallel experiments were carried out and the obtained values were averaged. The percent swelling was calculated from the equation:

$$S_w\% = [(W_s - W_i)/W_i] \times 100 \quad (2.1)$$

where  $W_i$  and  $W_s$  are the sample weights initially and after swelling, respectively.

### ***2.3.7 Mechanical Tests***

Tensile properties of films and compression characteristics of scaffolds were examined by a mechanical testing machine (Lloyd Instrument, Ltd., Fareham, UK), equipped with a 100 N load cell. For tensile test; film samples were cut as rectangular strips (10 mm x 40 mm) and for compression tests; porous 3-D samples were in cylindrical shapes. In tensile tests; the gauge length was 10 $\pm$ 2 mm and the width was 10 mm for each film sample, for compression tests the gauge length was 5 $\pm$ 1 mm. The thickness of each film specimen was determined by a micrometer having measurements from different parts and the average values were used in the calculations. At least 5 experiments were carried out for each type of films and 3-D scaffolds and average values of mechanical properties were calculated.

## **2.3.8 Cell Viability Tests**

### **2.3.8.1 Preparation of Scaffolds for Cell Seeding**

Crosslinked blends (xC, xC-G:3-1, xC-G:1-1, xG, where x shows crosslinking occurs) and composite films (xC/nsHA, xC-G:3-1/nsHA, xC-G:1-1/nsHA, where nsHA shows presence of non-sintered HA in the composition) (1x1 cm<sup>2</sup>) and 3-D spongy scaffolds (spxC-G/sHA, spxC-G/nsHA, where sp shows sponge structures) were rehydrated in 70% ethanol at 4°C for 3 h and washed with PBS three times in the wells of 24-well plates and then dried under laminar flow before cell seeding.

### **2.3.8.2 Cell Culture and Seeding**

SaOs-2 cells were cultured as monolayers in RPMI-1640 medium supplemented with 10% fetal bovine serum (FBS), penicillin (100 units/mL) and streptomycin (100 µg/mL), incubated under 5% CO<sub>2</sub> (CO<sub>2</sub> incubator, SANYO, Japan, Model MCO 175) at 37°C. Confluent SaOs-2 cells were detached from the flask surface using 0.05% trypsin/EDTA. The cells were centrifuged at 3000 rpm for 5 min and the pellet was resuspended in complete medium. The cells were counted by using Nucleocounter (Chemometec A/S, Denmark). Aliquots of 20 µL of cell suspension containing 2x10<sup>4</sup> cells were seeded on the sterile films placed in the wells while 1x10<sup>5</sup> cells were seeded on the 3-D scaffolds. After incubation for 1 h, complete RPMI-1640 medium (1 mL) was added and cells were grown at 37°C in the CO<sub>2</sub> incubator up to a week.

### **2.3.8.3 Cell Proliferation Test**

MTS cell proliferation assay was carried out to determine the cell density on the samples. After transferring of cell seeded films into a new, sterile 24-well plate and washing with sterile PBS, 1 mL of MTS/PES solution (10% in low glucose medium) was added to each sample in the 24-well plate and incubated for 1 h at 37°C in CO<sub>2</sub> incubator. After 2 h incubation, 200 µL of solution from each well was transferred to a new 96-well plate. Absorbance was measured at 490 nm using an Elisa Plate

Reader (Molecular Devices, Model Maxline, USA). Cell numbers were calculated after 24 h and after one week for 2-D and 3-D scaffolds (all experiments were performed in triplicate).

#### ***2.3.8.4 Cell Morphology***

Cell morphologies on the samples were examined by transmission microscopy (IX 70, Olympus, Japan), fluorescence microscopy (Leica DM2500, Germany), confocal microscopy (Leica TCS., SPE, Germany) and scanning electron microscopy (SEM, JEOL JSM-6400) after 1 and 7 days. For transmission microscopy examination, the cells were fixed in 1 mL of 4% paraformaldehyde (PFA) solution for 20 min and washed twice with PBS.

For fluorescence microscopy, PFA fixed cells were permeabilized in 1% (v/v) Triton X-100 solution at room temperature for 5 min and washed with PBS three times. Then samples were kept in blocking solution (1% BSA (bovine serum albumin) in PBS) at 37°C for 30 min and washed with PBS. Cells were stained with DAPI-phalloidin, washed twice with 0.1% BSA.

For confocal microscopy, propidium iodide (PI) (1:3000 dilution with distilled water) was used as the nuclear stain and after 1% (v/v) Triton X-100 treatment for 5 min, sponge samples were immersed in 800 µL PI solution for 15 min at room temperature, washed three times with distilled water (1 mL each time) and visualized with confocal microscopy.

For SEM imaging; the cells were fixed for 1 h in 1 mL 1% glutaraldehyde solution prepared in 0.1 M cacodylate buffer. Then washed with cacodylate buffer three times (1 mL each time), lyophilized, and sputter coated with gold.

## CHAPTER 3

### RESULTS AND DISCUSSION

#### 3.1 *Hydroxyapatite Synthesis*

Sintered and non-sintered hydroxyapatite powders were synthesized with a well-known wet synthesis procedure involved by Jarcho et al. Basically,  $\text{Ca}(\text{NO}_3)_2 \cdot 4\text{H}_2\text{O}$  and  $(\text{NH}_4)_2\text{HPO}_4$  were used as hydroxyapatite precursors and HA formation occurs in the basic media following the reaction shown in Figure 10.

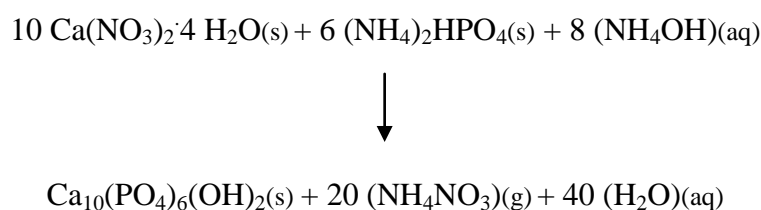


Figure 10 Hydroxyapatite synthesis.

As a novel approach, two types of hydroxyapatite (HA) as; non-sintered HA (nsHA) and sintered HA (sHA), were synthesized in the experiments to see their physicochemical and biocompatibility effects on the two-dimensional (2-D) and three-dimensional (3-D) chitosan-gelatin polymer-based scaffolds. Normally, sintering process with heat treatment at  $1000^\circ\text{C}$  increases the fusion of the atoms and

therefore crystallinity of the HA. So, final products with sintering process have high crystallinity while non-sintered HA particles show less crystalline structure. Deionized water usage is an important point in HA preparation because ionic substances even in trace amount can bind to ions of HA and change the crystal structure. Pulverization is another key factor in pretreatment process to increase the surface area of HA particles and enhance interaction between polymeric and ceramic matrices.

## **3.2 Hydroxyapatite Characterization Results**

### **3.2.1 X-Ray Diffraction (XRD) Examination**

XRD spectra of non-sintered and sintered hydroxyapatite powders are shown in Figure 11. It is seen that the 1000°C heat treatment caused higher crystallinity with sharper apatite peaks and there is no carbonate impurity displaying at 37° and 54° peaks [Vijayalakshmi et al., 2006]. Characteristic peaks of hydroxyapatite were shown at around 26.0° and 31.9° [Zhang et al., 2005].

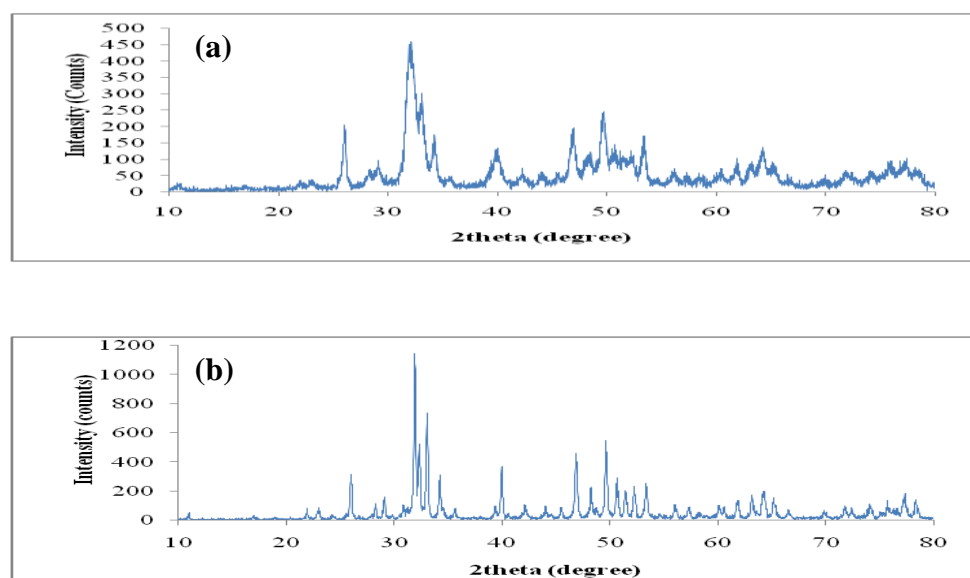


Figure 11 XRD patterns of hydroxyapatite powders (a) non-sintered, and (b) sintered.

Alternatively, in non-sintered hydroxyapatite sample XRD spectrum, those peaks are seen in broader range because of amorphous structure. So, XRD spectra of the samples without carbonate peaks verify the pure hydroxyapatite synthesis.

### 3.2.2 FTIR -Attenuated Total Reflectance Spectroscopy Analysis

FTIR spectra of non-sintered hydroxyapatite (nsHA) and sintered hydroxyapatite (sHA) are shown in Figure 12. In nsHA spectrum, a broad band appears between  $3250\text{ cm}^{-1}$  and  $3650\text{ cm}^{-1}$  deducing O-H stretching.  $\text{PO}_4^{3-}$  stretching peak appeared at  $1030\text{ cm}^{-1}$  and peaks at  $602\text{ cm}^{-1}$  and  $563\text{ cm}^{-1}$  indicate  $\text{PO}_4^{3-}$  bending vibrations. The small peak at  $860\text{ cm}^{-1}$  can be attributed to symmetric P-O stretching vibration. Those peaks get narrower or disappear when hydroxyapatite was exposed to  $1000^\circ\text{C}$  heat treatment.

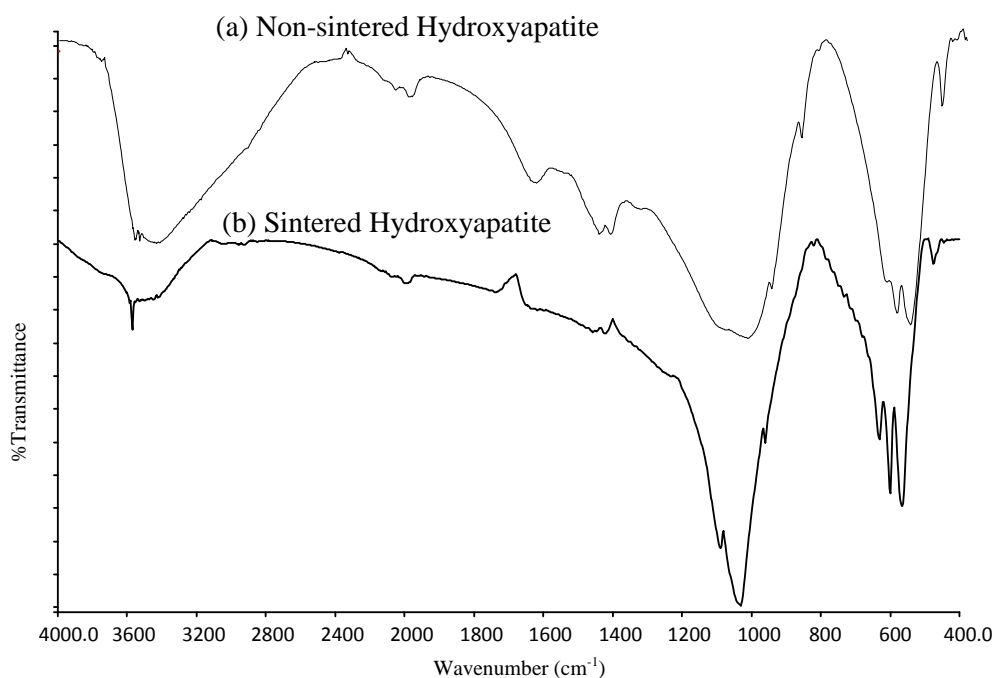


Figure 12 FTIR-ATR spectra of hydroxyapatite powder (a) non-sintered and (b) sintered.

In spectrum of sHA,  $\text{PO}_4^{3-}$  ions stretching bands are more clear at  $962\text{ cm}^{-1}$ ,  $1090\text{ cm}^{-1}$ ,  $1032\text{ cm}^{-1}$  and triple degenerate bending vibration of P-O peaks appeared at  $566\text{ cm}^{-1}$ ,  $602\text{ cm}^{-1}$  and  $632\text{ cm}^{-1}$ . OH stretching peak at  $3572\text{ cm}^{-1}$  also becomes sharper after heat treatment in sintered hydroxyapatite spectrum [Thamaraiselvi et al., 2006 and Li et al., 2007].

### 3.2.3 Morphologies of Hydroxyapatite Particles

Non-sintered and sintered hydroxyapatite morphologies can be seen from Figure 13. As it is seen from the SEM micrographs; aggregates of hydroxyapatite formed more crystalline, densely packed structures, when they were heated at  $1000^\circ\text{C}$  while non-sintered particles demonstrated amorphous structures with smaller flakes.

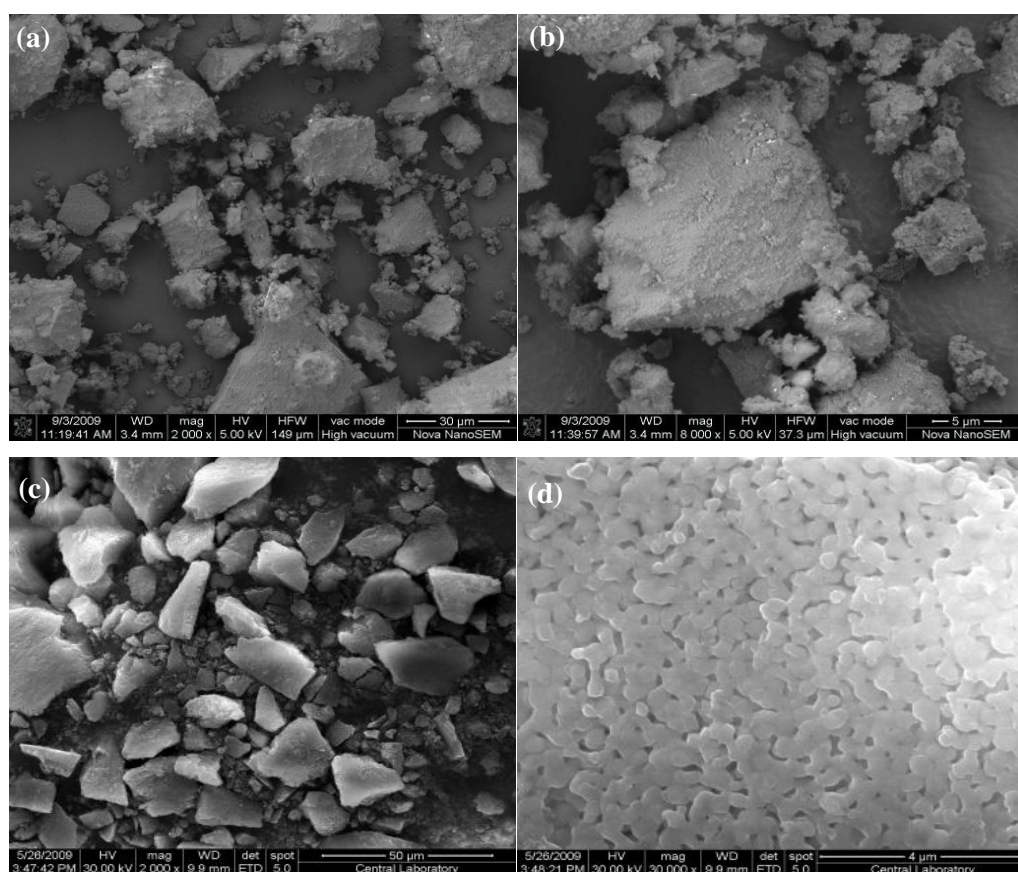


Figure 13 SEM micrographs of non-sintered (a and b) and sintered (c and d).



### 3.3 Film Preparation

Chitosan-gelatin blend films were prepared by solvent casting method resulting with solvent evaporation that leads thin and transparent C-G film formation. Since, C-G:1-3 blend films could not be removed from molds because of high brittleness of these films, they could not be used for further experiments. Pulverization of HA particles was one of the most important step in HA addition to increase the surface area of HA particles. Gelatin/non-sintered HA (G/nsHA) composite films had non-homogenous and brittle structures (as shown in Figure 14) and therefore, only C/nsHA, C-G:3-1/nsHA and C-G:1-1/nsHA composite films were used for the following experiments.

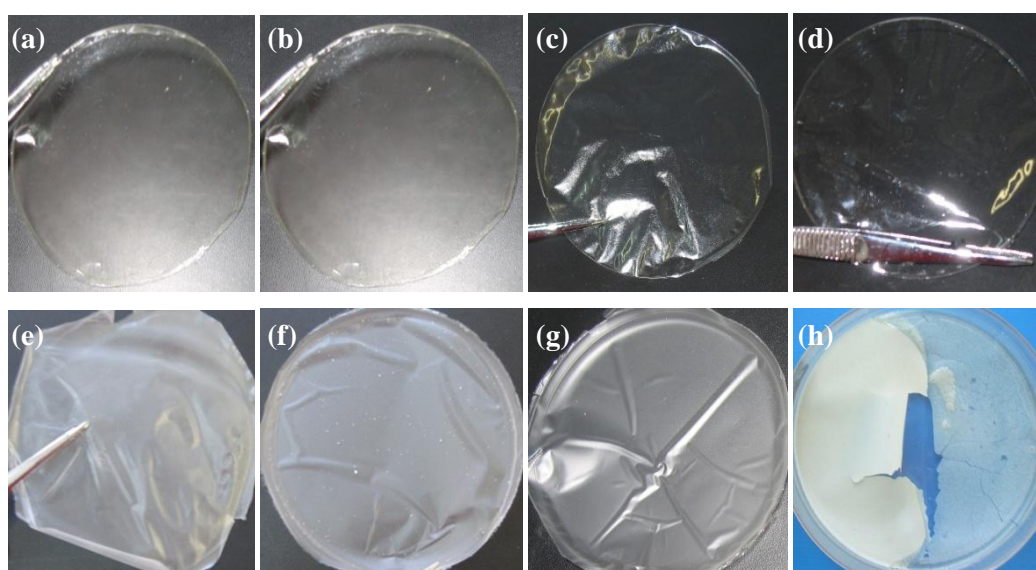


Figure 14 Pictures of (a)xC, (b)xC-G:3-1, (c)xC-G:1-1, (d)xG, (e)xC/nsHA, (f) xC-G:3-1/nsHA, (g) xC-G:1-1/nsHA, and (h) xG/nsHA films.

Water soluble EDC/NHS crosslinking agents with low toxicity were used in the experiments to form stable chitosan-gelatin structures. Crosslinker solution was prepared in ethanol to create a hydrophobic environment that prevents hydrolysis of

EDC [Nam et al., 2008]. The reason of NHS addition is to increase rate of reaction and degree of crosslinking [Damink et al., 1996].

EDC/NHS activates the carboxyl groups of gelatin and these activated carboxyl groups react with nucleophiles such as amino groups of chitosan or itself. Interactions between chitosan and gelatin induced by EDC/NHS crosslinking agent treatment is illustrated in Figure 15.

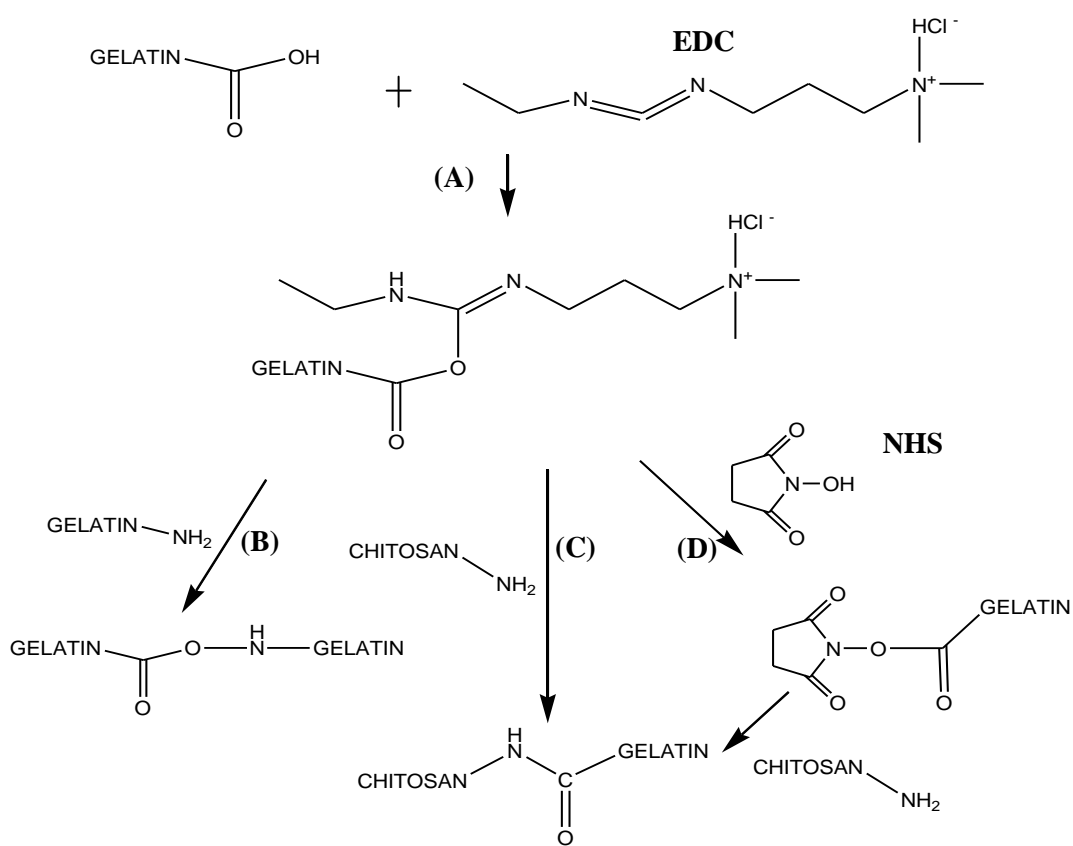


Figure 15 Schematic illustration of (A) gelatin carboxyl group activation by EDC and reaction of activated gelatin complex with (B) chitosan, (C) gelatin, and (D) NHS activated gelatin reactions.

As a result of these reactions, it is suggested that during the crosslinking of chitosan and gelatin, amide bonds formations have occurred. It was also claimed that ester bonds may form between hydroxyl and carboxyl groups in EDC/NHS presence [Zhang et al., 2005].

### **3.4 Film Characterization**

#### **3.4.1 FTIR -Attenuated Total Reflectance Spectroscopy Analysis**

FTIR-ATR spectra of uncrosslinked chitosan-gelatin (C-G), crosslinked chitosan-gelatin (xC-G) blend films and chitosan-gelatin/nsHA (xC-G/nsHA) composites are shown in Figure 16, Figure 17 and Figure 18.

FTIR spectrum of uncrosslinked chitosan film displayed characteristic peaks around  $892\text{ cm}^{-1}$  and  $1152\text{ cm}^{-1}$ , assigned to the saccharide structure and anti-symmetric stretching of C-O-C bridge. Furthermore,  $\text{-CH}_2$  bending peak at  $1402\text{ cm}^{-1}$  is another characteristic peak of chitosan. The spectrum of chitosan depicted absorption bands at  $1633\text{ cm}^{-1}$  for C=O stretching of the *N*-acetyl group (amide I band) and scissor vibration of amine group; at  $1537\text{ cm}^{-1}$  for N-H bending of amide II and scissor vibration of ammonium ions; at  $3180\text{ cm}^{-1}$  for stretching of O-H; at  $1063\text{ cm}^{-1}$  for skeletal vibration of C-O stretching, at  $2875\text{ cm}^{-1}$  for  $\text{CH}_2$  stretching vibration.

Uncrosslinked gelatin film was characterized by its C-N and N-H stretching amide II band at  $1537\text{ cm}^{-1}$  and C=O stretching peak of carboxylic group at  $1629\text{ cm}^{-1}$ . In the spectrum, the broad band around  $3280\text{ cm}^{-1}$  was the OH stretching. The band at  $2933\text{ cm}^{-1}$  was C-H stretching.

Since carbonyl group amount is higher in gelatin; the intensity of carbonyl peak at around  $1629\text{ cm}^{-1}$  increased with increasing gelatin concentration in both crosslinked and uncrosslinked blend film samples. Moreover, the amide III band; coming from C-N-H in-plane bending modes, was observed at around  $1239\text{ cm}^{-1}$  especially for xC-G:1-1 and xG samples which have higher gelatin concentration.

Crosslinked blend samples spectra at around  $650\text{ cm}^{-1}$  decreased or disappeared because of less C-H deformation than uncrosslinked blends. Crosslinked xC-G:1-1

and xC-G:3-1 blend films showed shifting in O-H and C-H stretching, at  $3250\text{ cm}^{-1}$  and  $2920\text{ cm}^{-1}$  with respect to the uncrosslinked blend samples. Since in EDC/NHS crosslinking process amide bonds form between  $\text{NH}_2$  groups and  $\text{COOH}$  groups, N-H stretching band at around  $1530\text{ cm}^{-1}$  decreased in crosslinked xC-G:3-1 and xC-G:1-1 when compared to uncrosslinked ones. C-H bending band at around  $1400\text{ cm}^{-1}$  decreased in crosslinked samples.

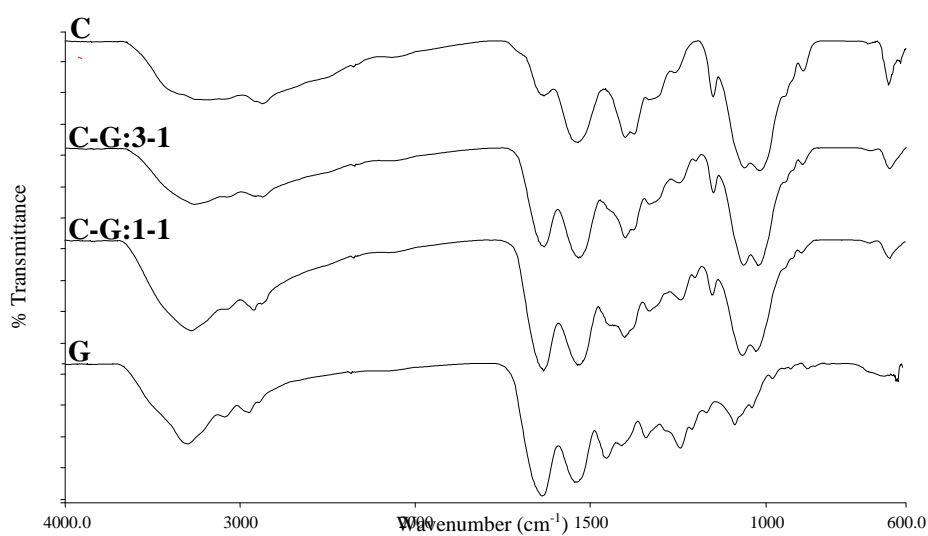


Figure 16 FTIR spectra of uncrosslinked chitosan-gelatin films.

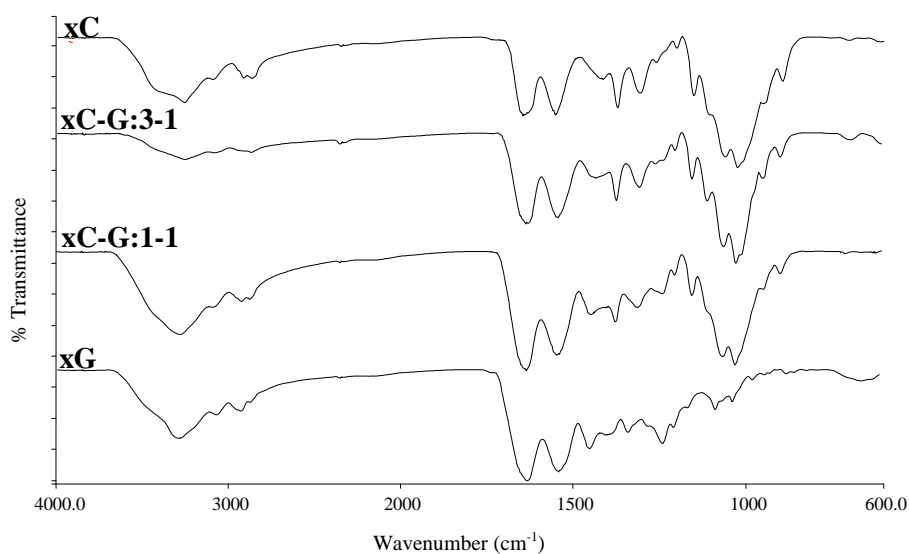


Figure 17 FTIR spectra of crosslinked chitosan-gelatin films.

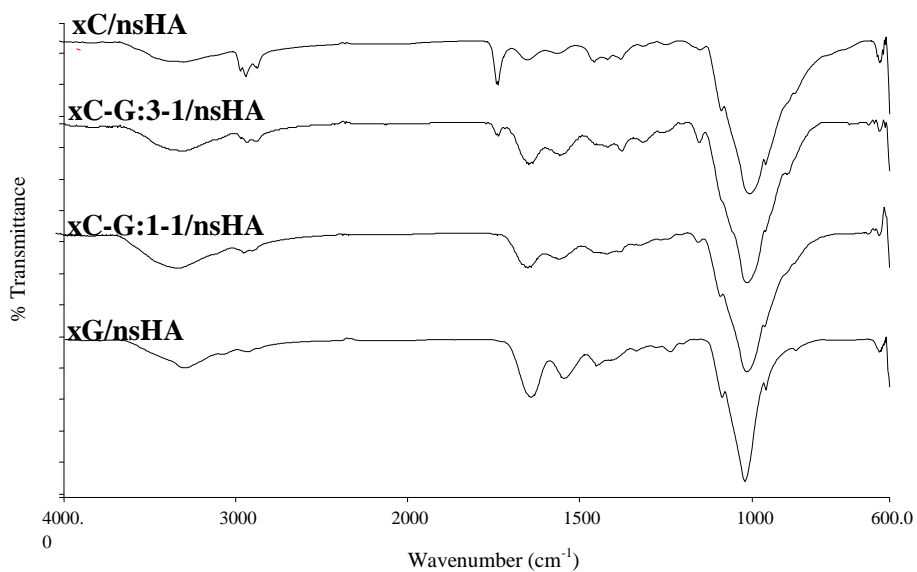


Figure 18 FTIR spectra of crosslinked chitosan-gelatin/non-sintered hydroxyapatite composite films.

In xC/nsHA spectrum, absorption band at  $2925\text{ cm}^{-1}$  can be attributed to aliphatic C-H stretching band. At  $1732\text{ cm}^{-1}$ , C=O band is appeared in xC/nsHA and xC-G:3-

1/nsHA spectra but it decreased or disappeared with increasing gelatin content [Yin et al., 2000 and Mohamed et al., 2008]. FTIR spectra of crosslinked chitosan-gelatin/nonsintered hydroxyapatite (xC-G/nsHA) composites displayed phosphate stretching bands at around  $962\text{ cm}^{-1}$  for all compositions. In the spectrum of all composites; the sharp band at  $1023\text{ cm}^{-1}$  and the bands at around  $603\text{ cm}^{-1}$  indicate asymmetric and bending vibration of phosphate groups of HA.

When crosslinked chitosan-gelatin blend and chitosan-gelatin/nsHA composite films were compared, it is obvious that C=O band of carboxylic group at around  $1630\text{ cm}^{-1}$  and  $\text{NH}_2$  band at around  $1530\text{ cm}^{-1}$ , amide III bands (combinations of C-N stretching and N-H bending deformation) around  $1370\text{-}1200\text{ cm}^{-1}$  decreased in all composites because of  $\text{Ca}^{2+}$  ions-carboxylic groups and  $\text{PO}_4^{3-}$  ions-amino groups interactions in composites. However, in xG/nsHA spectrum, these peaks do not decrease as much as in the others and it confirms the lack of hydroxyapatite-gelatin molecules interactions in xG/nsHA samples that show brittle structures and heterogeneous dispersion in SEM images as well. Another difference between crosslinked blend and composite FTIR spectra is the shifting of peaks around  $1020\text{-}1080\text{ cm}^{-1}$  because of overlapping of skeletal vibrations of chitosan C-O stretching and nsHA  $\text{PO}_4^{3-}$  vibrational peaks.

### ***3.4.2 Differential Scanning Calorimetry Results***

Thermal properties of the blend samples, as well as crosslinking effect and HA addition on thermal properties were examined by Differential Scanning Calorimetric (DSC). DSC curves of crosslinked chitosan-gelatin (xC-G) and chitosan-gelatin/nsHA (xC-G/nsHA) composites are shown in Figure 19 and Figure 20, respectively. Uncrosslinked chitosan-gelatin (C-G) DSC graphs were given in Appendix A.

According to DSC thermograms, endothermic peaks observed around  $50^\circ\text{C}\text{-}150^\circ\text{C}$  are due to removal of adsorbed water and exothermic peaks around  $300^\circ\text{C}$  are associated to decomposition temperatures of the samples [Wang et al., 2008].

The onset of thermal degradation of the chitosan film is observed at 250°C. It is difficult to identify the glass transition temperature ( $T_g$ ) of chitosan (150°C-170°C) since it is semicrystalline. Melting temperature ( $T_m$ ) of chitosan also can not be detected from DSC curve because rigid-rod backbone of chitosan contains strong inter- and intra- hydrogen bonds [Lee et al., 2000]. Nam et al. also reported that electrospun chitosan fiber with 85% deacetylation degree showed exothermic decomposition temperature at around 276°C [Nam et al., 2010].

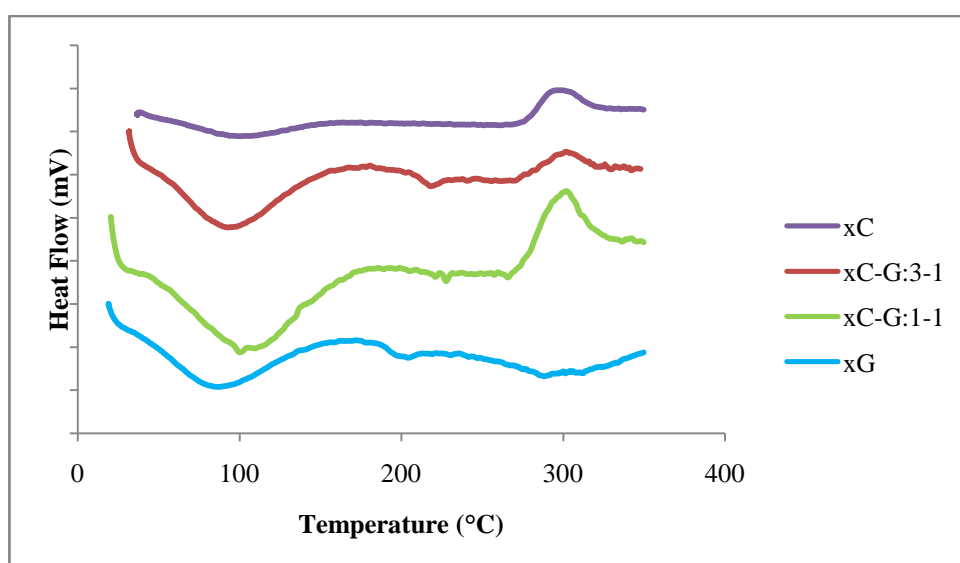


Figure 19 DSC of crosslinked chitosan-gelatin blend films.

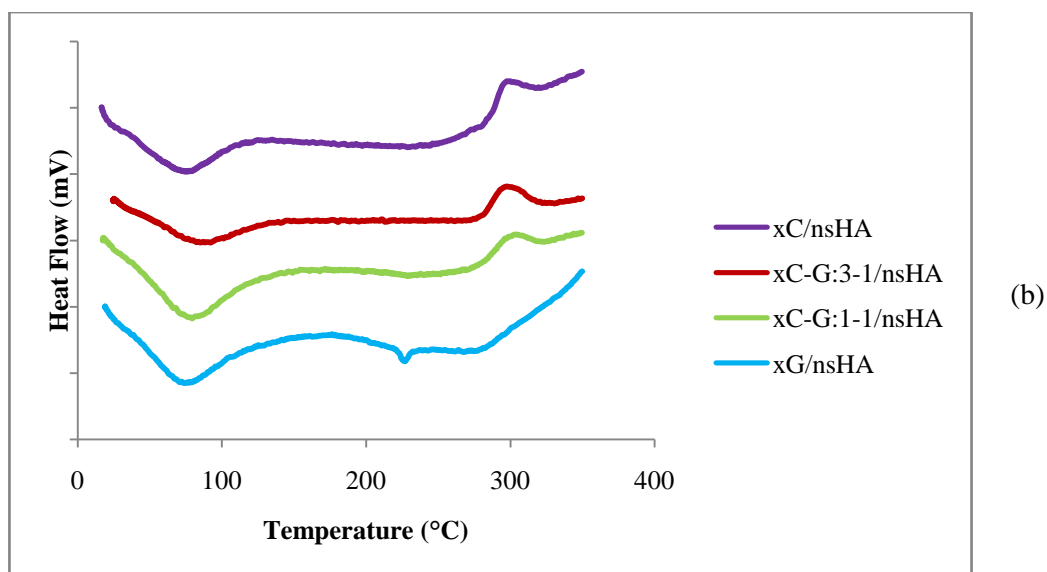


Figure 20 DSC of crosslinked chitosan-gelatin/nsHA composite films.

In the DSC curve of pure crosslinked gelatin film, absorbed water evaporation peak overlaps with denaturation temperature associated to the helix coil transition about 88°C as it was shown in other researches as well [Bigi et al., 2002]. The denaturation temperature of uncrosslinked gelatin films (241°C) shifted to higher values (288°C) with crosslinking, which increases the thermal stability, whereas hydroxyapatite addition lead to the least denaturation temperature at 75°C.

As it is seen in Table 9, the degradation temperatures of uncrosslinked C, C-G:3-1 and C-G:1-1 blend samples were increased with crosslinking process from about 281-290°C to 296-301°C, as expected.



Table 9 Adsorbed water evaporation and decomposition temperatures of chitosan-gelatin and chitosan-gelatin/non-sintered hydroxyapatite composite films.

<b>Sample</b>	<b>Adsorbed Water Evaporation Temperature (°C)</b>	<b>Decomposition Temperature (°C)</b>
<b>C</b>	97.22	281.49
<b>C-G:3-1</b>	98.27	290.51
<b>C-G:1-1</b>	97.54	288.34
<b>G</b>	88.33	241.40
<b>xC</b>	100.42	296.42
<b>xC-G:3-1</b>	94.08	301.43
<b>xC-G:1-1</b>	99.76	301.56
<b>xG</b>	86.20	288.06
<b>xC/nsHA</b>	74.69	297.71
<b>xC-G:3-1/nsHA</b>	85.77	296.5
<b>xC-G:1-1/nsHA</b>	78.77	303.94
<b>xG/nsHA</b>	74.65	226.35

It was stated that chitosan-gelatin scaffolds show two transitions peak in DSC graphs coming from dehydration of water molecules at below 200°C and for decompositions of samples at above 200°C [Thein-Han et al., 2009].

nsHA addition lead to shifting of decomposition temperature to higher degrees in composites, except for xC-G:3-1/nsHA sample. It may be because of the ionic interactions between  $\text{Ca}^{2+}$  and  $\text{PO}_4^{3-}$  groups of hydroxyapatite and  $\text{COO}^-$  and  $\text{NH}_3^+$  groups of chitosan-gelatin blends resulting with more stable structures in these composite samples.

xC-G/nsHA composite films DSC graphs demonstrated reduced water evaporation temperatures because of easier evaporation of unbounded water from highly hydrophilic amorphous hydroxyapatite particles.

### ***3.4.3 Mechanical Properties of Film Structures***

Mechanical properties of the blend and composite films were obtained by applying tension stress and recording the force applied and change in dimensions. The obtained results are given in Table 10. Since xG/nsHA films could not be obtained in necessary rectangular dimensions (10 mm x 40 mm), they could not be tested in mechanical analysis.

In the literature, it was reported that the mechanical properties of chitosan-gelatin structures are affected mainly from molecular weight and deacetylation degree of chitosan, water content in the film samples and the ratios of both components [Trung et al., 2006 and Kolodziejska et al., 2007]. Furthermore, Arvanitoyannis et al. suggested that protein-based film structures such as; gelatin films show very brittle and susceptible to cracking because of strong cohesive energy density of the polymer [Arvanitoyannis et al., 1998]. In fact, comparison of mechanical behaviors of these samples with literature is hard because preparation methods (plasticizer addition, crosslinking agents, solubilization method) and chitosan-gelatin ratios change among the studies. However, it can be said that reported mechanical characteristics of films prepared by similar methods were different from those obtained in this study. For example, Cheng et al., reported that chitosan films demonstrated E values at about 1.25 GPa and these values indicated 70% decrease with gelatin addition in chitosan-gelatin blend samples [Cheng et al., 2003]. In our study; hardness of the uncrosslinked and crosslinked blend films diminished about 50% and 60% with increasing gelatin content, respectively. However, E values of all chitosan samples were about 2.04-2.52 GPa.

Table 10 Mechanical properties of crosslinked (C-G) blend and (C-G/nsHA) composite films.

Sample	UTS (MPa)	E (GPa)	SAB (%)
<b>C</b>	139.25 ± 22.33	2.04 ± 0.70	11.64 ± 1.33
<b>C-G:3-1</b>	126.49 ± 11.07	1.89 ± 0.30	10.67 ± 3.57
<b>C-G:1-1</b>	103.46 ± 7.82	1.80 ± 0.24	7.80 ± 1.40
<b>G</b>	50.16 ± 6.94	0.97 ± 0.09	6.40 ± 1.42
<b>xC</b>	190.50 ± 13.33	2.52 ± 0.28	13.72 ± 1.17
<b>xC-G:3-1</b>	171.87 ± 16.20	2.61 ± 0.27	10.87 ± 4.07
<b>xC-G:1-1</b>	153.69 ± 18.00	2.77 ± 0.99	8.70 ± 2.90
<b>xG</b>	108.73 ± 18.44	1.04 ± 0.22	16.15 ± 3.50
<b>xC/nsHA</b>	140.04±4.47	2.32±0.24	11.59±1.35
<b>xC-G:3-1/nsHA</b>	99.75±15.87	2.13±0.28	7.59±1.01
<b>xC-G:1-1/nsHA</b>	88.07±13.28	2.23±0.12	6.9±1.13

According to the tensile test results; it was observed that the ultimate tensile strength (UTS) and Young's modulus (E) of uncrosslinked pure chitosan showed the highest values (UTS = 139 MPa, E = 2.04 GPa) in uncrosslinked blends and mechanical properties of all samples decreased with increasing gelatin content in the films, as expected. This behavior was due to the higher crystallinity and mechanical strength of chitosan when compared to gelatin. In addition, electrostatic interactions between the ammonium ( $-\text{NH}_3^+$ ) ions of the chitosan and the carboxylate ( $-\text{COO}^-$ ) ions of the gelatin may cause deformation in the crystallinity of chitosan and therefore have an effect on the decrease of tensile strength. The value of UTS of chitosan was found at about 139 MPa and gradually decreased to 103 MPa for C-G:1-1 samples. For pure gelatin UTS value was about 50 MPa.

Ultimate tensile strength, Young's modulus (E) and strain at break (SAB) values were increased as a result of crosslinking. It can be concluded that crosslinking caused to improved mechanical stability.

However, non-sintered hydroxyapatite addition into chitosan-gelatin blend films decreased the ultimate tensile strength values of samples in different chitosan-gelatin ratios. While Young's modulus results of xC-G and xC-G/nsHA films decreased in small amount (8%-23%), ultimate tensile strength and strain at break values reduced with nsHA addition in a significant range (26%-35%). It is reported that HA particles may lead to less ductility in polymer-HA composite structures and initial cracks may arise from larger HA particles in polymer matrix [Suchanek et al., 1998].

As a result, when tensile strength of cortical bone value between 50-150 MPa is considered, chitosan-gelatin/nonsintered hydroxyapatite composite films with UTS results in the range of 88-140 MPa have quite suitable UTS values for cortical bone tissue engineering applications.

#### ***3.4.4 Surface Hydrophilicity***

Since surface hydrophilicity has significant effect on cell adhesion; wettabilities of the samples were investigated by contact angle measurements with different liquids. Contact angle values of deionized water (DW), diiodomethane (DIM), formamide (FA) and dimethylsulfoxide (DMSO) on the surface of blend and composite films are given in Table 11. Although chitosan and gelatin are hydrophilic polymers (with  $\text{NH}_2$  and OH groups), water contact angle measurements were found as high as  $114^\circ$  and  $98^\circ$  for uncrosslinked chitosan and gelatin samples, respectively, most probably due to the hydrophobic backbone of the polymer. For the blends; it was observed a gradual decrease with crosslinking process and increase with increasing gelatin content. For example, water contact angle of chitosan is  $114^\circ$  and it decreased to  $84^\circ$  when it is crosslinked. The most significant change in water contact angle after crosslinking is in xC-G:1-1 film with the most hydrophilic character ( $\theta=53^\circ$ ). These changes may be due to the reorientation of polar functional groups toward to the top surface of blend films after crosslinking process especially in crosslinked films with chitosan-gelatin:1-1 ratio. When water contact angle of chitosan is compared with literature, it can be suggested that crosslinked sample has more similar value to contact angle of 2% (w/w) chitosan film prepared in 1% (v/v) acetic acid (same mass

and volume values with this study) that has showed 88° contact angle [Kuo et al., 2005]. Moreover gelatin showed the least water contact angle value (98°) in uncrosslinked samples and the second least value (77°) in crosslinked ones. Ai et al., also reported that glutaraldehyde crosslinked gelatin showed decreasing contact angle with crosslinking process from about 84° to 74° [Ai et al., 2002].

In composites, nsHA added chitosan exhibited 71° water contact angle and the enhanced hydrophilicity caused by nsHA addition in composite constructs with water contact angles 62° and 70° for xC-G:3-1/nsHA and xC-G:1-1/nsHA, respectively. This result may be assigned to availability of hydrophilic -OH groups of hydroxyapatite.

Table 11 Contact angle values of the uncrosslinked, crosslinked (x) chitosan-gelatin blend and crosslinked chitosan-gelatin/nsHA composite (x/nsHA) films.

		Contact Angle (Degree)											
Sample Liquid	C			C-G:3-1			C-G:1-1			G			
	-	x	x/ns HA	-	x	x/ns HA	-	x	x/ns HA	-	x	x/ns HA	
DW	113.9	84.4	70.81	105.0	82.4	62.42	105.1	53.0	69.94	98.3	77.3	-	
DIM	46.6	37.7	40.20	40.0	34.1	40.23	40.7	28.2	35.34	40.0	36.3	-	
FA	54.5	43.3	40.71	46.3	48.4	38.88	46.1	37.2	42.51	32.4	28.9	-	
DMSO	58.0	16.7	17.08	25.6	14.4	19.58	20.4	14.6	16.38	15.3	18.5	-	

For the liquids, used in the calculation of SFE values of the prepared films, the surface tension and its components were obtained from literature [Cantin et al., 2006 and Ozcan et al., 2007] and given in Table 12.

Table 12 Surface free energy parameters (acidic and basic components) of test liquids according to acid-base approach.

	<b>Total SFE</b>	<b>Lifshitz–Van der Waals component</b>	<b>Acid-Base interaction</b>	<b>Acidic component</b>	<b>Basic component</b>
<b>Liquid</b>	$\gamma_L$ (mJ/m <sup>2</sup> )	$\gamma_L^{LW}$ (mJ/m <sup>2</sup> )	$\gamma_L^{AB}$ (mJ/m <sup>2</sup> )	$\gamma_L^+$ (mJ/m <sup>2</sup> )	$\gamma_L^-$ (mJ/m <sup>2</sup> )
<b>DW</b>	72.8	21.8	51	25.5	25.5
<b>DIM</b>	50.8	50.8	0	0	0
<b>FA</b>	58.0	39	19	2.3	39.6
<b>DMSO</b>	44	36	8	0.5	32

The calculated SFE results of samples from different approaches (as explained in Section 1.5.2) are given in Table 13. It was observed that the results are very much dependent on the method used in calculation and changes between 32 mJ/m<sup>2</sup> and 56 mJ/m<sup>2</sup>. According to Acid-Base and Harmonic approaches, total SFE values of uncrosslinked samples do not show significant fluctuations with increasing gelatin content. When compared with the literature, chitosan SFE value calculated with Harmonic approach (40 mJ/m<sup>2</sup>) showed similar value with chitosan prepared by similar methods (38 mJ/m<sup>2</sup>) [Wang et al., 2009]. In Zisman and Geometric approaches, it is obvious that SFE values of uncrosslinked blends increase with gelatin content from 38 mJ/m<sup>2</sup> to 46 mJ/m<sup>2</sup> and from 43 mJ/m<sup>2</sup> to 50 mJ/m<sup>2</sup>, respectively. This may be because of high number of COOH and NH<sub>2</sub> groups in gelatin structure that increase the SFE of surfaces and decrease water contact angle.

Acid Base and Harmonic approaches indicate that total SFE values of uncrosslinked films were increased when blend films were crosslinked with EDC/NHS. As the total SFE value of sample surface is close to total SFE of liquid drop, sample becomes more wettable. So, according to Acid-Base approach; total SFE of xC-G:1-1 blend sample with 46.32 mJ/m<sup>2</sup> showed the highest and closest value to total SFE of water and this result supported the contact angle measurement demonstrating xC-G:1-1 blend sample as the most wettable surface with water contact angle of 53°.

Table 13 SFE values of chitosan-gelatin films.

Sample	Zisman $\gamma$ (mJ/m <sup>2</sup> )	Harmonic $\gamma$ (mJ/m <sup>2</sup> )	Geometric $\gamma$ (mJ/m <sup>2</sup> )	Acid Base $\gamma$ (mJ/m <sup>2</sup> )
C	37.96	39.61	42.81	32.34
C-G:3-1	44.74	45.15	49.49	33.71
C-G:1-1	45.17	45.28	50.02	32.48
G	46.03	47.43	50.14	33.84
xC	44.38	46.57	45.32	42.77
xC-G:3-1	44.43	46.70	45.18	44.46
xC-G:1-1	41.56	55.71	51.87	46.32
xG	44.74	49.66	47.25	45.46
xC/nsHA	42.10	48.41	45.33	44.59
xC-G:3-1/nsHA	39.51	50.79	47.17	45.07
xC-G:1-1/nsHA	42.87	49.09	46.07	45.62

There is not a significant trend in crosslinked nsHA added composite samples when they were compared to crosslinked blend samples. However, if uncrosslinked samples are considered, according to Harmonic and Acid Base approaches nsHA addition increased total SFE values. For example, for chitosan films, total SFE values increased from about 40 mJ/m<sup>2</sup> to 48 mJ/m<sup>2</sup> for Harmonic approach and from 32 mJ/m<sup>2</sup> to 45 mJ/m<sup>2</sup> for Acid Base approach. This change may be due to contribution of high amount of OH groups from hydroxyapatite structures.

### 3.4.5 Surface Morphology Analysis

Surface morphology of the film structures is one of the important parameters in initial cell attachment. Thus, SEM images of the sample surfaces were examined to provide information about roughness and homogeneity of the blend and composite samples (Figure 21).

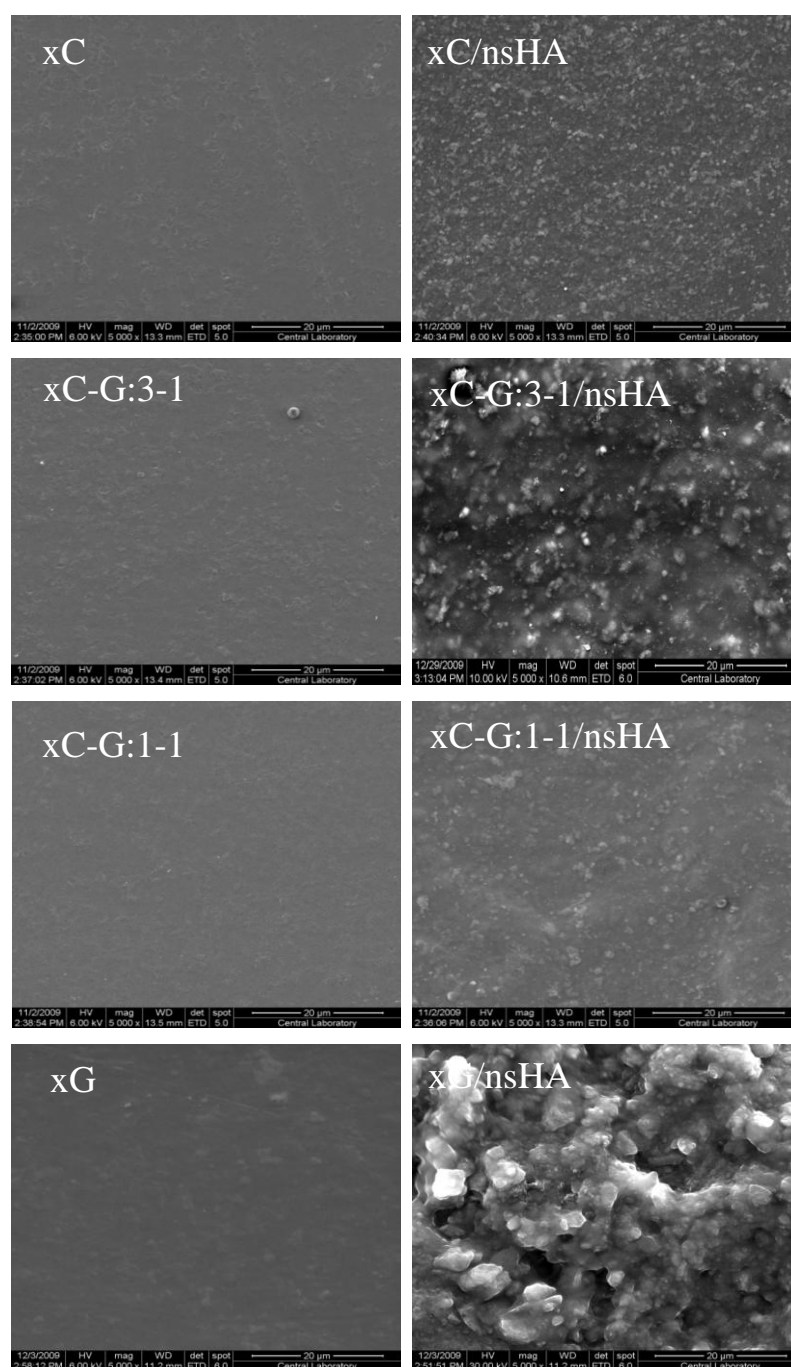


Figure 21 SEM micrographs of crosslinked chitosan-gelatin (left column) and chitosan-gelatin/nsHA composite (right column) films X5000.

Scanning electron microscopy (SEM) images of chitosan-gelatin blend films indicate the presence of smooth surfaces without phase disengagement supporting the idea of



homogenous chitosan-gelatin blend formation while chitosan-gelatin/nsHA images showed rough surfaces with homogenous hydroxyapatite particle dispersion through the chitosan-gelatin blend and embedded nsHA particles into polymeric matrix without distinct polymer-nsHA interfaces. Phase separation in SEM image of xG/nsHA film confirms the FTIR and DSC results; lack of chemical interactions between nsHA particles and gelatin molecules.

### ***3.4.6 Swelling Behavior of Film Structures***

Dissolution of uncrosslinked blend samples were quite fast in aqueous medium therefore, only crosslinked films and composites were tested in swelling tests.

Table 14, Figure 22 and Figure 23 show the percent swelling ratios that were calculated by Equation 2.1 as a function of time.

xC and xC-G:3-1 samples reached to equilibrium swelling state in 3 h and 6 h, respectively. The equilibrium swelling degree of crosslinked chitosan showed the least value ( $155.3\pm 11.5\%$ ) and chitosan-gelatin:3-1 film had the second least equilibrium value ( $172.4\pm 4.3\%$ ). In crosslinked chitosan-gelatin blend films, maximum equilibrium swelling degree ( $333.0\pm 16.9\%$ ) was observed for xC-G:1-1. Kim et al., reported that the swelling ratio would be enhanced by the increasing of free –OH, –NH<sub>2</sub> and –NHOC(=O)CH<sub>3</sub> groups of the chitosan [Kim et al., 2005]. However, Haider et al. claimed that chitosan amount increase also lead to generation of network structure (through the electrostatic interactions between NH<sub>3</sub><sup>+</sup> of chitosan and COO<sup>-</sup> ions of gelatin) that result with improved stiffness in complex chains of structure and swelling ratio may decrease [Haider et al., 2008]. So, by combining these two approaches; it may be said that swelling ratio may show the highest value with the combination of these two opposite effects in xC-G:1-1 film sample. Contact angle values also verified that these hydrophilic groups amount was higher in xC-G:1-1 films.

Table 14 Swelling ratios (% w/w) of crosslinked blend and composite films.

Sample Time (h)	xC	xC-G:3-1	xC-G:1-1	xG	xC/nsHA	xC-G:3-1/nsHA	xC-G:1-1/nsHA
1	150.6±10.9	168.4±3.0	319.9±7.2	232.1±4.7	137.6±2.3	159.2±1.2	162.7±2.2
3	154.6±10.9	172.4±4.3	321.2±15.9	262.7±0.6	137.5±2.1	157.0±9.9	162.7±2.2
6	155.3±11.5	172.5±4.3	324.1±12.5	262.2±5.5	139.6±0.5	167.3±0.9	167.3±0.8
12	155.9±12.1	172.6±4.2	327.8±17.1	264.8±4.6	142.5±2.1	167.3±0.9	173.6±2.0
24	156.1±11.8	172.6±4.2	333.0±16.9	268.7±0.5	149.4±9.3	173.5±2.1	181.7±5.6
48	156.1±11.8	172.6±4.2	335.6±16.7	270.7±0.3	153.4±15.0	177.5±3.5	186.3±4.2

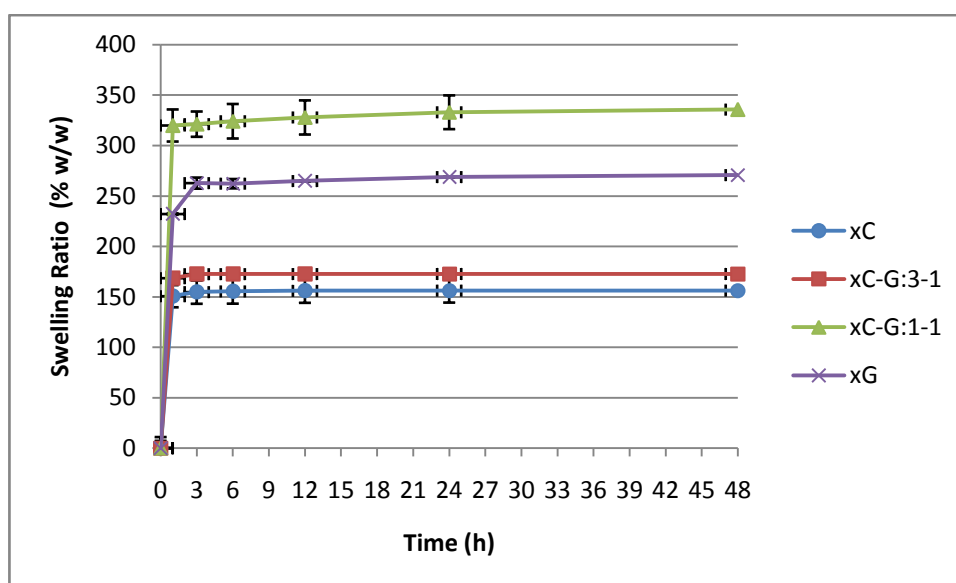


Figure 22 Swelling behavior of crosslinked chitosan-gelatin blends.

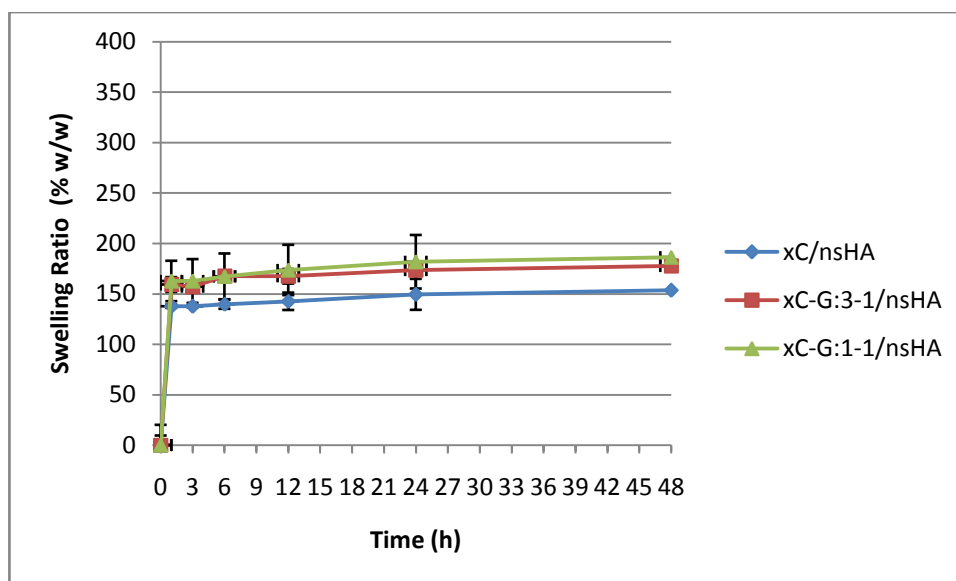


Figure 23 Swelling behavior of crosslinked chitosan-gelatin/nsHA composite samples.

Swelling ratio results of crosslinked chitosan-gelatin/nsHA composite samples indicated that xC-G:1-1/nsHA films had the highest swelling ratios increasing from  $162.7 \pm 2.2\%$  to  $186.3 \pm 4.2\%$  from 1 h to 48 h. xC-G:3-1/nsHA films showed a small decrease in swellability and had swelling ratio of  $177.5 \pm 3.5\%$  at 48 h. xC/nsHA films demonstrated the least swellability ( $153.4 \pm 15.0\%$  at 48 h) in composite constructs as in the example of chitosan in blend samples. The reason of decreasing swelling ratio of composite samples with respect to polymeric blends may be the interactions of HA with polymeric groups such as;  $-\text{COO}^-$  and  $-\text{NH}_3^+$ . As a result, as described before, these groups that may enhance swellability of the samples, may decrease in content.

### 3.4.7 Cell Affinity and Proliferation of Film Structures

Uncrosslinked chitosan-gelatin blend structures degraded quite rapidly in aqueous media, therefore, only crosslinked samples were examined in cell adhesion and

proliferation tests. MTS assay results of SaOs-2 cells on crosslinked film samples are given in Figure 24.

Cell attachment and proliferation as a function of time on the tissue engineered constructs are very important properties that show cytocompatibility and thus suitability of the surfaces for bone tissue engineering approaches.

MTS assay showed that in the first day, among the crosslinked chitosan-gelatin blend films, pure gelatin showed the highest cell attachment ( $5754 \pm 3083$  cells/cm<sup>2</sup>); chitosan had higher cell number ( $4654 \pm 965$  cells/cm<sup>2</sup>) than its blends xC-G:3-1 and xC-G:1-1 films ( $3144 \pm 434$  cells/cm<sup>2</sup>). However, among the chitosan-gelatin blend samples, SaOs-2 cell proliferation on day 7 increased with the increase in gelatin content. This can be explained by on the presence of RGD sequences in gelatin that promote cell attachment to the surfaces of the films. Gelatin films (xG) showed higher cell number ( $44597 \pm 188$  cells/cm<sup>2</sup>) than chitosan ( $15363 \pm 931$  cells/cm<sup>2</sup>) in blend films at day 7. This significantly higher proliferation indicates the superior cellular compatibility of the gelatin containing scaffolds.

Among the chitosan-gelatin/nsHA composite structures, the effect of increase in gelatin content was a decrease in cell number, especially detectable on day 7. xC/nsHA indicated the highest cell proliferation on day 1 ( $4736 \pm 2536$  cells/cm<sup>2</sup>) and day 7 ( $25283 \pm 2962$  cells/cm<sup>2</sup>). This might be the result of a gelatin-HA interaction (between COO<sup>-</sup> and NH<sub>3</sub><sup>+</sup> groups of amino acid sequences and Ca<sup>2+</sup> and PO<sub>4</sub><sup>3-</sup> ions of HA) leading to inhibition of RGD-like sequences. It was claimed that after crosslinking process, the distance between gelatin and hydroxyapatite decreases within the critical length and higher concentration of Ca<sup>2+</sup> and COO<sup>-</sup> may have higher chance to bind each other [Chang et al., 2003]. So, cell proliferation decreases to  $17987 \pm 3893$  cells/cm<sup>2</sup> and  $13018 \pm 427$  cells/cm<sup>2</sup> for xC-G:3-1/nsHA and xC-G:1-1/nsHA, respectively.

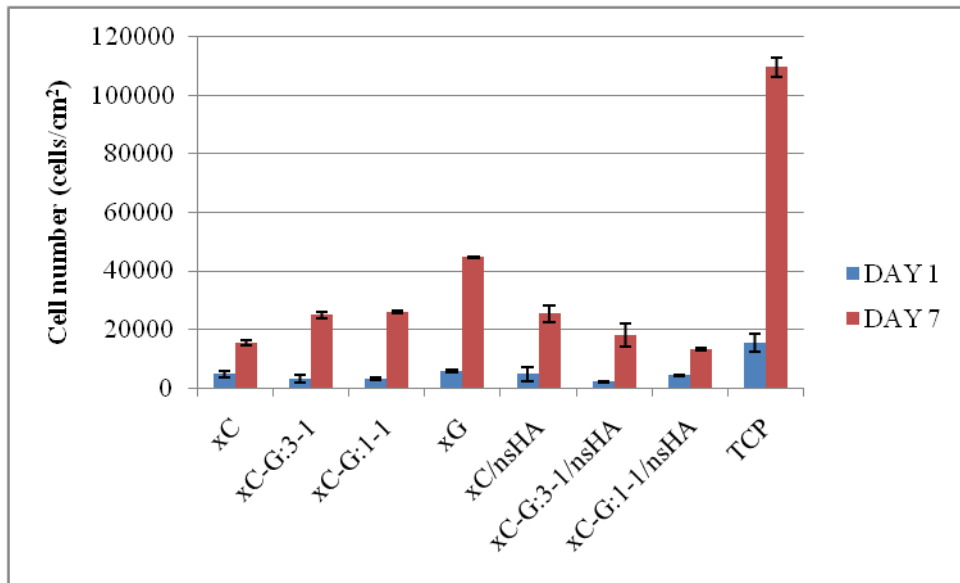


Figure 24 SaOs-2 proliferation on films.

Fluorescence micrographs of SaOs-2 cells cultured on crosslinked chitosan-gelatin blend films were obtained to study the cells attached to the the film surfaces (Figure 25). DAPI and Phalloidin stained cells have blue nuclei and green cytoplasm. It is a commonly used staining method with chitosan-based scaffolds that have autofluorescence. Fluorescence micrographs reflect that increasing gelatin amount in blend samples stimulates the attachment of osteosarcoma cells on film structures.

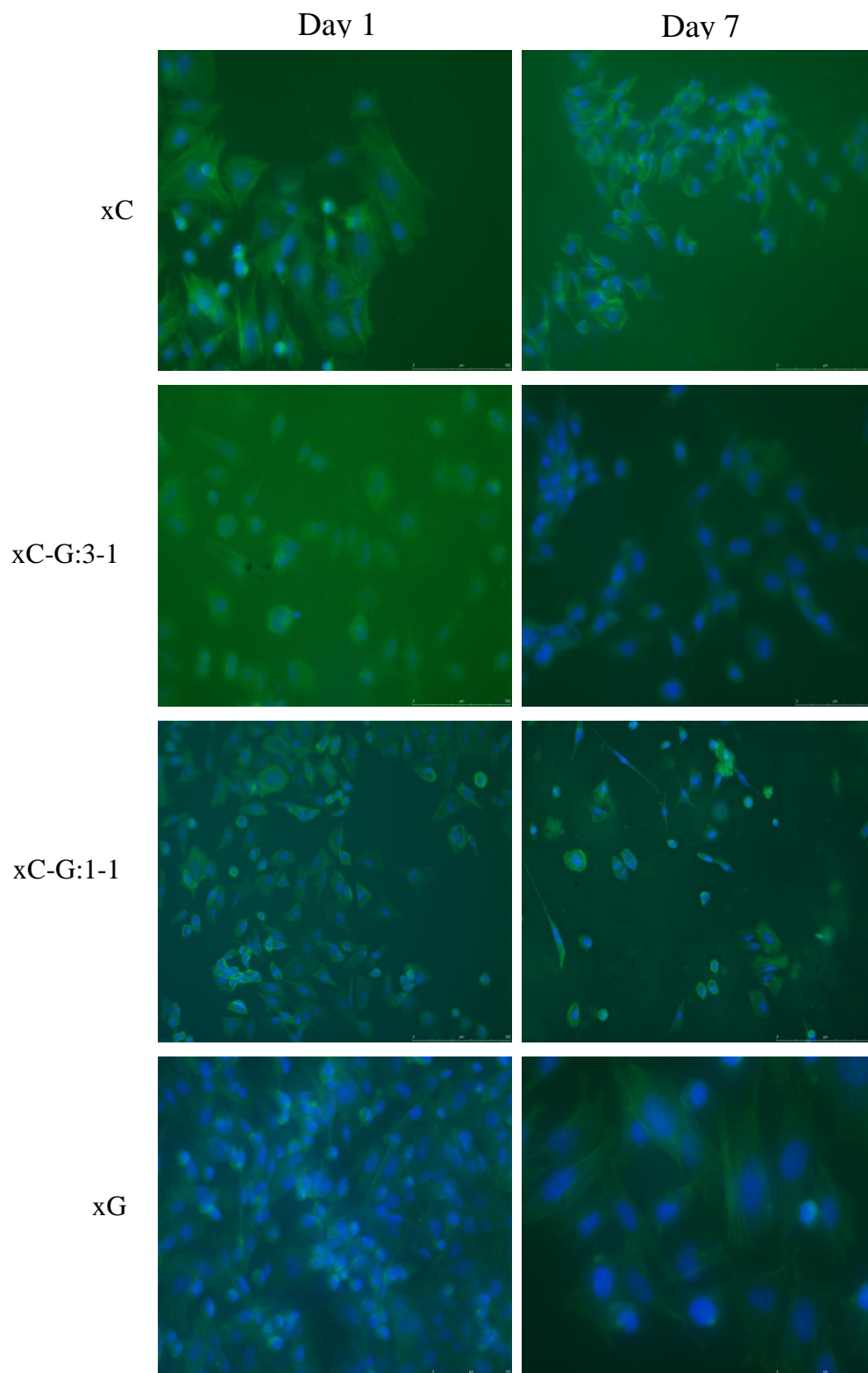


Figure 25 Fluorescence microscopy images of crosslinked chitosan-gelatin blend films with SaOs-2 cells cultured on them for 1 and 7 days (x20).

DAPI (nuclei) and phalloidin (cytoplasm) stained chitosan-gelatin/nsHA composites showed comparable cell proliferation and higher cell viabilities on xC/nsHA and xC-G:3-1/nsHA composite films with respect to xC-G:1-1 film at day 7 (Figure 26). Moreover, adherent cells enhanced on all films from day 1 to 7.

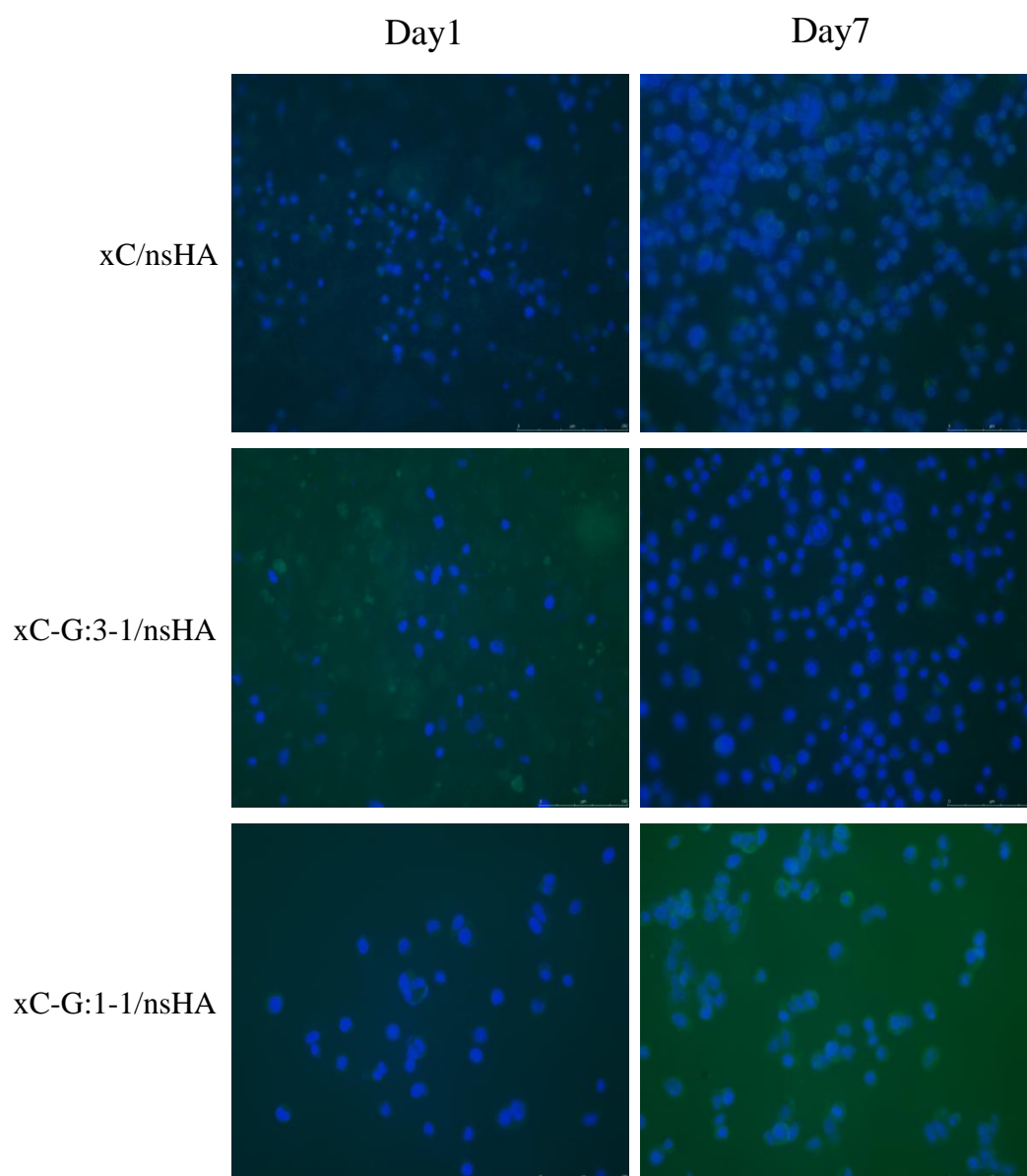


Figure 26 Fluorescence microscopy images of crosslinked chitosan-gelatin/nsHA composite films seeded with SaOs-2 cells. After 1 and 7 days (x20).

Since cell-material interactions on film structures were not observed clearly by fluorescence microscopy, SEM micrographs of all the prepared samples were obtained. SEM images of blend films (Figure 27) with SaOs-2 cells demonstrated that cell spreading was remarkable on day 7, while they had more spherical shapes on day 1. xC films demonstrated the least cell spreading at day 1 whereas star-like spread cells were seen on gelatin added blend samples. Furthermore, cell densities also were higher on the films with increased gelatin amount. For example, it is obviously seen that high coverage of xC-G:1-1 and xG film surfaces with increasing cell densities on day 7.



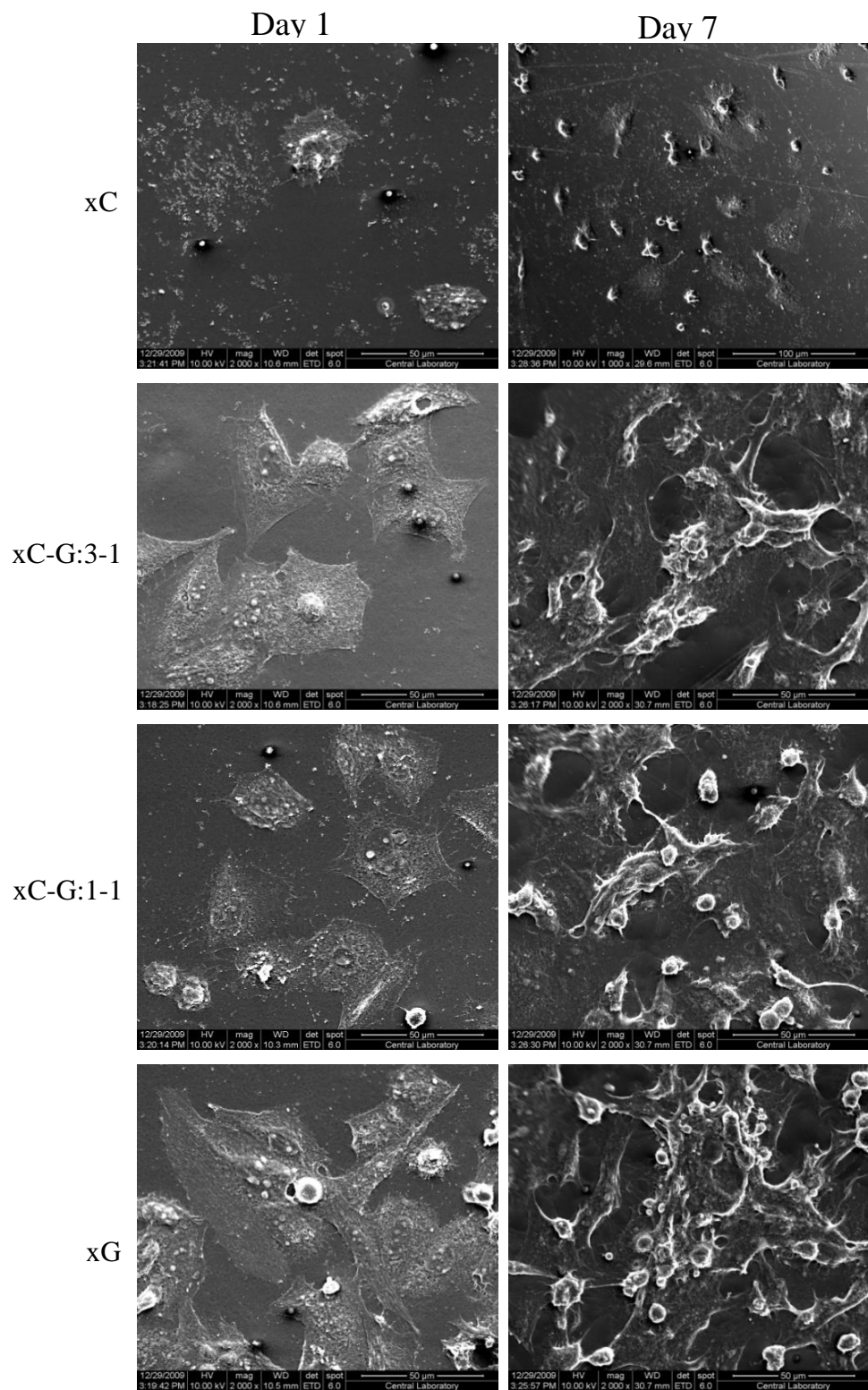


Figure 27 SEM images of cell morphology of SaOs-2 cells seeded on crosslinked chitosan-gelatin blend films cultured for 1 day and 7 days.

In SEM images of composite films (Figure 28), it is obvious that cells were spread on nsHA added surfaces after 7 days even though they showed spherical shapes on Day 1. Contrary to the expectations from the MTS values the SEM micrographs do not show a significant difference in cell spreading between the films with different chitosan-gelatin ratios. Rizzi et al., reported that SEM images of biodegradable polymer/non-sintered HA films (prepared by PCL and PLA) showed that the human osteoblasts spread in higher degree on the film regions of exposed non-sintered HA compared to polymer coated surfaces [Rizzi et al., 2001]. So, according to the SEM micrographs of this study, it can be suggested that nsHA particles encouraged cells spreading if sufficient were exposed at the surface of the scaffold.

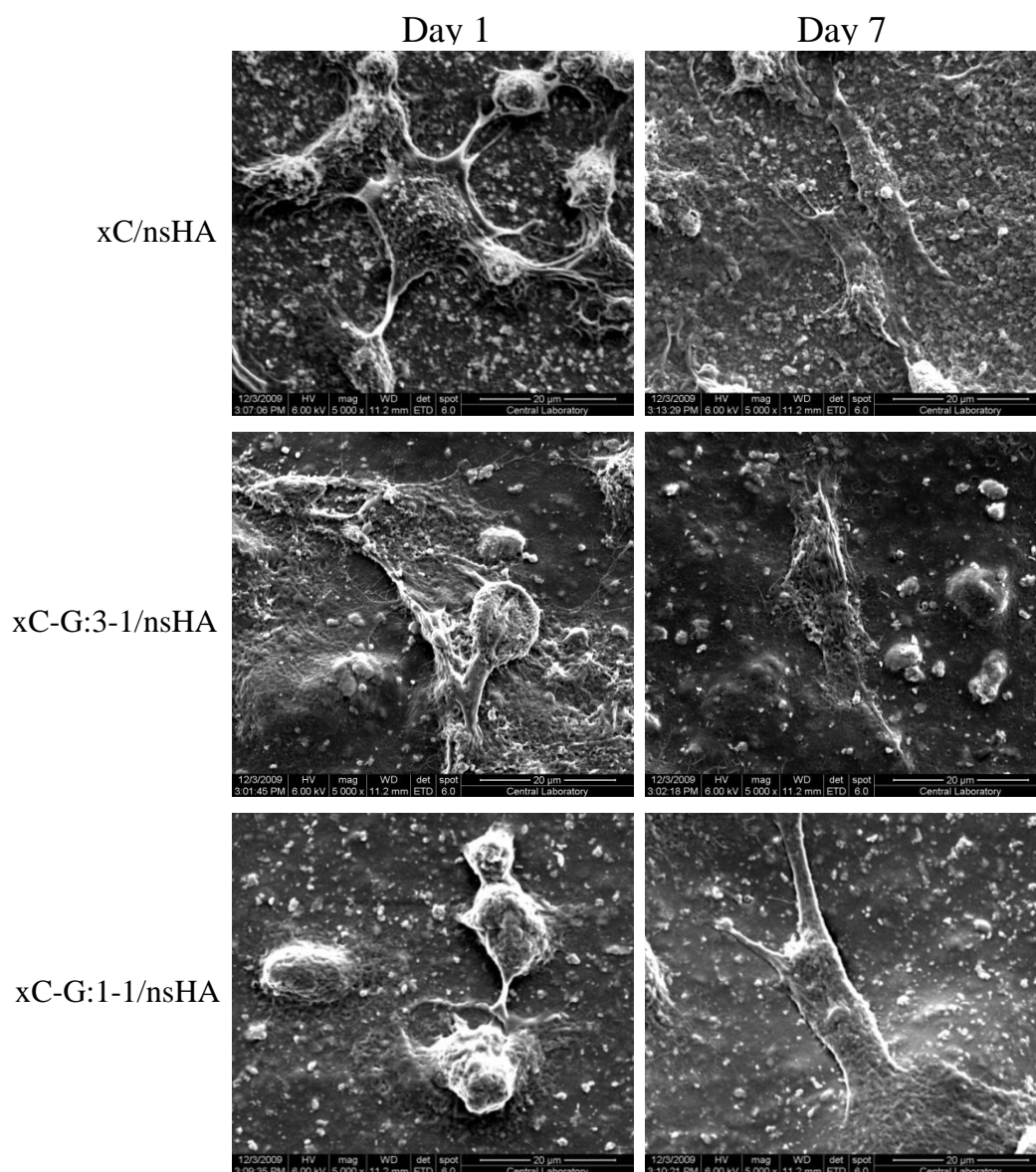


Figure 28 SEM images of SaOs-2 cells seeded on crosslinked chitosan-gelatin/nsHA composite films and cultured for 7 days.

### 3.5 Porous Scaffold Preparation

Before freeze-drying, chitosan-gelatin solutions were frozen at  $-80^{\circ}\text{C}$ , on  $\text{N}_2(\text{liq})$  and in  $\text{N}_2(\text{liq})$  to observe the effect of this temperature on scaffold structure. At the end of the freeze-drying process, scaffolds that were frozen at  $-80^{\circ}\text{C}$  and in  $\text{N}_2(\text{liq})$ ,

showed laminar three-dimensional structures while scaffolds that were frozen on  $N_2(\text{liq})$  had irregular shaped pores with homogenous distribution in the sponge (Figure 29).

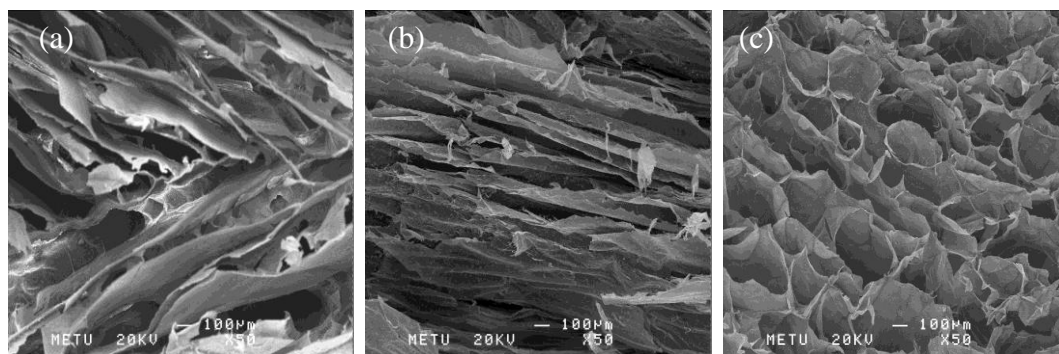


Figure 29 SEM micrographs of spxC-G:1-1/sHA porous scaffolds frozen (a) at  $-80^{\circ}\text{C}$  (b) in  $N_2(\text{liq})$ , and (c) on  $N_2(\text{liq})$ .

In the rest of the study scaffolds were frozen on  $N_2(\text{liq})$  before lyophilization. Considering the results obtained from the characterization of C-G film samples, C-G:1-1 was chosen as the optimum composition for 3-D scaffold preparation.

### **3.6 Porous Scaffold Characterization**

#### **3.6.1 FTIR-ATR Examination**

EDC/NHS crosslinking process of all scaffolds was applied in an aqueous media during two days. During this period the added sintered or non-sintered hydroxyapatite particles may have degraded or left the porous composite structures because of exposure to ethanol or highly alkaline solutions or the neutralization step of crosslinking that took at least two days (Section 2.2.2.3). However, FTIR results confirmed the presence of hydroxyapatite particles in crosslinked and freeze-dried chitosan-gelatin three-dimensional constructs as was shown by the  $\text{PO}_4^{3-}$  peaks at  $961\text{ cm}^{-1}$ ,  $603\text{ cm}^{-1}$  and OH vibration peak of HA at  $629\text{ cm}^{-1}$  (Figure 30).

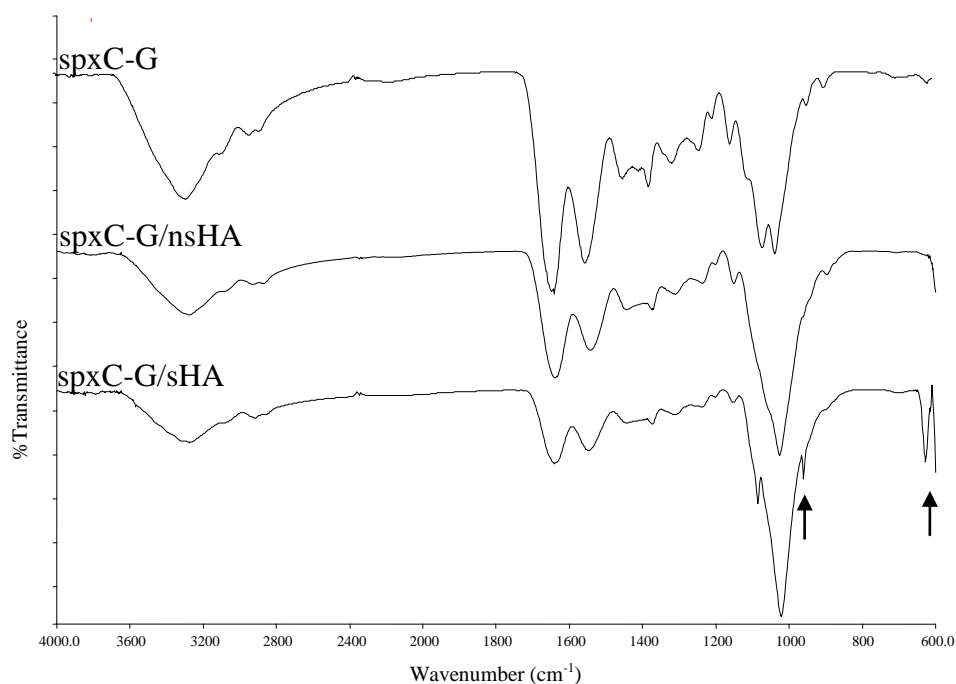


Figure 30 FTIR-ATR analysis of crosslinked various chitosan-gelatin sponges.

### 3.6.2 Scaffold Morphology

SEM images of the chitosan-gelatin (spxC-G), chitosan-gelatin/non-sintered hydroxyapatite (spxC-G/nsHA) and chitosan-gelatin/sintered hydroxyapatite (spx(C-G/sHA) scaffolds are given in Figure 31. Pore sizes, ranged from 100  $\mu\text{m}$  to 500  $\mu\text{m}$ , and therefore they are suitable for vascularization process according to the literature [Hutmacher et al., 2007]. In the scaffolds the lowest pore size was formed in spxC-G/nsHA samples about 100  $\mu\text{m}$  while spxC-G and spxC-G/sHA showed larger pore sizes about 200  $\mu\text{m}$  and 500  $\mu\text{m}$ , respectively. Pore walls of spxC-G and spxC-G/sHA samples showed similar thicknesses (5-10  $\mu\text{m}$ ) but it seemed that spxC-G/nsHA had thicker pore walls (50-60  $\mu\text{m}$ ).

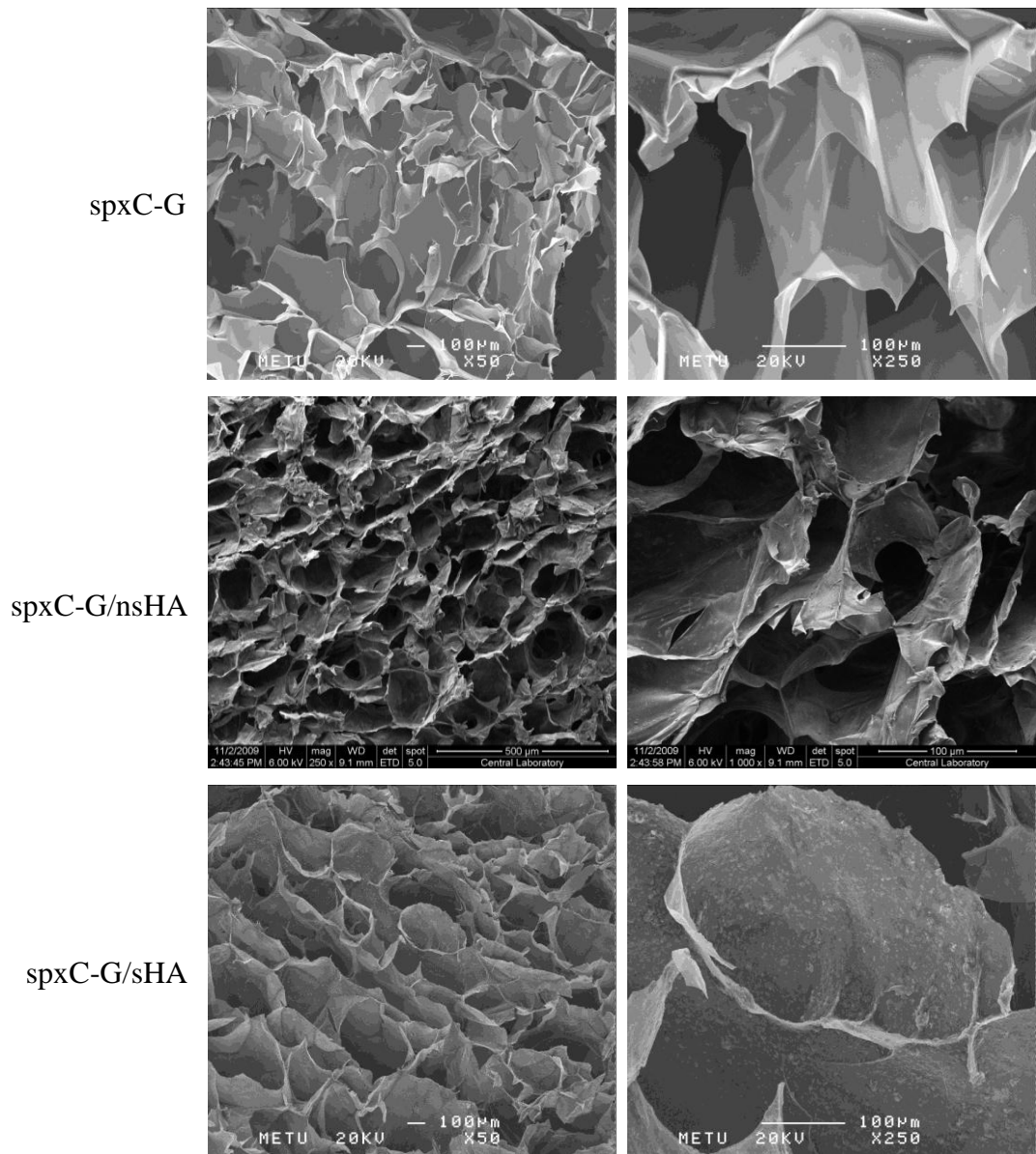


Figure 31 Scanning electron microscopy images of chitosan-gelatin-based three-dimensional porous scaffolds. Second column presents the magnified version of the first column.

SEM images also verified that non-sintered and sintered HA particles remain on the scaffold surface of spxC-G/nsHA and spxC-G/sHA after crosslinking treatment despite 48 h aqueous medium exposure.

Homogenous, irregular pore distribution can be observed in all three-dimensional porous scaffold samples that are essential properties of the scaffolds to provide transfer of nutrients for cells and subsequent tissue ingrowth. Moreover, hydroxyapatite addition did not cause to failure of structures. Pore walls of the scaffolds had uniform HA distribution and particle sizes about 5-10  $\mu\text{m}$  as it can be seen from Figure 32. These HA embedded pore walls may enhance cell affinities towards the scaffolds with good biocompatibility of hydroxyapatite.

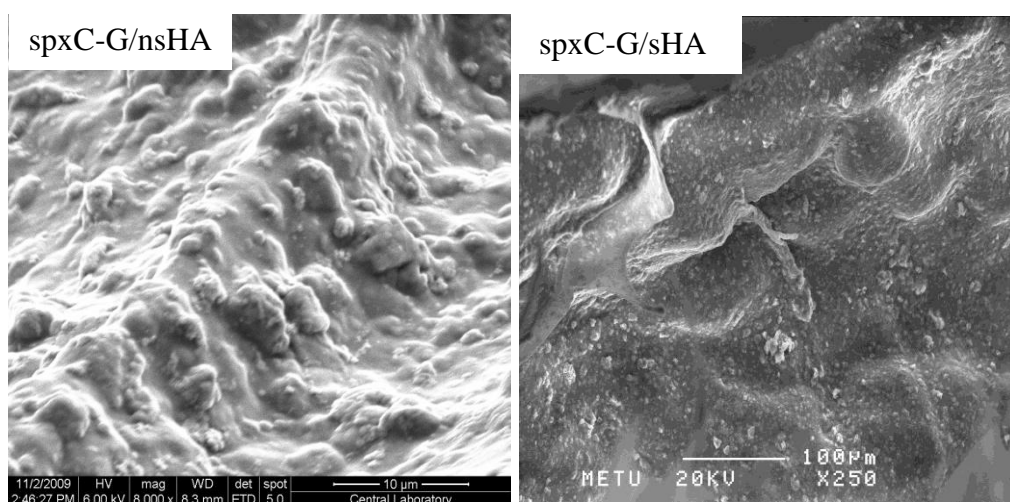


Figure 32 Scanning electron microscopy images of chitosan-gelatin/non-sintered hydroxyapatite (x5000) magnitude and chitosan-gelatin/sintered hydroxyapatite scaffolds pore walls (x250) magnitude.

### 3.6.3 Mechanical Properties

Compression tests were carried out for the chitosan-gelatin and chitosan-gelatin/hydroxyapatite scaffolds and the obtained compressive elastic modulus (E) and ultimate compression strength (UCS) values are given in Figure 33 and Figure

34, respectively. The results indicated that HA addition enhanced the ultimate compression strength of the materials from  $1.33\pm 0.19$  MPa for spxC-G to  $3.03\pm 0.82$  MPa and  $3.16\pm 0.39$  MPa for spxC-G/nsHA and spxC-G/sHA, respectively. Young's modulus values also enhanced with the HA addition from  $0.12\pm 0.03$  GPa for spxC-G to  $0.33\pm 0.07$  GPa and  $0.31\pm 0.04$  GPa for spxC-G/nsHA and spxC-G/sHA, respectively. So, approximately 300% increase in mechanical properties was achieved after both nsHA and sHA addition into polymeric matrices.

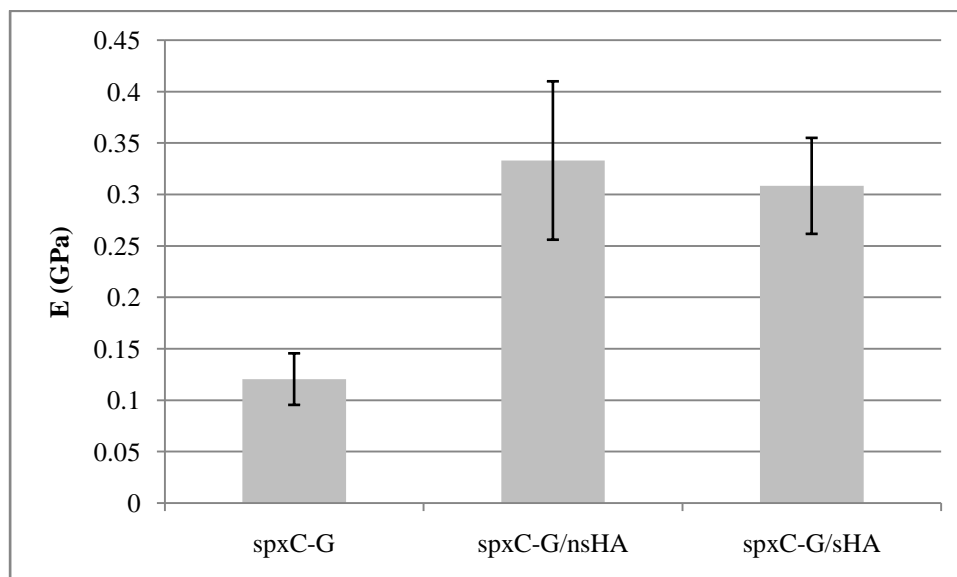


Figure 33 Comparison of Young's modulus (E) of crosslinked chitosan-gelatin, chitosan-gelatin/non-sintered hydroxyapatite, chitosan-gelatin/sintered hydroxyapatite porous scaffolds, obtained in compression tests.



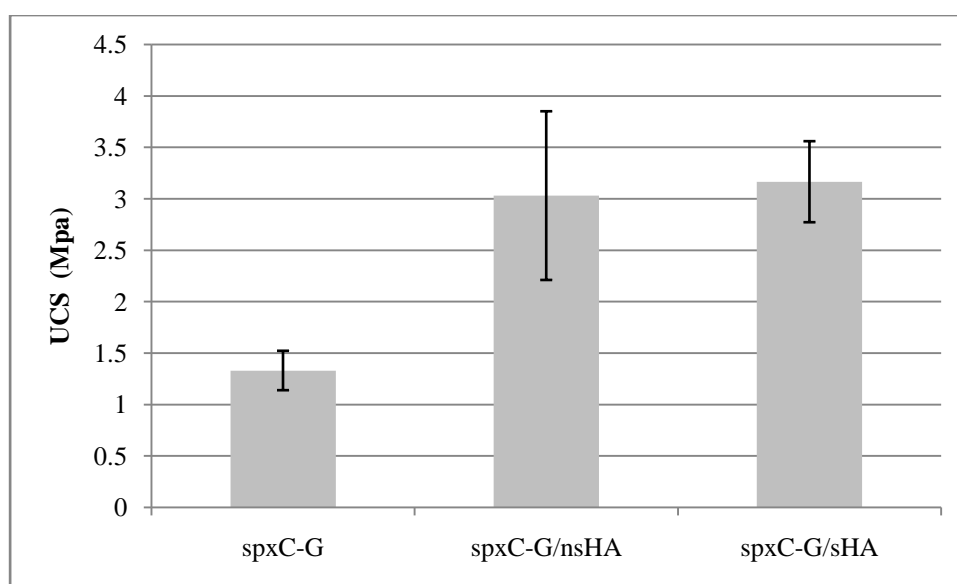


Figure 34 Ultimate compression strengths (UCS) of crosslinked chitosan-gelatin, chitosan-gelatin/non-sintered hydroxyapatite, chitosan-gelatin/sintered hydroxyapatite porous scaffolds.

Compressive strength of cancellous bone is in the range of 2-12 Mpa and Young's modulus values are around 0.05-0.5 MPa [Hench et al., 1993]. Thus, hydroxyapatite incorporated chitosan-gelatin structures that have shown UCS values at around 3 MPa and Young's modulus with about 0.3 MPa, can be applied in cancellous bone tissue engineering approaches as can be seen from Table 15.

Table 15 Comparison of Young's modulus (E) and Ultimate Compression Strength of crosslinked Chitosan-Gelatin and Chitosan-Gelatin/Hydroxyapatite porous scaffolds with those of cancellous bone.

Sample	UCS (MPa)	E (GPa)
Cancellous Bone	2-12	0.05-0.5
spxC-G	1.33 ± 0.19	0.12 ± 0.03
spxC-G/nsHA	3.03 ± 0.82	0.33 ± 0.08
spxC-G/sHA	3.17 ± 0.39	0.31 ± 0.05

### 3.6.4 Cell Viability on Porous Structures

The suitability of the scaffolds for cell spreading was examined by determining the cell proliferation with MTS assay (Figure 35) and observing the morphologies of cells by microscopy. 100,000 cells/cm<sup>2</sup> were seeded onto porous structures for 7 days and the highest cell proliferation was obtained with the sintered HA incorporated composite scaffolds and lowest with spxC-G/nsHA sponges. The reason for this may be the differences in pore size. SEM images of the scaffolds showed that the least pore size was observed in spxC-G/nsHA (about 100  $\mu$ m) whereas spxC-G/sHA demonstrated the largest pore sizes (about 500  $\mu$ m).

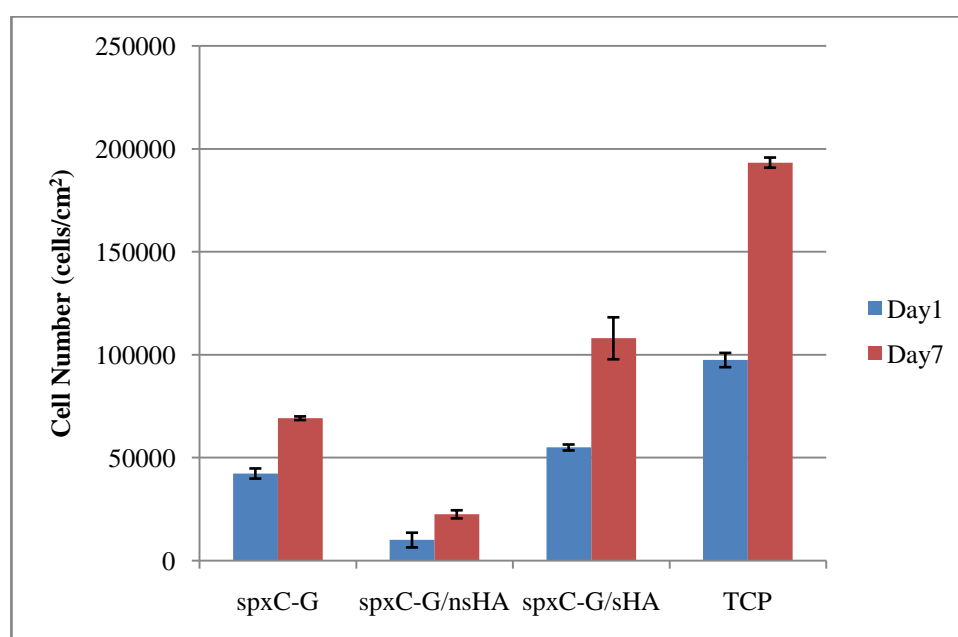


Figure 35 SaOs-2 osteosarcoma proliferation on sponges assessed by MTS assay.

Confocal microscopy was used to evaluate cell distribution and cell penetration through the pores of the cell seeded scaffolds. Confocal microscopy images (Figure 36) of propidium iodide-stained SaOs-2 cells cultured on spxC-G, spxC-G/nsHA and spxC-G/sHA sponges supported the MTS results with higher cell number in spxC-

G/sHA sample on Day 7. In addition, z-stack confocal images of the cross-section revealed that the cells had infiltrated about 100  $\mu\text{m}$  through spxC-G scaffolds while only about 60  $\mu\text{m}$  depth in spxC-G/sHA scaffolds. In spite of the highest cell number of spxC-G/sHA, spxC-G scaffolds showed the highest penetration. spxC-G/sHA constructs showed the least cell distribution and penetration, it may be because of the smallest pore sizes that are very critical in cell penetration and viability in scaffolds.

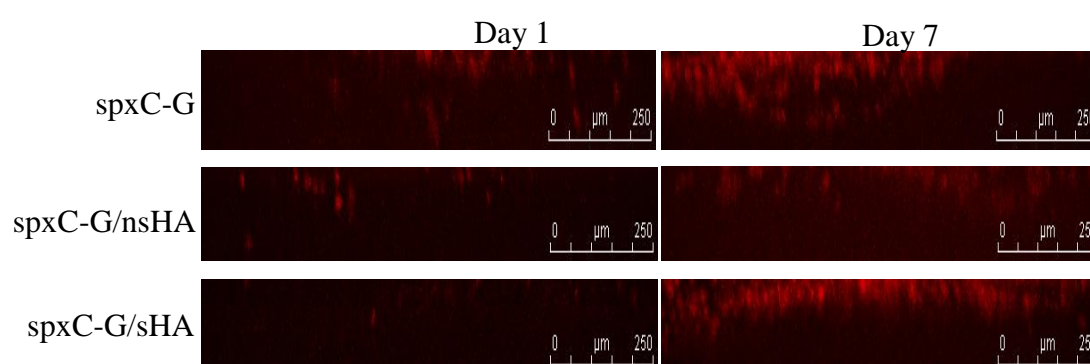


Figure 36 Confocal images of the cross-section of SaOs-2 cells seeded crosslinked chitosan-gelatin blend, chitosan-gelatin/nsHA and chitosan-gelatin/sHA composite porous scaffolds cultured for 1 and 7 days.

Cells migrated down the pores are shown by SEM micrographs of the scaffolds (Figure 37). SEM images indicate that cells have spherical shape with low spreading on all samples on Day 1. However, on Day 7, cells appear to have spread and adhered on the pore walls.

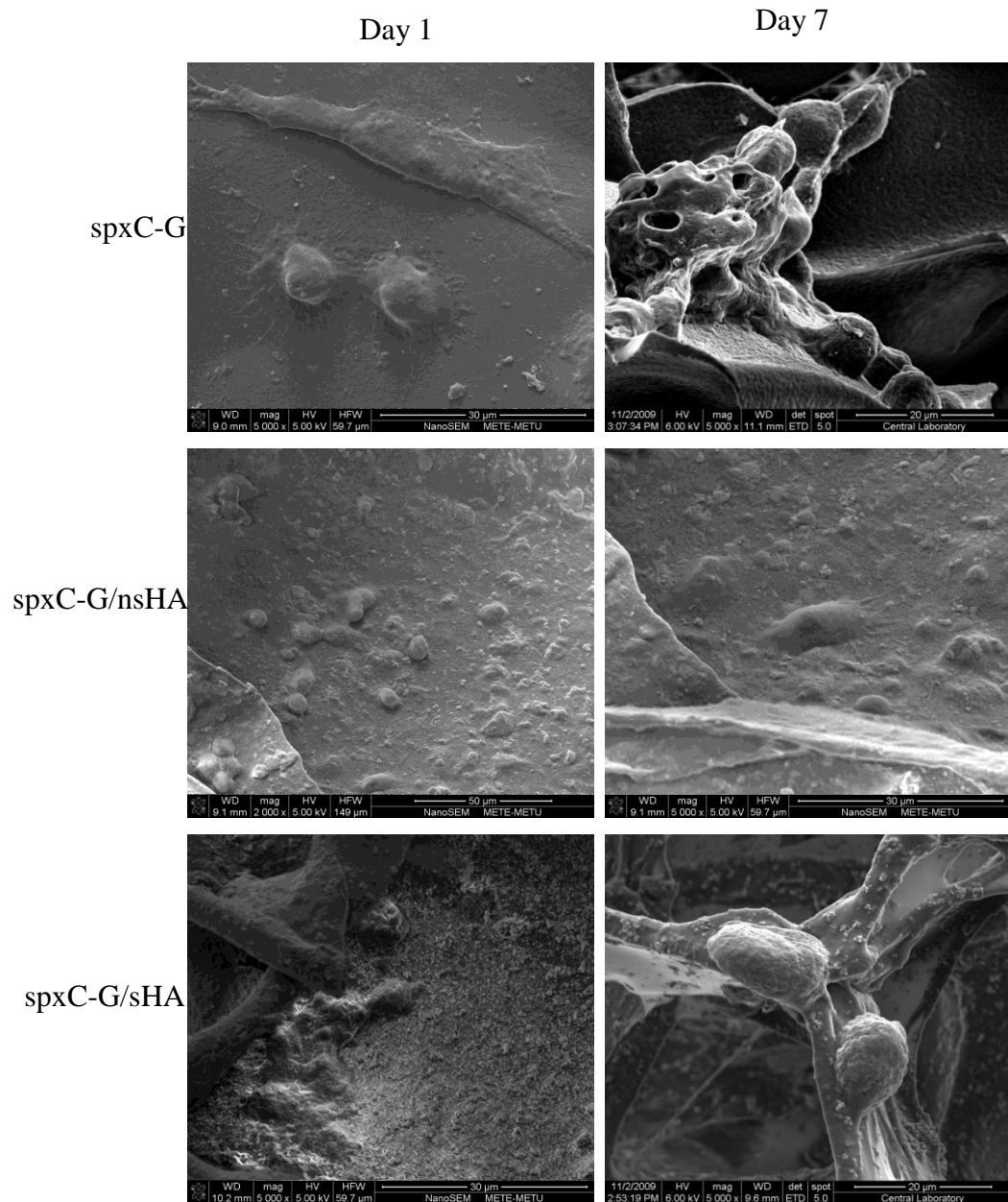


Figure 37 SEM images of SaOs-2 cells seeded on crosslinked chitosan-gelatin blend, chitosan-gelatin/nsHA and chitosan-gelatin/sHA composite porous scaffolds cultured for 1 and 7 days.

Interestingly, it was suggested that the osteoblast cells seeded on chitosan-gelatin/sintered-hydroxyapatite 3-D scaffolds may be located under the surface of the

porous walls of the scaffolds because the scaffold material may resorb partially. So, it was claimed that osteoblasts may bury themselves during this process [Zhao et al., 2002]. Since hydroxyapatite particles embedded on the pore walls are not distinguishable from buried cell structures in Figure 37 it is possible to claim the same for this study. If this approach is verified, the result of MTS assay with lowest cell proliferation in xC-G/nsHA scaffolds can be explained. Some other studies, explained the reason of increasing cell proliferation in HA added scaffolds as the effect of basic adsorption products that prevents the formation of acidic environment for cells [Shikinami et al., 1998 and Zhao et al., 2006].

It can be resulted that according to the confocal and SEM micrographs of chitosan-gelatin blend, chitosan-gelatin/nsHA and chitosan-gelatin/sHA composites, SaOs-2 osteosarcoma cells adhered and spread on the 3-D constructs but MTS assay results demonstrated that sHA addition indicated higher cell proliferation.

## CHAPTER 4

### CONCLUSIONS

Chitosan and gelatin are biocompatible and biodegradable natural polymers and hydroxyapatite is a bone-like mineral that is widely used to improve osteogenic properties of tissue engineered constructs. This study focused on the characterization of 2-D and 3-D chitosan-gelatin blend and chitosan-gelatin/hydroxyapatite composite structures for hard tissue engineering approaches. The results obtained in current study can be summarized as follows:

- According to FTIR-ATR, X-Ray and SEM analysis of the synthesized hydroxyapatite particles; highly pure amorphous and crystalline hydroxyapatite properties were obtained for non-sintered and sintered hydroxyapatite, respectively.
- In chitosan-gelatin films prepared with different chitosan-gelatin ratios, EDC/NHS crosslinking agents were used to crosslink water-soluble structures and FTIR-ATR results verified that this crosslinking process was successfully achieved. So, in further steps within the aqueous media only crosslinked samples were examined.
- To improve the osteogenic properties of the natural polymeric films non-sintered hydroxyapatite particles were added into these samples and homogenous distribution of hydroxyapatite particles in the polymeric matrix was obtained after crosslinking process. Since sintered-HA addition resulted with non-homogenous distribution and fragile constructs, only non-sintered

HA added samples with different chitosan-gelatin ratios were used in characterization tests.

- In thermal analysis; DSC curves showed that the decomposition temperatures of chitosan-gelatin blends increased with crosslinking process due to higher stability. In chitosan-gelatin/hydroxyapatite composite films, hydroxyapatite addition increased the decomposition temperatures of xC/nsHA and xC-G:1-1/nsHA composites. It may be because of the ionic interactions between  $\text{Ca}^{2+}$  and  $\text{PO}_4^{3-}$  groups of hydroxyapatite and  $\text{COO}^-$  and  $\text{NH}_3^+$  groups of chitosan-gelatin blends resulting with more stable structures in these composite samples. However, crosslinked xG/nsHA composites showed the least decomposition temperature due to heterogenous nsHA distribution of particles within the polymer as it was seen in SEM micrographs.
- Mechanical properties of the crosslinked samples showed higher ultimate tensile strength, hardness and strain at break values when compared to uncrosslinked ones. Moreover semi-crystalline chitosan addition also enhanced the mechanical behavior of the blend film samples. After nsHA addition, UTS and E values of films decreased. Because HA particles may lead to less ductility in polymer-HA composites and initial cracks may arise from larger HA particles in polymer matrix. 2-D chitosan-gelatin/nsHA film structures may be the candidate materials for cortical bone tissue engineering when similar mechanical results of cortical bone with these films were considered.
- Surface hydrophilicity results demonstrated that xC-G:1-1 films had the most hydrophilic behaviour among the crosslinked blend samples and swelling test results supported this behavior of film with the highest degree of swelling.
- Assays with human osteosarcoma SaOs-2 cells demonstrated that gelatin addition enhanced the cell proliferation in chitosan-gelatin blend samples mostly because of the presence of RGD-like sequences in gelatin that enhance cell attachment whereas in chitosan-gelatin/hydroxyapatite composite structures the trend of cell proliferation was in the opposite

direction and a decrease in cell number was observed as the gelatin content was increased. The reason of this decrease may be the reaction of HA particles and gelatin in a way that inhibits RGD-like sequences.

- To improve the similarity of the scaffolds to natural extracellular matrix, three-dimensional porous chitosan-gelatin/hydroxyapatite scaffolds were fabricated by lyophilization method. In these types of constructs both non-sintered and sintered HA added composite production was achieved. Chitosan-gelatin ratio was chosen as 1-1 in porous scaffold production according to crosslinked polymeric blend film characterization results.
- FTIR-ATR results and SEM images of porous scaffolds confirmed the stability of HA particles even after 24-hour crosslinking process in aqueous media.
- Mechanical results of samples indicated that both non-sintered and sintered HA addition lead to increased Young's modulus and ultimate compression strength. Moreover HA added porous composite samples showed very similar mechanical behavior to human spongy bone mechanical properties. So, these products may have the potential to be used in spongy bone tissue engineering.
- spC-G/sHA scaffolds showed the highest SaOs-2 cell affinities within the porous sponge samples. This may be because of greater pore sizes, about 500  $\mu\text{m}$ , with respect to spC-G scaffolds with pore sizes about 200  $\mu\text{m}$  and spC-G/nsHA scaffolds with pore sizes about 100  $\mu\text{m}$ . Confocal and SEM images also verified the cell attachment on the pore walls of the constructs.

As a conclusion, biocompatibility of chitosan-gelatin protein-based scaffolds can be improved with bioactive ceramics hydroxyapatite addition and the effects of the modification highly depends on the composition of polymer, type of hydroxyapatite and shape of structure. In addition, chitosan-gelatin/hydroxyapatite scaffolds have the potential to use in hard tissue engineering applications and in order to have detailed information about cell-material interaction, *in vivo* histological examinations of the samples are needed.



## REFERENCES

Abbasian, A., Ghaffarian, S. R., Mohammadi, N., Fallahi, D. 'Sensitivity of surface free energy analysis methods to the contact angle changes attributed to the thickness effect in thin films', *Journal of Applied Polymer Science*, 93: 1972-1980, 2004.

Abshagen, K., Schrodi, I., Gerber, T., Vollmar, B. 'In vivo analysis of biocompatibility and vascularization of the synthetic bone grafting substitute NanoBone<sup>®</sup>', *Journal of Biomedical Materials Research Part A*, 91: 2, 557-566, 2009.

Agnihotri, S.A., Mallikarjuna, N.N., Aminabhavi, T.M. 'Recent advances on chitosan-based micro- and nanoparticles in drug delivery', *Journal of Controlled Release*, 100: 5-28, 2004.

Ai, H., Mills, D.K., Jonathan, A.S., Jones, S.A. 'Gelatin-glutaraldehyde cross-linking on silicone rubber to increase endothelial cell adhesion and growth', *In Vitro Cell. Dev. Biol.-Animal*, 38: 487-492, 2002.

Altman, G.H., Diaz, F., Jakuba, C., Calabro, T., Horan, R.L., Chen, J., Lu, H., Richmond, J., Kaplan, D.L. 'Silk-based biomaterials', *Biomaterials*, 24: 401-416, 2003.

Anderson, D.D., Adams, D.J., Hale, J.E. 'Mechanical effects of forces acting on bone, cartilage, ligaments and tendons', in *Biomechanics and Biology of Movement*, Nigg, B.M., Macintosh, B.R., Master, J. eds., Human Kinetics Pub., 289-290, 2000.

Anselme, K. 'Osteoblast adhesion on biomaterials: Review', *Biomaterials*, 21: 667-681, 2000

Arvanitoyannis, I.S., Nakayama, A., Aiba, S-I. 'Chitosan and gelatin based edible films state diagrams, mechanical and permeation properties', 37: 371-382, 1998.

Atala, A., 'Review: Engineering tissues, organs and cells', J. Tissue Eng. Regen. Med., 1: 83-96, 2007.

Badylak, S.F. 'The extracellular matrix as a scaffold for tissue reconstruction', Seminars in cell and developmental biology, 13: 377-383, 2002.

Bao, C., Zhang, B., Li, Y., Sun, L., Yao, J., Zhang, X. 'In vivo bone tissue engineering' in Tissue engineering: Roles, materials and applications, Barnes, S.J., Harris, L.P. eds., Nova Science Pub, New York, 191-242, 2008.

Barnes, S.J., Harris, L.P. 'Tissue engineering: Roles, materials and applications', Nova Science Pub, New York, 2008.

Basmanav, B., Kose, G.T., Hasirci, V. 'Sequential growth factor delivery from complexed microspheres for bone tissue engineering', F. Biomaterials, 29: 4195-4204, 2008.

Belloncle, V.V., Rousseau, M. 'Effect of the surface free energy on the behaviour of surface and guided waves', Ultrasonics, 45: 188-195, 2006.

Bienengräber, V., Gerber, Th., Henkel, K.O., Bayerlein, T., Proff, P. Gedrange, G. 'The clinical application of a new synthetic bone grafting material in oral and maxillofacial surgery', Folia Morphol., 65: 84-88, 2006.

Bigi, A., Cojazzi, G., Panzavolta, S., Roveri, N., Rubini, K. 'Stabilization of gelatin films by crosslinking with genipin', Biomaterials, 23: 4827-4832, 2002.

Black, J. 'Biological performance of materials: fundamentals of biocompatibility', CRC Press Taylor and Francis Group, Northwest Florida, 2006.

Blazewicz, M. , Paluszkiewicz, C. ‘Characterization of biomaterials used for bone regeneration by FTIR spectroscopy’, *J Molecular Structure*, 563-564: 147-152, 2001.

Bonadio, J., Smiley, E., Patil, P., Goldstein, S. ‘Localized, direct plasmid gene delivery in vivo: prolonged therapy results in reproducible tissue regeneration’, *Nature Med*, 7: 753-759, 1999.

Braga, P.C., Ricci, D. ‘Methods in Molecular Biology Vol.242. Atomic Force Microscopy in Biomedical Methods and Applications’, Humana Press, New Jersey, 4-13, 2004.

Brunette, D.M., Chehroudi, B. ‘The effects of the surface topography of micromachined titanium substrata on cell behavior in vitro and in vivo’, *J Biomech Eng*, 121:49–57, 1999.

Bu, W., Wu, L., Hou, X., Fan, H., Hu, C., Zhang, X. ‘Investigation on Solvent Casting Films of Surfactant-Encapsulated Clusters’, *Journal of Colloid and Interface Science*, 251: 120–124, 2002.

Buckwalter, J.A., ‘Musculoskeletal tissues and the musculoskeletal system’ in Turek’s *Orthopaedics Principles and their Applications*, Wenstein, S.L., Buckwalter, J.A. eds., Lippincott Company, 2005.

Byrd, H.S., Hobar, P.C., Shewmake, K. ‘Augmentation of the craniofacial skeleton with porous hydroxyapatite granules’, *Plast Reconstr Surg*, 91: 15–22, 1993.

Cantin, S., Bouteau, M., Benhabib, F., Perrot, F. ‘Surface free energy evaluation of well-ordered Langmuir–Blodgett surfaces comparison of different approaches’, *Colloid. Surface. A.*, 276: 107–115, 2006.

Carmeliet, P. ‘Mechanisms of angiogenesis and arteriogenesis’, *Nat Med*, 6: 389-395, 2000.

Carole, A. ‘Cells for tissue engineering’, *Trends in Biotechnology*, 18: 17-19, 2000.

Carter, B., Norton, M.G. 'Ceramic Materials: Science and engineering', Springer Science and Media, New York, 3-4, 2007.

Chang, M.C., Ko, C.C., Douglas, W.H. 'Preparation of hydroxyapatite-gelatin nanocomposite' *Journal of Biomaterials*, 2853-2862, 2003.

Chen, Y-S., Chang, J-Y., Cheng, C-Y., Tsai, F-J., Yao, C-H., Liu, B-S. 'An in vivo evaluation of a biodegradable genipin-cross-linked gelatin peripheral nerve guide conduit material', *Biomaterials*, 26: 3911-3918, 2005.

Cheng, M., Deng, J., Yang, F., Gong, Y., Zhao, N., Zhang, X. 'Study on physical properties and nerve cell affinity of composite films from chitosan and gelatin solutions', *Biomaterials*, 24: 2871-2880, 2003.

Chevalier, J., Gremillard, L. 'Ceramics for medical applications: A picture for the next 20 years', *Journal of the European Ceramic Society*, 29: 1245–1255, 2009.

Chomarat, N., Robert, L., Seris J.L., Kern, P. 'Comparative efficiency of pepsin and proctase for the preparation of bovine skin gelatin', *Enzyme and microbial technology*, 16: 756-760, 1994.

Chu, C-C. 'Biodegradable polymers: An Overview' in 'Encyclopedia of Biomaterials and Biomedical Engineering', Wnek G.E., Bowlin, G.L. eds. Informa Healthcare, New York, 195, 2008.

Damink, L.H.H.O., Dijkstra, P.J., van Luyn, M. J. A., van Wachem, P. B., Nieuwenhuis, P., Feijen, J. 'Cross-linking of dermal sheep collagen using a water-soluble carbodiimide', *Biomaterials*, 17: 765-773, 1996.

Dang , J.M., Leong, K.W. 'Natural polymers for gene delivery and tissue engineering', *Advanced Drug Delivery Reviews*, 58: 487– 499, 2006.

Davies, R.C., Neuberger, A., Wilson, B.M. 'The dependence of lysozyme activity on pH and ionic strength', *Biochem Biophys Acta*, 178: 294–305, 1969.

de Oliveira, H.C.L., Fonseca, J.L.C., Pereira, M.R. 'Chitosan-poly(acrylic acid) polyelectrolyte complex membranes: preparation, characterization and permeability studies', *Journal of Biomaterials Science, Polymer Edition*, 19: 143-160, 2008.

DeFail, A.J., Edington, H.D., Matthews, S., Lee, W-C.C., Kacey G. 'Controlled release of bioactive doxorubicin from microspheres embedded within gelatin scaffolds', *Marra Journal of Biomedical Materials Research Part B: Applied Biomaterials*, 79A: 954–962, 2006.

Deng, C-M., He, L-Z., Zhao, M., Yang, D., Liu, Y. 'Biological properties of the chitosan-gelatin sponge wound dressing', *Carbohydrate Polymers*, 69: 583–589, 2007

Di Martino, A., Sittinger, M., Risbud, M.V. 'Review; Chitosan: A versatile biopolymer for orthopaedic tissue-engineering', *Biomaterials*, 26: 5983–5990, 2005.

Djagny, K.B., Wang, Z., Xu, S. 'Gelatin: a valuable protein for food and pharmaceutical industries: review', *Crit. Rev. Food Sci. Nutr.*, 41: 481–492, 2001.

Dogan S., Demirer S., Kepenekci I., Erkek B., Kiziltay A., Hasirci N., Muftuoglu S., Nazikoglu A., Renda N., Dincer U.D., Elhan A., Kuterdem E. 'Epidermal growth factor-containing wound closure enhances wound healing in non-diabetic and diabetic rats', *International Wound Journal*, 2009.

Dornish, M., Kaplan, D., Skaugrud, O. 'Standards and guidelines for biopolymers in tissue-engineered medical products', *Ann N Y Acad Sci*, 944: 388–97, 2001.

Druecke, D., Langer, S., Lamme, E., Pieper, J., Ugarkovic, M., Steinau, H.U., Homann, H.H. 'Neovascularization of poly(ether ester) block-copolymer scaffolds in vivo: Long-term investigations using intravital fluorescent microscopy', *J Biomed Mater Res Pt A*, 68: 10-18, 2004.

Ducheyne, P., Qiu, Q. 'Bioactive ceramics: the effect of surface reactivity on bone formation and bone cell function', *Biomaterials*, 20: 2287-2303, 1999.

El-Ghannam, A., Ducheyne, P., Shapiro, I.M. 'Effect of serum protein adsorption on osteoblast adhesion to bioactive glass and hydroxyapatite', *J Orthop Res*, 17: 340-5, 1999.

El-Ghannam, A., Ducheyne, P., Shapiro, I.M. 'Formation of surface reaction products on bioactive glass and their effects on the expression of the osteoblastic phenotype and the deposition of mineralized extracellular matrix', *Biomaterials*, 18: 295-303, 1997.

Erbil, Y. 'Surface chemistry of solid and liquid interfaces', Blackwell Pub., Oxford, 85, 2006.

Everaerts, F., Torrianni, M., Hendriks, M., Feijen, J. 'Biomechanical properties of carbodiimide crosslinked collagen: Influence of the formation of ester crosslinks', *Journal of Biomedical Materials Research*, 85: 547-555, 2008.

Freshney, R.I. 'Basic principles of cell culture' in *Culture of Cell for Tissue Engineering*, Vunjak-Novakovic, G., Freshney, R.I. eds., John Wiley Sons Pub, New Jersey, 4-5, 2006.

Gades M.D., Stern J.S. Chitosan supplementation and fat absorption in men and women, *Journal of the American Dietetic Association*, 105: 72-77, 2005.

Garner, J.P. 'Tissue Engineering in Surgery', *The Surgeon*, 2: 70-78, 2004.

Geiger, M., Li, R.H., Friess, W. 'Collagen sponges for bone regeneration with rhBMP-2', *Adv. Drug Deliv. Rev.*, 55:1613-1629, 2003.

George, M., Abraham, T.E. 'Review: Polyionic hydrocolloids for the intestinal delivery of protein drugs: alginate and chitosan', *J. Control. Release* 114;1-14, 2006.

Gerike, W., Bienengräber, V., Henkel, K.-O., Bayerlein, T., Proff, P., Gedrange, T., Gerber, Th. 'The manufacture of synthetic non-sintered and degradable bone grafting substitutes', *Folia Morphol.* 65;1, 54-55, 2006.

Giannoudis, P.V., Pountos, I. 'Tissue regeneration: The past, the present and the future', *Injury Int. J. Care Injured*, 36S: 2-5, 2005.

Gibson, L. 'New tissue scaffold regrows cartilage and bone', *MIT TechTalk*, 53: 4, 2009.

Gindl, M., Sinn, G., Gindl, W., Reiterer, A., Tschegg, S. 'A comparison of different methods to calculate the surface free energy of wood using contact angle measurements', *Colloids and Surfaces A: Physicochemical and Engineering Aspects*, 181:279-287, 2001.

Goldstein, J., Newbury, D., Joy, D., Lyman, C., Echlin, P., Lifshin, E., Sawyer, L., Micael, J. 'Scanning electron microscopy and x-ray microanalysis', Plenum Press, New York, 1, 2003.

Griffith, L., Naughton, G. 'Tissue engineering-current challenges and expanding opportunities', 295: 1009-1014, 2002.

Guelcher, S.A., Hollinger, J.O. 'An introduction to biomaterials', Taylor and Francis Group Press, Florida, 1, 2006.

Guilak, F., Awad, H.A., Fermor, B., Leddy, H.A., Gimple, J.M. 'Adipose-derived adult stem cells for cartilage tissue engineering', *J. Biorheology*, 41: 389-399, 2004.

Gunatillake, P.A., Adhikari, R. 'Biodegradable synthetic polymers for tissue engineering', *European cells and materials*, 5: 1-16, 2003.

Guo, C., Xue-Guang Liu, Jian-Zhong Huo, Chun Jiang, Xue-Jun Wen, Zheng-Rong Chen, 'Novel gene-modified-tissue engineering of cartilage using stable transforming growth factor- $\beta$ 1-transfected mesenchymal stem cells grown on chitosan scaffolds', *Journal of Bioscience and Bioengineering*, 103: 547-556, 2007.

Guo, T., Zhao, J., Chang, J., Ding, Z., Hong, H., Chena, J., Zhanga, J. 'Porous chitosan-gelatin scaffold containing plasmid DNA encoding transforming growth factor-b1 for chondrocytes proliferation', *Biomaterials*, 27: 1095–1103, 2006.

Haider, S., Park, S-Y., Lee, S-H. 'Preparation, swelling and electro-mechano-chemical behaviors of a gelatin-chitosan blend membrane', *Soft Matter*, 4:485-492, 2008.

Hench, L. 'Sol-gel materials for bioceramic applications', *Curr Opin Solid State Mater Sci*, 2: 604–610, 1997.

Hench, L., Splinter R., Greenlee T, Allen W. 'Bonding mechanisms at the interface of ceramic prosthetic materials', *J Biomed Eng*, 2: 117-41, 1971

Hench, L.L., Wilson, J. 'Advanced Series in Ceramics vol 1: An introduction to bioceramics', McLaren, M., Niesz, D.E., ed., World Scientific Pub, London, 1-4, 1993.

Hiroshi U., Takashi M., Toru F. 'Topical formulations and wound healing applications of chitosan', *Advanced Drug Delivery Reviews*, 52: 105-115, 2001.

Hong, H., Liu, C., Wu, W. 'Preparation and Characterization of Chitosan/PEG/Gelatin Composites for Tissue Engineering', *Journal of Applied Polymer Science*, 114: 1220-1225, 2009.

Höhne, G.W.H., Hemminger, W.F., Flammersheim, H.-J. 'Differential scanning calorimetry', Springer, Germany, 2003.



Hsu, S.H., Whu, S.W., Hsieh, S.C., Tsai, C.L., Chen, D.C., Tan, T.S. 'Evaluation of chitosan–alginate–hyaluronate complexes modified by an RGD-containing protein as tissue-engineering scaffolds for cartilage regeneration', *Artif Organs*, 28: 693–703, 2004.

Huang, Y., Onyeri, S., Siewe, M., Moshfeghian, A., Madihally, S.V. 'In vitro characterization of chitosan–gelatin scaffolds for tissue engineering', *Biomaterials*, 26: 7616-7627, 2005.

Hutmacher, D.W. 'Scaffolds in tissue engineering bone and cartilage', *Biomaterials*, 21: 2529-2543, 2000.

Hutmacher, D.W., Kirsch, A., Ackermann, K.L., Huerzeler, M.B. 'Matrix and carrier materials for bone growth factors-state of the art and future perspectives', in *Biological matrices and tissue reconstruction*. Stark, G.B., Horch, R., Tancos, E., eds., Springer, Heidelberg, 197-206, 1998.

Ignatiusa, A., Blessinga, H., Liederta, A., Schmidta, C., Neidlinger-Wilkea, C., Kaspara, D., Friemertb, B., Claesa, L. 'Tissue engineering of bone: effects of mechanical strain on osteoblastic cells in type I collagen matrices', *Biomaterials*, 26: 311–318, 2005.

Imen, E.H., Nakamura, M., Mie, M., Kobatake, E. 'Construction of multifunctional proteins for tissue engineering: Epidermal growth factor with collagen binding and cell adhesive activities', *Journal of Biotechnology*, 139: 19-25, 2009.

Ishihara, M., Nakanishi, K., Ono, K., Sato, M., Kikuchi, M., Saito, Y., Yura, H., Matsui, T., Hattori, H., Uenoyama, M., Kurita, A. 'Photocrosslinkable chitosan as a dressing for wound occlusion and accelerator in healing process', *Biomaterials*, 23: 833–840, 2002.

Ito, A., Mase, A., Takizawa, Y., Shinkai, M., Honda, H., Hata, K.I., Ueda, M., Kobayashi, T. 'Transglutaminase-mediated gelatin matrices incorporating cell adhesion factors as a biomaterial for tissue engineering', *J Biosci Bioeng*, 95: 196–9, 2003.

Jack, K.S., Velayudhan, S., Luckman, P., Trau, M., Lisbeth Grøndahl, L. Cooper-White, J. 'The fabrication and characterization of biodegradable HA/PHBV nanoparticle–polymer composite scaffolds', *Acta Biomaterialia*, 5: 2657-2667, 2009.

Jagur-Grodzinski, J. 'Polymeric gels and hydrogels for biomedical and pharmaceutical applications', *Polymers advanced Technologies*, 21: 27-47, 2009.

Jarcho, M., Bolen, C.H. 'Hydroxylapatite synthesis and characterization in dense polycrystalline form', *Journal of materials science*, 11: 2027-2035, 1976.

Jiankang H., Dichena L., Yaxiong L., Bo Y., Hanxiang Z., Qin L., Bingheng L., Yi L. Preparation of chitosan–gelatin hybrid scaffolds with well-organized microstructures for hepatic tissue engineering. *Acta Biomaterialia*, 5: 453-461, 2009 .

Johns, P., Courts, A. 'The science and technology of gelatin', Ward, A.G., Courts, A., ed., Academic Press, London, 138, 1977.

Kalfas, I.H., 'Principles of bone healing', *Neurosurg Focus*, 10:4, 2001.

Kaplan DL. 'Biopolymers from Renewable Resources', Berlin, Springer-Verlag, 1998.

Kawai, K., Suzuki, S., Tabata, Y., Ikada, Y., Nishimura Y. 'Accelerated tissue regeneration through incorporation of basic fibroblast growth factor-impregnated gelatin microspheres into artificial dermis', *Biomaterials*, 21;5, 489-499, 2000.

Keene, G.S., Robinson, A.H.N., Bowditch, M.G., Edwards, D.J. 'Key topics in orthopaedic trauma surgery', Bios Scientific Pub, Oxford, 11-14, 1999

Kenar, H., Kose, G.T., Hasirci, V. 'Tissue engineering of bone on micropatterned biodegradable polyester films', *Biomaterials*, 27;885–895, 2006.

Khor, E., Lim, L.Y. 'Implantable applications of chitin and chitosan', *Biomaterials*, 24;2339–2349, 2003.

Kikuchi, M., Koyama, Y., Yamada, T., Imamura, Y., Okada, T., Shirahama, N., Akita, K., Takakuda, K., Tanaka, J. 'Development of guided bone regeneration membrane composed of  $\beta$ -tricalcium phosphate and poly (-lactide-co-glycolide-co-caprolactone) composites', *Biomaterials*, 25: 5979-5986, 2004.

Kilpadi, K.L., Sawyer, A.A., Prince, C.W., Chang, P., Bellis, S.L. 'Primary human marrow stromal cells and Saos-2 osteosarcoma cells use different mechanisms to adhere to hydroxylapatite', *Journal of Biomedical Materials Research Part B: Applied Biomaterials*, 68A;2, 273 – 285, 2003.

Kim, B.S., Mooney, D.J. 'Development of biocompatible synthetic extracellular matrices for tissue engineering', *Trends Biotechnol.*, 16;5, 224–230, 2001.

Kim, H-W, Kim, H-E, Salih, V. 'Stimulation of osteoblast responses to biomimetic nanocomposites of gelatin–hydroxyapatite for tissue engineering scaffolds', *Biomaterials*, 26:5221-5230, 2005.

Kimura, Y., Ozeki, M., Inamoto, Y., Tabata, Y. 'Adipose tissue engineering based on human preadipocytes combined with gelatin microspheres containing basic fibroblast growth factor', *Biomaterials*, 24:2513-2521, 2003.

Kirkpatrick, C.J., Peters, K., Hermanns, M.I, Bittinger, F., Krump-Konvalinkova, V., Fuchs, S., Unger, R.E. 'In vitro methodologies to evaluate biocompatibility: status quo and perspective', *ITBM-RBM*, 26: 192-199, 2005.

Klokkevold, P.R., Vandemark, L., Kenney, E.B., Bernard, G.W. 'Osteogenesis enhanced by chitosan (poly-N-acetyl glucosaminoglycan) in vitro', *J Peridont*, 67:1170–5, 1996.

Kokubo, T., Kim, H-M., Kawashita, M. 'Novel bioactive materials with different mechanical properties', *Biomaterials*, 24;2161–2175, 2003.

Kolodziejska, I., Piotrowska, B. 'The water vapour permeability, mechanical properties and solubility of fish gelatin–chitosan films modified with transglutaminase or 1-ethyl-3-(3-dimethylaminopropyl) carbodiimide (EDC) and plasticized with glycerol', *Food Chemistry*, 103: 295-300, 2007.

Kong, L., Gao, Y., Lu, G., Gong, Y., Zhao, N., Zhang, X. 'A study on the bioactivity of chitosan/nano-hydroxyapatite composite scaffolds for bone tissue engineering', *European Polymer Journal*, 42: 3171-3179, 2006.

Kose, G.T., Korkusuz, F., Korkusuz P., Hasirci, V. 'In vivo tissue engineering of bone using poly(3-hydroxybutyric acid-co-3-hydroxyvaleric acid) and collagen scaffolds', *Tissue Engineering*, 10: 1234–1250, 2004.

Krajewska B. 'Membrane-based processes performed with use of chitin/chitosan materials', *Sep Purif Technol*, 41:305–12, 2005.

Kuijpers A.J., Engbers G.H.M., Feijen J., De Smedt S.C., Meyvis T.K.L., Demeester J., Krijgsveld J., Zaat S.A.J., Dankert J. 'Characterization of the network structure of carbodiimide cross-linked gelatin gels', *Macromolecules*, 32: 3325-3333, 1999.

Kumar, M.N.V.R. 'A review of chitin and chitosan applications', *Reactive and Functional Polymers*, 46;1–27, 2000.

Kumar, S.G., Kalpagam, V., Nandi, U.S., Vasantharajan, V.N. 'Biodegradation of gelatin-g-Poly(ethyl Acrylate) copolymers', *Journal of Applied Polymer Science*, 26: 3633-3641, 1981.

Kuo, S.M., Chang, S.J., Hsu, Y.T., Chen, T.V. 'Evaluation of Alginate coated Chitosan Membrane for Guided Tissue Regeneration', Engineering in Medicine and Biology 27th Annual Conference, 4878-4881, 2005.

Lacefield, W., Clare, A. 'Ceramics and Glasses' in Handbook of biomaterials evaluation. Scientific, technical and clinical testing of implant materials, Von Recum, A.F., ed., Taylor and Francis, Philadelphia, 145-146, 1999.

Lalan, S., Pomerantseva, I., Vacanti, J.P. 'Tissue engineering and its potential impact on surgery', World J. Surg. 25: 1458–1466, 2001.

Lee, S.J., Kim, S.S., Lee, Y.M. 'Interpenetrating polymer network hydrogels based on poly(ethylene glycol) macromer and chitosan', Carbohydrate Polymers, 41: 197–205, 2000.

Li, J., Chen, Y., Yin, Y., Yao, F., Yao, K. 'Modulation of nano-hydroxyapatite size via formation on chitosan–gelatin network film in situ', Biomaterials, 28: 781-790, 2007.

Li, J., Dou, Y., Yang, J., Yin, Y., Zhang, H., Yao, F., Wang, H., Yao, K. 'Surface characterization and biocompatibility of micro- and nano-hydroxyapatite/chitosan-gelatin network films', Materials Science and Engineering C, 29: 1207–1215, 2009.

Li, Z., Ramay, H.R., Hauch, K.D., Xiao, D., Zhang, M. 'Chitosan–alginate hybrid scaffolds for bone tissue engineering', Biomaterials, 26; 18, 3919-3928, 2005.

Liao, S., Chan, C.K., Ramakrishna, S. 'Stem cells and biomimetic materials strategies for tissue engineering', Materials Science and Engineering: C, 28:1189-1202, 2008.

Liu, C., Xia, Z., Czernuszka, J.T. 'Review paper design and development of three-dimensional scaffolds for tissue engineering', Trans IChemE, 85A;1051–1064, 2007.

Liu, Y., Lu, Y., Tian, X., Cui, G., Zhao, Y., Yang, Q., Yu, S., Xing, G., Zhang, B., 'Segmental bone regeneration using an rhBMP-2-loaded gelatin/nanohydroxyapatite/fibrin scaffold in a rabbit model', *Biomaterials*, 30; 31, 6276-6285, 2009.

Lu, L., Garcia, C.A., Mikos, A.G. 'In vitro degradation of thin poly(dl-lactic-co-glycolic acid) films', *J Biomed Mater Res*, 46:236-44, 1999.

Lu, L., Zhu, X., Valenzuela, R.G., Currier, B.L., Yaszemski, M.J. 'Biodegradable Polymer Scaffolds for Cartilage Tissue Engineering', *Clinical Orthopaedics and Related Research*, 391;S251-S270, 2001.

Lucchesi, C., Barbanti, S.H., Joazeiro, P.P., Duek, E.A.R. 'Cell culture on PCL/PLGA blends', *Journal of Applied Polymer Science*, 115:2609-2615, 2010.

Lysaght, M.J., Reyes, J. 'Review: The growth of tissue engineering', *J. Tissue Engineering*, 7;5, 485-493, 2001.

Ma, P.X., 'Scaffolds for tissue fabrication', *Materials Today*, 7;5:30-40, 2004.

Ma, P.X., Elisseeff, J. 'Scaffolding in tissue engineering', Taylor and Francis Group, Florida, 2006.

Madhumathi, K., Shalumon, K.T., Divya Rania, V.V., Tamurab, H., Furuikeb, T. 'Wet chemical synthesis of chitosan hydrogel-hydroxyapatite composite membranes for tissue engineering applications', *International Journal of Biological Macromolecules*, 45:12-15, 2009.

Madhally, S.V., Matthew, H.W.T. 'Porous chitosan scaffolds for tissue engineering', *Biomaterials*, 20:1133-1142, 1999.

Malafaya, P.B., Silva, G.A., Reis, R.L. 'Natural-origin polymers as carriers and scaffolds for biomolecules and cell delivery in tissue engineering applications', *Advanced Drug Delivery Reviews*, 59; 207-233, 2007.

Mamoru, S., Tetsuhiko, I., Manabu, K. 'Method for synthesis of hydroxyapatite, and hydroxyapatite complex and method for preparing the same', US Patent 6592989, 2003.

Manafi, S.A., Yazdani, B., Rahimiopour, M.R., Sadrnezhad, S.K., Amin, M.H., Razavi, M. 'Synthesis of nano-hydroxyapatite under a sonochemical/hydrothermal condition', *Biomedical Materials*, 3,1-6, 2008.

Mao, J.S., Zhao, L.G., Yin, Y.J., Yao, K.D. 'Structure and properties of bilayer chitosan–gelatin scaffolds', *Biomaterials*, 24,1067–1074, 2003.

Marks, S.C., Odgren, P.R. 'Structure and development of the skeleton' in *Principles of bone biology*, Bilezikian, J.P., Raisz, L.G., Rodan, G.A., ed, Academic Press, San Diego, 3–15, 2002.

Martuccia, J.F., Ruseckaitea, R.A., Vázquez, A. 'Creep of glutaraldehyde-crosslinked gelatin films', *Materials Science and Engineering: A*, 435-436: 681-686, 2006.

Mayr-Wohlfart, U., Fiedler, J., Gunther, K.-P., Puhl, W., Kessler, S. 'Proliferation and differentiation rates of a human osteoblast-like cell line (SaOS-2) in contact with different bone substitute materials', *J Biomed Mat Research Part B: Applied Biomaterials*, 57;1, 132 – 139, 2001.

Mizutani, A., Fujita, T., Watanabe, S., Sakakida, K., Okada, Y. 'Experiments on antigenicity and osteogenicity in allotransplanted cancellous bone.' *Int Orthop*, 14:243–8, 1990.

Mohamed, K.R., Mostafa, A.A. 'Preparation and bioactivity evaluation of hydroxyapatite-titania/chitosangelatin polymeric biocomposites', *Materials Science and Engineering C*, 28: 1087–1099, 2008.

Mohanty, A.K., Misra, M., Hinrichsen, G. 'Biofibres, biodegradable polymers and biocomposites: An overview', *Macromolecular Materials and Engineering*, 276: 1-24, 2000.

Moore, J.R., Phillips, T.W., Weiland, A.J., Randolph, M.A. 'Allogenic transplants of bone revascularized by microvascular anastomoses: a preliminary study.' *J Orthop Res*, 1:352-60, 1984.

Murphy, M.B., Mikos, A.G. 'Polymer Scaffold Fabrication', in *Principles of Tissue Engineering*, Lanza, R.P., Langer, R., Vacanti, J.P., ed., Elsevier Inc., 2007.

Muzzarelli R.A.A., Biagini, G., Bellardini, M., Simonelli, L., Castaldini, C., Fratto G. 'Osteoconduction exerted by N-methylpyrrolidinone chitosan used in dental surgery, *Biomaterials*', 14: 39-43, 1993.

Nam, Y.S., Park, W.H., Ihm, D., Hudson, S.M. 'Effect of the degree of deacetylation on the thermal decomposition of chitin and chitosan nanofibers', *Carbohydrate Polymers*, In Press, 2010.

Naughton, G.K., Tolbert, W.R., Grillo, T.M. 'Emerging developments in tissue engineering and cell technology', *Tissue Eng*;1(2):211-9, 1995.

Norland, R.E. 'Fish gelatin', in *Advances in fisheries technology and biotechnology for increased profitability*, Voight, M.N, Botta, J.K. ed., Lancaster: Technomic Publishing Co.,325-333, 1990.

O'Brien, F.J., Harley, B.A., Yannas, I.V., Gibson, L. 'Influence of freezing rate on pore structure in freeze-dried collagen-GAG scaffolds', *Biomaterials*, 25:1077-1086, 2004.

Oliveira, J.M., Silva, S.S., Malafaya, P.B., Rodrigues, M.T., Kotobuki, N., Hirose, M., Gomes, M.E., Mano, J.F., Ohgushi, H., Reis, R.L. 'Macroporous hydroxyapatite scaffolds for bone tissue engineering applications: Physicochemical characterization



and assessment of rat bone marrow stromal cell viability', *J Biomed Mater Res A*, 91;1,175-86, 2009.

Ong S.Y., Wu J., Moochhala S.M., Tan M.H., Lu J. Development of a chitosan-based wound dressing with improved hemostatic and antimicrobial properties, *Biomaterials*, 29: 4323-4332, 2008.

Ozcan, C., Hasirci, N. 'Evaluation of Surface Free Energy for PMMA Films', *Journal of Applied Polymer Science*, 108: 438–446, 2008.

Park, J., Lakes, R.S. 'Biomaterials: an introduction', Springer Science Business Media, New York, 2007.

Pautke, C., Schieker, M., Tischer, T., Kolk, A., Neth, P., Mutschler, W., Milz, S. 'Characterization of Osteosarcoma Cell Lines MG-63, SaOs-2 and U-2 OS in Comparison to Human Osteoblasts', *Anticancer Research*, 24;6, 3743-3748, 2004.

Peter, M, Binulal, N.S., Soumya, S., Nair, S.V., Furuike, T., Tamura, H., Jayakumar, R. 'Nanocomposite scaffolds of bioactive glass ceramic nanoparticles disseminated chitosan matrix for tissue engineering applications', *Carbohydrate Polymers*, 79(2):284-289, 2010.

Pfizer Co. 'Gelfoam® absorbable gelatin compressed sponge', [http://www.pfizer.com/files/products/uspi\\_gelfoam\\_sponge.pdf](http://www.pfizer.com/files/products/uspi_gelfoam_sponge.pdf), 2007.

Pomfret, E.A., Sung, R.S., Allan, J., Kinghabwala, M., Melancon, J.K., Roberts, J.P. 'Solving the organ shortage crisis: 7th annual American society of transplant surgeons' state-of-the-art winter symposium', *American Journal of Transplantation*, 8: 745-752, 2008.

Ponsonnet, L., Reybier, K., Jaffrezic, N., Comte, V., Lagnau, C., Lissac, M., Martelet, C. 'Relationship between surface properties (roughness, wettability) of

titanium and titanium alloys and cell behaviour', *Materials Science and Engineering C*, 23: 551–560, 2003.

Quarto, R., Mastrogiacomo, M., Cancedda, R., Kutepov, S.M., Mukhachev, V., Lavroukov, A., Kon, E., Marcacci, M. 'Repair of large bone defects with the use of autologous bone marrow stromal cells.', *N Engl J Med*, 6:344-385, 2001.

Rabea, E.I., Badawy, M.E.-T., Stevens, C.V., Smaghe, G., Steurbaut, W. 'Reviews: Chitosan as antimicrobial agent: Applications and mode of action', *Biomacromolecules*, 4(6): 1457-1465, 2003.

Rafat, M., Li, F., Fagerholm, P., Lagali, N.S., Watsky, M.A., Munger, R., Matsuura, T., Griffith, M. 'PEG-stabilized carbodiimide crosslinked collagen–chitosan hydrogels for corneal tissue engineering', *Biomaterials*, 29:1-13, 2008.

Rey, L. 'Glimpses into the realm of freeze-drying: Fundamental issues' in *Drugs and the pharmaceutical sciences vol 137. Freeze-drying/lyophilization of pharmaceutical and biological products*, Rey, L., May, J.C., ed., Marcel Dekker Inc., New York, 3-4, 2004.

Rezwana, K., Chena, Q.Z., Blakera, J.J., Boccaccini, A.R. 'Review: Biodegradable and bioactive porous polymer/inorganic composite scaffolds for bone tissue engineering', *Biomaterials* 27;18, 3413-3431, 2006.

Rizzi, S.C., Heath, D.J., Coombes, A.G.A., Bock, N., Textor, M., Downes, S. 'Biodegradable polymer/hydroxyapatite composites: Surface analysis and initial attachment of human osteoblasts', *Journal of Biomedical Materials*, 55: 475-486, 2001.

Rochet, N., Balaguer, T., Boukhechba, F., Laugier, J.-P., Quincey, D., Goncalves, S., Carle G.F. 'Differentiation and activity of human preosteoclasts on chitosan enriched calcium phosphate cement', *Biomaterials*, 30(26): 4260-4267, 2009.

Rohanizadeh, R., Swain, M.V., Mason, R.S. 'Gelatin sponges (Gelfoam®) as a scaffold for osteoblasts', *J Mater Sci: Mater Med*, 19:1173–1182, 2008.

Rosellini, E., Cristallini, C., Barbani, N., Vozzi, G., Giusti, P. 'Preparation and characterization of alginate/gelatin blend films for cardiac tissue engineering', *Journal of Biomedical Materials Research Part A*, 91; 2, 447-453, 2009.

Rosso, F., Giordano, A., Barbarisi, M., Barbarisi, A. 'From cell-ECM interactions to tissue engineering', *Journal of cellular physiology*, 199:174–180, 2004.

Sailaja, G.S., Ramesh, P., Kumary, T.V., Varma, H.K. 'Human osteosarcoma cell adhesion behaviour on hydroxyapatite integrated chitosan–poly(acrylic acid) polyelectrolyte complex', *Acta Biomaterialia*, 2:651–657, 2006.

Saltzman, W.M. 'Tissue engineering: Engineering principles for the design of replacement organs and tissue', New York, Oxford Press, 16, 2004.

Sarasam A.R., Brown P., Khajotia S.S., Dmytryk J.J., Madhally S.V. Antibacterial activity of chitosan-based matrices on oral pathogens, *Journal of Materials Science: Materials in Medicine*, 19: 1083-1090, 2008

Schnettjer, R., Alt, V., Dingeldein, E., Pfefferle, H-J., Kilian, O., Meyer, C., Heiss, C., Wensch, S. 'Bone ingrowth in bFGF-coated hydroxyapatite ceramic implants', *Biomaterials*, 24:4603–4608, 2003.

Seol, Y-J., Lee, J-Y., Park, Y-J., Lee, Y-M., Ku, Y., Rhyu, I-C., Lee, S-J., Han, S-B., Chung, C-P. 'Chitosan sponges as tissue engineering scaffolds for bone formation', *Biotechnology Letters*, 26: 1037–1041, 2004.

Shareef, M.Y., Messer, P.E. 'Fabrication, characterization and fracture study of a machinable hydroxyapatite ceramic', *Biomaterials*, 14;1, 69–75, 1993.

Shea, L.D., Wang, D., Franceschi, R.T., Mooney, D.J. 'Engineered Bone Development from a Pre-Osteoblast Cell Line on Three-Dimensional Scaffolds', *J Tissue Engineering*, 6;6, 2004.

Sheridan, M.H., Shea, L.D., Peters, M.C., Mooney, D.J. 'Bioabsorbable polymer scaffolds for tissue engineering capable of sustained growth factor delivery, *Journal of Controlled Release*, 24:91-102, 2000.

Shikinami, Y., Okuno, M. 'Bioresorbable devices made of forged composites of hydroxyapatite (HA) particles and poly-L-lactide (PLLA): part I. Basic characteristics', *Biomaterials*, 20: 859-77, 1998.

Shum-Tim, D., Stock, U., Hrkach, J., Shinoka, T., Lien, J., Moses, M.A., Stamp, A., Taylor, G., Moran, A.M., Landis, W., Langer, R., Vacanti, J.P., Mayer, J.E. 'Tissue engineering of autologous aorta using a new biodegradable polymer', *Ann Thorac Surg*, 68:2298-2304, 1999.

Siemann, U. 'Solvent cast technology: a versatile tool for thin film production', *Progr Colloid Polym Sci*, 130: 1-14, 2005.

Suchanek, W., Yoshimura, M. 'Processing and properties of hydroxyapatite-based biomaterials for use as hard tissue replacement implants', *Journal of Materials Research*, 13: 94-117, 1998.

Suheyla Kas, H. 'Review chitosan: properties, preparations and application to microparticulate systems', *J. Microencapsul*, 14; 689-711, 1997.

Suna, J-S., Wuc, S.Y-H. and Feng-Huei Linc, 'The role of muscle-derived stem cells in bone tissue engineering', *Biomaterials*, 26;18, 3953-3960, 2005.

Supova, M. 'Problem of hydroxyapatite dispersion in polymer matrices: a review', *Journal of Materials Science: Materials in Medicine*, 20: 1201-1213, 2009.

Tabata, Y., Ikada, Y. 'Protein release from gelatin matrices', *Adv. Drug Deliv. Rev.*, 31;287–301, 1998.

Tang, X.J., Gui, L., Lü, X.Y. 'Hard tissue compatibility of natural hydroxyapatite/chitosan composite', *Biomedical Materials*, 3;1-9, 2008.

Teoh, S.H. 'Fatigue of biomaterials: a review', *International Journal of Fatigue*, 22;825–837, 2000.

Thamaraiselvi, T.V., Prabakaran, K., Rajeswari, S. 'Synthesis of Hydroxyapatite that Mimic Bone Minerology', *Trends Biomaterials Artificial Organs*, 19. 81-83, 2006.

Thamaraiselvi, T.V., Rajeswari, S. 'Biological evaluation of bioceramic materials: Review', *Trends Biomaterials Artificial Organs*, 18:9-17, 2004.

Thein-Han, W.W., Saikhun, J., Pholpramoo, J., Misra, R.D.K., Kitiyanant, Y. 'Chitosan–gelatin scaffolds for tissue engineering: Physico-chemical properties and biological response of buffalo embryonic stem cells and transfectant of GFP–buffalo embryonic stem cells', *Acta Biomaterialia*, 5: 3453-3466, 2009.

Trung, T.S., Thein-Han, W.W., Quia, N.T., Nga, C-H., Stevens, W.F. 'Functional characteristics of shrimp chitosan and its membranes as affected by the degree of deacetylation', *Bioresource Technology*, 97: 659-663, 2006.

Ulubayram, K., Aksu, E., Deliloglu, G.S.I., Serbetci, K., Hasirci, N. 'Cytotoxicity evaluation of gelatin sponges prepared with different cross-linking agents', *Journal of Biomaterials Science, Polymer Edition*, 13(11): 1203-1219, 2002.

Ulubayram, K., Cakar, A.N., Korkusuz, P., Ertan, C., Hasirci, N. 'EGF containing gelatin-based wound dressings', *Biomaterials*, 22;1345-1356, 2001.

Ulubayram, K., Eroglu, I., Hasirci, N. 'Gelatin Microspheres and Sponges for Delivery of Macromolecules', *J Biomater Appl*, 16: 227, 2002

Van Wachem, P.B., Plantinga, J.A., Wissink, M.J., Beernink, R., Poot, A.A., Engbers, G.H.M., Beugeling, T., van Aken, W.G., Feijen, J., van Luyn, M.J.A. 'In vivo biocompatibility of carbodiimide-crosslinked collagen scaffolds: effects of crosslink density, heparin immobilization, and bFGF loading', *J Biomed Mater Res*, 55: 368–378, 2001.

Venugopal, J., Vadgama, P., Kumar, T.S.S., Ramakrishna, S. 'Biocomposite nanofibres and osteoblasts for bone tissue engineering', *Nanotechnology*, 18,2007.

Vijayalakshmi, U., Rajeswari, S. 'Preparation and Characterization of Microcrystalline Hydroxyapatite Using Sol Gel Method', *Trends Biomaterials Artificial Organs*, 19: 57-62, 2006.

Vincent, J. F.V. 'Structural Biomaterials', Princeton University Press, New Jersey, 3,1990.

Vorhies, J.S., Nemunaitis, J.J. 'Synthetic vs. Natural/Biodegradable Polymers for Delivery of shRNA-Based Cancer Therapies.' *Methods in molecular biology, Macromolecular Drug delivery*, Humana Press, 480, 2009.

Wang, A., Ao, Q., Cao, W., Zhao, C., Gong, Y., Zhao, N., Zhang, X. 'Fiber-Based Chitosan Tubular Scaffolds for Soft Tissue Engineering: Fabrication and in Vitro Evaluation', *J Tsinghua Science &Technology* 10;4, 449-453, 2005.

Wang, H-Q., Bai, L., Shen, B-R., Yan, Z-Q., Jiang, Z-L. 'Coculture with endothelial cells enhances vascular smooth muscle cell adhesion and spreading via activation of b1-integrin and phosphatidylinositol 3-kinase/Akt', *European Journal of Cell Biology*, 86:51-62, 2007.

Wang, X., Wang, X., Tan, Y., Zhang, Bo., Gu, Z., Li, X. 'Synthesis and evaluation of collagen–chitosan–hydroxyapatite nanocomposites for bone grafting', *Journal of Biomedical Materials Research Part A*, 89: 1079-1087, 2008.

Wang, Y., Yin, S., Ren, L., Zhao, L. 'Surface characterization of the chitosan membrane after oxygen plasma treatment and its aging effect', *Biomedical Materials*, 4: 1-7,2009.

Wang, Y-X., Robertson, J.L., Spillman, W.B., Claus, R.O. 'Effects of the Chemical Structure and the Surface Properties of Polymeric Biomaterials on Their Biocompatibility', *Pharmaceutical Research*,21; 8, 2004.

Wei, G., Ma, P.X. 'Structure and properties of nano-hydroxyapatite/polymer composite scaffolds for bone tissue engineering', 25: 4749-4757, 2003.

White, S.C., Atchison, K.A., Gornbein, J.A., Nattiv, A., Paganini, A., Service, S.K., 'Risk factors for fractures in older men and women: The leisure world cohort study', *Hard Gender Medicine* 3:2, 2006.

Widmer, M.S., Mikos, A.G., 'Fabrication of Biodegradable Polymer Scaffolds for Tissue Engineering, in *Frontiers in Tissue Engineering*, Patrick, Jr. C.W., Mikos, A.G., McIntire, L.V. ed., Elsevier Science, New York, 107-120, 1998.

Wiesmann, H.P., Nazer, N., Klatt, C., Szuwart, T., Meyer, U. 'Bone tissue engineering by primary osteoblast-like cells in a monolayer system and 3-dimensional collagen gel', *Oral Maxillofac Surg*, 61(12):1455-62, 2003.

Wise, D.L., Trantolo, D.J., Altobelli, D.E., Yaszemski, M.J., Gresser, J.D., Schwartz, E.R. 'Encyclopedic handbook of biomaterials and bioengineering part:A volume2' , Marcel Dekker Inc, New York, 1465-1467, 1995.

Woodard, J.R., Hildorea, A.J., Lanb, S.K., Park, C.J., Morgan, A.W., Eurell, J.A.C., Clark, S.G., Wheeler, M.B., Jamison, R.D., Johnson, A.J.W. 'The mechanical properties and osteoconductivity of hydroxyapatite bone scaffolds with multi-scale porosity', *Biomaterials*, 28; 45–54, 2007.

Wu, C.K.A., Pettit, A. R. Toulson, S. Grøndahl, L. Mackie, E. J. Cassady , A.I. 'Responses in vivo to purified poly(3-hydroxybutyrate-co-3-hydroxyvalerate) implanted in a murine tibial defect model', *Journal of Biomedical Materials Research Part A* 91:845-854,2009.

Xia, Z., Breward, C.J.W. 'Tissue Engineering of Bone: The role of osteoblasts and osteoclasts', Description for a problem studied at the UK Mathematics-in-Medicine Study Group, Strathclyde, 2004.

Xiaoyan A., Jun Y., Min W., Haiyue Z., Li C., Kangde Y., Fanglian Y., Preparation of chitosan–gelatin scaffold containing tetrandrine-loaded nano-aggregates and its controlled release behavior, *International Journal of Pharmaceutics*, 350: 257–264, 2008.

Xin-Yuan, S., Tian-Wei, T. 'New Contact Lens Based on Chitosan/Gelatin Composites', *Journal of Bioactive and Compatible Polymers*, 19:467, 2004.

Xu, H.H.K., Simon, C.G. 'Fast setting calcium phosphate–chitosan scaffold: mechanical properties and biocompatibility', *Biomaterials*, 26;12, 1337-1348, 2005.

Yang, S., Leong, K., Du, Z., Chuar, C. 'Review: The design of scaffolds for use in tissue engineering, Part I. Traditional Factors', *Tissue Eng*, 7; 6, 2001.

Yao, C-H., Liu, B-S., Chang, C-J., Hsu, S-H., Chen, Y-S. 'Preparation of networks of gelatin and genipin as degradable biomaterials', *Materials Chemistry and Physics*, 83;204–208, 2004.

Yilgor, P., Sousa, R.A., Reis, R.L.,Hasirci, N., Hasirci, V. '3-D plotted PCL scaffolds for stem cell based bone tissue engineering', *Macromol. Symp.*, 269:92–99, 2008.

Yin, Y.J., Zhao, F., Song, X.F., Yao, K.D., Lu, W.W., Leong, J.C. 'Preparation and characterization of hydroxyapatite/chitosan-gelatin network composite', *Journal of Applied Polymer Science*, 77: 2929-2938, 2000.



Yoshikawa, H., Myoui, A. 'Bone tissue engineering with porous hydroxyapatite ceramics', *J Artif Organs*, 8:131–136, 2005.

Young, S., Wong, M., Tabata, Y., Mikos, A.G. 'Gelatin as a delivery vehicle for the controlled release of bioactive molecules', *J Controlled Release*, 109;1–3, 256–274, 2005.

Yucel, D., Kose, G., Hasirci, V. 'Polyester based nerve guidance conduit design', *Biomaterials*, 31: 1596-1603, 2010.

Zhang, R., Tang, M., Bowyer, A., Eisenthal, R., Hubble, J. 'A novel pH- and ionic-strength sensitive carboxy methyl dextran hydrogel', *Biomaterials*, 26, 4677-4683, 2005.

Zhang, Wang, Y., Shi, B., Cheng, X. 'A platelet-derived growth factor releasing chitosan/coral composite scaffold for periodontal tissue engineering', *Biomaterials*, 28: 1515-1522, 2007.

Zhang, Y., Ouyang, H., Lim, C.T., Ramakrishna, S., Huang, Z-M. 'Electrospinning of gelatin fibers and gelatin/PCL composite fibrous scaffolds', *J of Biomedical Materials*, 72:156, 2004.

Zhao, F. 'Preparation and histological evaluation of biomimetic three-dimensional hydroxyapatite/chitosan-gelatin network composite scaffolds', *Biomaterials*, 23: 3227–3234, 2002.

Zhao, F., Grayson, W.L., Ma, T., Bunnell B., Lu, W.W. 'Effects of hydroxyapatite in 3-D chitosan-gelatin polymer network on human mesenchymal stem cell construct development', *Biomaterials*, 27: 1859-1867, 2006

Zheng, J.P., Wang, C.Z., Wang, X.X., Wang, H.Y., Zhuang, H., Yao, K.D. 'Preparation of biomimetic three-dimensional gelatin/montmorillonite–chitosan scaffold for tissue engineering', *Reactive & Functional Polymers*, 67;780–788, 2007.

Zheng, M.H., Hinterkeuser, K., Solomon, K., Kunert, V., Pavlos, N. J., Xu, J. 'Collagen-Derived Biomaterials in Bone and Cartilage Repair', *Macromol. Symp.*, 253;179–185, 2007.

Zivanovic, S., Li J., Davidson P.M., Kit K., Physical, Mechanical and Antibacterial Properties of Chitosan/PEO Blend Films. *Biomacromolecules*, 8: 1505-1510, 2007.

## APPENDICES

### APPENDIX A

#### DSC CURVES OF C-G BLEND FILMS

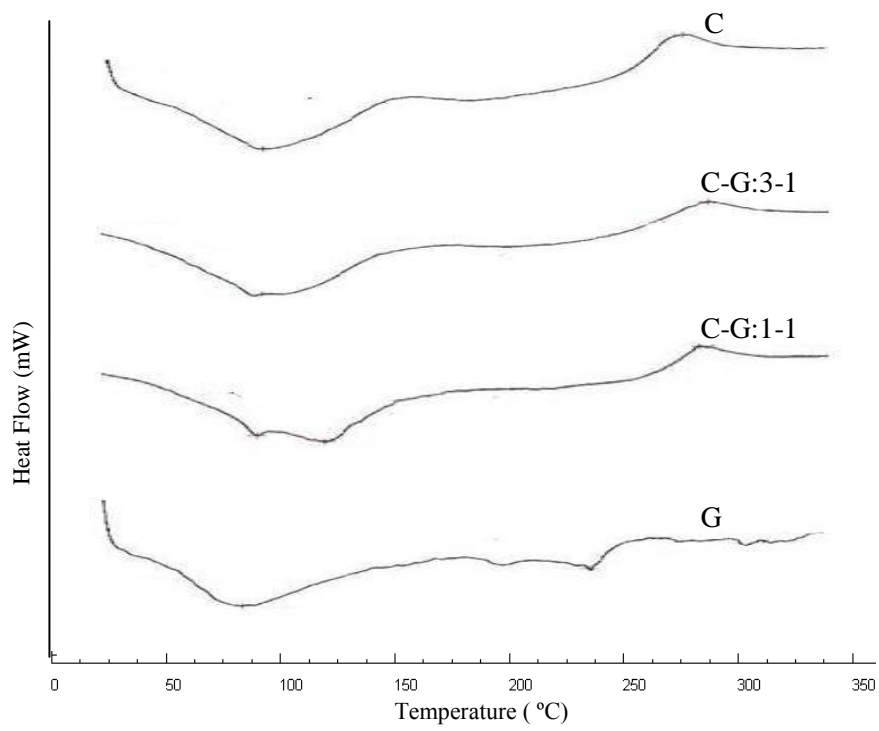


Figure 38 DSC analysis of uncrosslinked chitosan-gelatin films.